

1977

Pretensioning of single-crossarm stayed columns.

Hisham Hussein. Hafez
University of Windsor

Follow this and additional works at: <http://scholar.uwindsor.ca/etd>

Recommended Citation

Hafez, Hisham Hussein, "Pretensioning of single-crossarm stayed columns." (1977). *Electronic Theses and Dissertations*. Paper 3183.

This online database contains the full-text of PhD dissertations and Masters' theses of University of Windsor students from 1954 forward. These documents are made available for personal study and research purposes only, in accordance with the Canadian Copyright Act and the Creative Commons license—CC BY-NC-ND (Attribution, Non-Commercial, No Derivative Works). Under this license, works must always be attributed to the copyright holder (original author), cannot be used for any commercial purposes, and may not be altered. Any other use would require the permission of the copyright holder. Students may inquire about withdrawing their dissertation and/or thesis from this database. For additional inquiries, please contact the repository administrator via email (scholarship@uwindsor.ca) or by telephone at 519-253-3000ext. 3208.



National Library of Canada

Cataloguing Branch
Canadian Theses Division

Ottawa, Canada
K1A 0N4

Bibliothèque nationale du Canada

Direction du catalogage
Division des thèses canadiennes

NOTICE

The quality of this microfiche is heavily dependent upon the quality of the original thesis submitted for microfilming. Every effort has been made to ensure the highest quality of reproduction possible.

If pages are missing, contact the university which granted the degree.

Some pages may have indistinct print especially if the original pages were typed with a poor typewriter ribbon or if the university sent us a poor photocopy.

Previously copyrighted materials (journal articles, published tests, etc.) are not filmed.

Reproduction in full or in part of this film is governed by the Canadian Copyright Act, R.S.C. 1970, c. C-30. Please read the authorization forms which accompany this thesis.

**THIS DISSERTATION
HAS BEEN MICROFILMED
EXACTLY AS RECEIVED**

AVIS

La qualité de cette microfiche dépend grandement de la qualité de la thèse soumise au microfilmage. Nous avons tout fait pour assurer une qualité supérieure de reproduction.

S'il manque des pages, veuillez communiquer avec l'université qui a conféré le grade.

La qualité d'impression de certaines pages peut laisser à désirer, surtout si les pages originales ont été dactylographiées à l'aide d'un ruban usé ou si l'université nous a fait parvenir une photocopie de mauvaise qualité.

Les documents qui font déjà l'objet d'un droit d'auteur (articles de revue, examens publiés, etc.) ne sont pas microfilmés.

La reproduction, même partielle, de ce microfilm est soumise à la Loi canadienne sur le droit d'auteur, SRC 1970, c. C-30. Veuillez prendre connaissance des formules d'autorisation qui accompagnent cette thèse.

**LA THÈSE A ÉTÉ
MICROFILMÉE TELLE QUE
NOUS L'AVONS REÇUE**

PRETENSIONING OF
SINGLE-CROSSARM STAYED COLUMNS

by

Hisham Hussein Hafez

A Thesis
submitted to the Faculty of Graduate Studies
through the Department of
Civil Engineering in Partial Fulfillment
of the requirements for the Degree
of Master of Applied Science at
The University of Windsor

Windsor, Ontario, Canada

1977

© Hisham Hussein Hafez, 1977

058075

To My Family

ABSTRACT

PRETENSIONING OF SINGLE-CROSSARM STAYED COLUMNS

by

Hisham Hussein Hafez

The elastic buckling load of a concentrically loaded, pin-ended, slender metal column may be increased many times over its Euler load by reinforcing it with an assemblage of pretensioned stays and rigidly connected crossarm members. In this thesis, the effect of pretensioning the stays on the buckling load of single-crossarm stayed columns is presented. The optimum required pretension is derived. Also, the minimum effective pretension and the maximum possible pretension are developed. A geometrical study of the loaded column has been used to obtain these values.

The derived relationships were applied to numerical examples to demonstrate the influence of various stayed column parameters on the optimum and minimum effective pretension, and the maximum buckling load. The results indicate the significant change in the optimum pretension when the stay diameter, the stay modulus of elasticity and the crossarm member length are varied. The results also indicate the increase in the minimum effective pretension with the increase in either the stay diameter or the stay modulus of elasticity.

A series of tests were conducted on a single-crossarm stayed column model. The experimental results, obtained by varying the initial pretension, are compared with the predicted values. Both of the theoretical and experimental results indicate the great influence of the value of pretension, when below the optimum pretension, on the buckling load of the column.

ACKNOWLEDGEMENTS

The author wishes to express his sincere gratitude to his advisor, Dr. M. C. Temple, for his guidance, suggestions and continuous encouragement throughout the preparation of this thesis. The author records his special thanks to Dr. North for his valuable remarks regarding the experimental part.

Thanks are due to:

- the structural engineering staff members and friends for their valuable discussions.
- the technicians of the Civil Engineering laboratory for their assistance in the preparation of the model.
- the Computer Centre at the University of Windsor for running the computer programs.

The author is grateful to the financial support provided by the Defence Research Board through grant No. 1678-08.

TABLE OF CONTENTS

ABSTRACT	iv
ACKNOWLEDGEMENTS	vi
TABLE OF CONTENTS	vii
LIST OF ILLUSTRATIONS	ix
LIST OF ABBREVIATIONS	xiii
CHAPTER 1 INTRODUCTION	1
1.1 General	1
1.2 The Problem to Be Studied	2
1.3 Method and Scope of Work	2
CHAPTER 2 LITERATURE REVIEW	5
2.1 General	5
2.2 Pin-Connected Crossarm Stayed Columns	5
2.3 Rigidly Connected Crossarm Stayed Columns	6
CHAPTER 3 ANALYTICAL STUDY OF THE TENSION IN THE STAYS	10
3.1 General	10
3.2 Basic Assumptions	11
3.3 Buckling Load and Pretension Relationships	12
3.3.1 Definitions	12
3.3.2 Geometrical Analysis	13
CHAPTER 4 COMPUTER SOLUTION	26
4.1 General	26
4.2 Solution for the Maximum Buckling Load	27
4.3 Description of Computer Program	31
4.4 Limitations of Computer Program	33
CHAPTER 5 EFFECT OF STAYED COLUMN PARAMETERS	35
5.1 General	35
5.2 Numerical Example	35
5.3 Effect of Crossarm Member Length	36
5.4 Effect of Stay Diameter	40
5.5 Effect of Stay Modulus of Elasticity	44

CHAPTER 6	EXPERIMENTAL PROCEDURE AND RESULTS	49
6.1	General	49
6.2	Tested Column Properties	49
6.2.1	Geometric Properties	49
6.2.2	Material Properties	51
6.3	Experimental Equipment	51
6.4	Experimental Procedure	53
6.4.1	Equipment Preparation	53
6.4.2	Column Preparation	54
6.4.3	Column Testing	56
6.4.4	An Important Precaution	57
6.5	Experimental Results	59
CHAPTER 7	ANALYSIS OF EXPERIMENTAL RESULTS	60
7.1	General	60
7.2	Analytical Relationships between Buckling Load and Pretension for a Plane Single-Crossarm Stayed Column	60
7.3	Equivalent Stay Modulus of Elasticity	64
7.4	Comparison of Observed and Predicted Buckling Loads and Residual Tension in the Stays	66
7.4.1	Case of Initial Pretension Less than the Minimum Effective Pretension	66
7.4.2	Case of Initial Pretension between the Minimum Effective and Optimum Pretension	67
7.4.3	Case of Initial Pretension Greater than the Optimum Pretension	68
CHAPTER 8	CONCLUSIONS AND RECOMMENDATIONS	69
8.1	General	69
8.2	Conclusions	69
8.3	Future Research	72
ILLUSTRATIONS	73
APPENDIX I	LISTING OF COMPUTER PROGRAM	123
APPENDIX II	DEFLECTION OF A RING BEAM UNDER TENSION	129
BIBLIOGRAPHY	135
VITA AUCTORIS	136

LIST OF ILLUSTRATIONS

Figure		Page
1.1	Single-Crossarm Stayed Column	73
1.2	Double- and Triple-Crossarm Stayed Columns ..	74
2.1	Buckling Modes of Pin-Ended Single-Crossarm Stayed Column	75
3.1	Known Limits	76
3.2	Equilibrium Force Systems of Stayed Column (After Smith, McCaffrey, and Ellis)	77
3.3	Change in Length of Stays Due to Axial Deformation (After Smith, McCaffrey, and Ellis)	78
3.4	Initial Pretension versus Buckling Load	79
4.1	Beam Element for Two-Dimensional Structures .	80
4.2	Finite Elements and Assumed Possible Node Displacements for a Single-Crossarm Stayed Column	81
5.1	Effect of Crossarm Length for a Stay Diameter of 3/16 in. and Modulus of Elasticity of 9400 ksi	82
5.2	Effect of Crossarm Length for a Stay Diameter of 3/16 in. and Modulus of Elasticity of 19500 ksi	83
5.3	Effect of Crossarm Length for a Stay Diameter of 3/16 in. and Modulus of Elasticity of 29600 ksi	84
5.4	Effect of Crossarm Length for a Stay Diameter of 7/16 in. and Modulus of Elasticity of 9400 ksi	85
5.5	Effect of Crossarm Length for a Stay Diameter of 7/16 in. and Modulus of Elasticity of 19500 ksi	86

Figure	Page
5.6 Effect of Crossarm Length for a Stay Diameter of 7/16 in. and Modulus of Elasticity of 29600 ksi	87
5.7 Effect of Crossarm Length for a Stay Diameter of 7/8 in. and Various Values of Stay Modulus of Elasticity	88
5.8 Effect of Stay Diameter for a Ratio of l/l_{ca} of Ten and Stay Modulus of Elasticity of 9400 ksi	89
5.9 Effect of Stay Diameter for a Ratio of l/l_{ca} of Ten and Stay Modulus of Elasticity of 19500 ksi	90
5.10 Effect of Stay Diameter for a Ratio of l/l_{ca} of Ten and Stay Modulus of Elasticity of 29600 ksi	91
5.11 Effect of Stay Diameter for a Ratio of l/l_{ca} of Six and Stay Modulus of Elasticity of 9400 ksi	92
5.12 Effect of Stay Diameter for a Ratio of l/l_{ca} of Six and Stay Modulus of Elasticity of 19500 ksi	93
5.13 Effect of Stay Diameter for a Ratio of l/l_{ca} of Six and Stay Modulus of Elasticity of 29600 ksi	94
5.14 Effect of Stay Diameter for a Ratio of l/l_{ca} of One and Various Values of Stay Modulus of Elasticity	95
5.15 Effect of Stay Modulus of Elasticity for a Ratio of l/l_{ca} of Ten and Stay Diameter of 3/16 in.	96
5.16 Effect of Stay Modulus of Elasticity for a Ratio of l/l_{ca} of Ten and Stay Diameter of 7/16 in.	97
5.17 Effect of Stay Modulus of Elasticity for a Ratio of l/l_{ca} of Ten and Stay Diameter of 7/8 in.	98
5.18 Effect of Stay Modulus of Elasticity for a Ratio of l/l_{ca} of Six and Stay Diameter of 3/16 in.	99

Figure		Page
5.19	Effect of Stay Modulus of Elasticity for a Ratio of l/l_{ca} of Six and Stay Diameter of 7/16 in.	100
5.20	* Effect of Stay Modulus of Elasticity for a Ratio of l/l_{ca} of Six and Stay Diameter of 7/8 in.	101
5.21	Effect of Stay Modulus of Elasticity for a Ratio of l/l_{ca} of One and Various Values of Stay Diameter	102
6.1	Plane Single-Crossarm Stayed Column	103
6.2	Ring Beam Load Cell	104
6.3	Universal Flat Load Cell	105
6.4	Hydraulic Jack	106
6.5	Strain Indicators	107
6.6	Column Base	107
6.7	Positions of Strain Gages on the Stayed Column	108
6.8	Top Plate of the Column	109
6.9	Lateral Support of the Column	110
6.10	Load versus Deflection and Tension in the Stays for an Initial Pretension of 20 lbs ...	111
6.11	Load versus Deflection and Tension in the Stays for an Initial Pretension of 37 lbs ...	112
6.12	Load versus Deflection and Tension in the Stays for an Initial Pretension of 80 lbs ...	113
6.13	Load versus Deflection and Tension in the Stays for an Initial Pretension of 100 lbs ..	114
6.14	Load versus Deflection and Tension in the Stays for an Initial Pretension of 150 lbs ..	115
6.15	Load versus Deflection and Tension in the Stays for an Initial Pretension of 175 lbs ..	116
6.16	Load versus Deflection and Tension in the Stays for an Initial Pretension of 200 lbs ..	117

Figure	Page
6.17	Load versus Deflection and Tension in the Stays for an Initial Pretension of 240 lbs .. 118
6.18	Load versus Deflection and Tension in the Stays for an Initial Pretension of 280 lbs .. 119
6.19	Load versus Deflection and Tension in the Stays for an Initial Pretension of 400 lbs .. 120
6.20	Load versus Deflection and Tension in the Stays for an Initial Pretension of 500 lbs .. 121
6.21	Comparison between Theoretical and Experimental Buckling Loads and Residual Pretension 122
A.1	Ring Beam Subjected to Tension Force along One of its Diameters 134
A.2	Quadrant of the Ring Beam and Differential Element to Be Studied 134

LIST OF ABBREVIATIONS

English Alphabet

A	= cross-sectional area
A_b	= cross-sectional area of ring beam
A_c	= cross-sectional area of column
A_{ca}	= cross-sectional area of crossarm member
A_r	= cross-sectional area of rod
A_s	= cross-sectional area of stay
C_1, C_2	= constants of proportionality for a space single-crossarm stayed column, see Eqs. 3.20 and 3.27
C_3	= constant of proportionality for a space or plane single-crossarm stayed column, see Eq. 3.33
C_1, C_2'	= constants of proportionality for a plane single-crossarm stayed column, see Eqs 7.11 and 7.15
c	= distance from the centroidal axis
D_o	= outer diameter of column
D_s	= diameter of stay
E	= modulus of elasticity
E_b	= modulus of elasticity of ring beam material
E_c	= modulus of elasticity of column material
E_{ca}	= modulus of elasticity of crossarm member material
E_e	= equivalent stay modulus of elasticity
E_r	= modulus of elasticity of rod material
E_s	= modulus of elasticity of stay material

F_f	= final compressive force on crossarm member, see Eq. 3.6
F_i	= initial compressive force on crossarm member, see Eq. 3.3
$\{F\}$	= vector of loads at the nodes
G_b	= modulus of rigidity of ring beam material
I	= moment of inertia of cross-sectional area
I_b	= moment of inertia of ring beam
I_c	= moment of inertia of column
$[I]$	= unit matrix
K_c	= axial stiffness of column, see Eq. 3.9
K_{ca}	= axial stiffness of crossarm member, see Eq. 3.12
K_s	= stiffness of stay, see Eq. 3.15
$[K]$	= master stiffness matrix
$[K_E]$	= master elastic stiffness matrix
$[K_G]$	= master geometric stiffness matrix
$[K_G^*]$	= master geometric stiffness matrix for unit load
$[\tilde{k}_E]$	= elastic stiffness matrix for beam column element in local coordinate system
$[\tilde{k}_G]$	= geometric stiffness matrix for beam column element in local coordinate system
L	= length of column
L_1	= length of beam column element
l	= length of column between support points, see Fig. 1.1
l_{ca}	= length of crossarm member
l_r	= actual length of rods used in one stay
l_s	= length of stay
l_t	= theoretical length of stay calculated in

	computer program
M	= bending moment
M_A	= internal bending moment at end of ring beam quadrant, see Fig. A.2 and Eq. A.13
N	= normal force
n_1	= number of stays connected to column end
n_2	= number of stays connected to end of crossarm member
P	= axial load in column
P^*	= unit load
P_a	= external applied axial load on column
P_{cr}	= buckling load of stayed column
P_E	= Euler load, see Eq. 3.28
P_f	= final axial force on column
P_i	= initial axial force on column
P_{in}	= initial loading at which geometric stiffness matrix is calculated
P_{max}	= maximum theoretical buckling load of stayed column
P_{min}	= buckling load corresponding to minimum effective pretension
R	= mean radius of ring beam
R_{cs}	= rate of change of slope of elastic curve
S	= actual stiffness of stay used in tested column
T	= tension force in ring beam, see Fig. A.1
T_f	= final tension in stay
T_i	= initial pretension force in stay
T_{max}	= maximum possible pretension
T_{min}	= minimum effective pretension

T_{opt}	= optimum pretension
T_r	= residual pretension
T_1, T_2	= tension in stays on convex side of column
T_3, T_4	= tension in stays on concave side of column
U	= total strain energy in ring beam
u_1, u_2	= element nodal displacements in x direction
V	= shearing force
v_1, v_2	= element nodal displacements in y direction
X, Y	= global coordinate axes
x, y	= local coordinate axes

Greek Letters

α	= angle between stays and column, see Fig. 1.1
γ	= $1/\lambda$
Δ_a	= maximum allowable deflection of column at crossarm level, see Eq. 6.3
Δ_c	= shortening of column due to applied load
Δ_{ca}	= elongation of crossarm member due to applied load
$\Delta d\theta$	= change in the angle $d\theta$ between two normal sections, a differential distance apart, in ring beam quadrant, see Fig. A.2
ΔL_i	= shortening of column due to pretensioning
Δl_{ca}	= shortening of crossarm member due to pretensioning
Δ_r	= elongation of actual length of rods used in one stay
Δ_s	= shortening in length of stay due to applied load
$\{\Delta\}$	= vector of nodal displacements
δ_b	= deflection of ring beam, see Eq. 7.17



- δ_c = experimental deflection of column at crossarm level
- θ = angle of inclination of section under consideration in ring beam quadrant, see Fig. A.2
- θ_1, θ_2 = element rotational displacements at nodes
- λ = eigenvalue
- σ = fiber stress
- σ_y = yield stress of column material

CHAPTER 1

INTRODUCTION

1.1 General

A stayed column is a slender metal column reinforced with an assemblage of pretensioned stays and rigidly connected crossarm members. This assemblage causes the increase of the elastic buckling load of the column many times by introducing restraint against translation and rotation at the levels of the crossarms. Stayed columns are classified as single-, double-, and triple-crossarm stayed columns according to the number of sets of crossarm members distributed along its length. These columns can be used as supports to hold plates in place during erection of large plate structures, as side booms for the mast of a derrick, as masts for ships, etc.

A single-crossarm stayed column is shown in Fig. 1.1. The crossarms are arranged in a cruciform manner. Because of symmetry, the column can be considered as a two-dimensional structure, and buckling will occur in one plane, a plane containing one of the crossarms. Possible arrangements for double- and triple-crossarm stayed columns are shown in Fig. 1.2. Stayed columns with more than three crossarms are also possible.

1.2 The Problem to Be Studied

In the last five years, research and published papers dealing with stayed columns were mainly concerned with the value of the maximum buckling load. Two analytical methods to determine this load were developed. The first used a differential calculus approach to predict the buckling load for single-crossarm stayed columns. The second method was more general and used a finite element method to solve the buckling problem of any stayed column.

In all the previous studies, it was assumed that a small amount of tension existed in the stays just prior to buckling. The required initial pretension was not computed. Only a few experiments have been performed to date, and they indicate that the critical load is significantly affected by the variation of the initial pretension in the stays. But no relationship has been derived to predict analytically its influence.

The purpose of this research is to get the complete relationship between the initial pretension of a single-crossarm stayed column and the corresponding buckling load. The theoretical derivation is verified experimentally.

1.3 Method and Scope of Work

The stays should be pretensioned to remain effective during the application of the load. If not pretensioned, they would become slack and ineffective. The nature of the problem implies the use of a geometric approach to derive

the relationship between the initial pretension and the corresponding buckling load. A relationship between the increment of applied load and the corresponding change in tension in the stays was developed.

First, the work done in the field of stayed columns has been discussed, and the conclusions drawn by each research worker has been presented. This is important since the optimum pretension depends on the maximum value of the buckling load derived previously.

Then, the theoretical study of the loaded column followed, leading to:

- 1) The optimum pretension required to give the maximum critical load,
- 2) The minimum effective pretension over which the buckling load of the column begins to increase above the Euler load, and
- 3) The residual tension in the stays at the instant of buckling in case of an initial pretension larger than the optimum pretension.

The maximum possible pretension, which is defined as the pretension causing buckling without any external applied load, was derived to complete the principal points on an initial pretension-buckling load curve.

A computer program was developed to predict these values and the corresponding buckling loads for either a real column with four crossarm members or a model column with

two crossarms only. A model column is shown in Fig. 6.1.

Numerical examples were solved, using the computer program, to study the influence of some stayed column parameters on the optimum and minimum effective pretension, and buckling load.

Finally, the experimental work began. A series of tests were performed on one model column. The pretension in the stays was varied and the corresponding buckling loads were obtained. The theoretical and experimental values were compared. Reasonable agreement was obtained.

CHAPTER 2

LITERATURE REVIEW

2.1 General

Previous research in the field of stayed columns may be divided into two parts. Each part deals with a different type of column. First attempts were concerned with pin-ended columns with tension ties and hinged crossarms. After discovering the effect of welding the crossarms to the column on the increase of the buckling strength of the column, the research work began to deal with rigidly connected crossarm members to pin-ended columns. The two parts are discussed below with special emphasis on the conclusions drawn by each research worker.

2.2 Pin-Connected Crossarm Stayed Columns

Two papers studying this preliminary type of stayed column were published. In 1963, Chu and Berge^{(1)*} analysed a slender pin-ended column stayed with tension ties arranged in equilateral rosettes around the column and bearing on several intermediate points along the column through hogging frames. The connections between the

* Numbers in parenthesis refer to cited references in the Bibliography.

hogging frames and the column, and between the ties and the frame were assumed to be ideal hinges. They developed a general solution for the elastic buckling load of the column which indicated that the maximum possible buckling load would be a four-fold strength increase over the Euler column. Any increase in the number of symmetrically placed intermediate frames did not affect the strength increase. To verify the analytical solution, model stayed columns were tested, and the test results were found to agree satisfactorily with the predicted strength increase.

Then, in 1967, Mauch and Felton⁽²⁾ continued the work of Chu and Berge by developing an analytical foundation for the rational design of their columns, such as exists for simple columns. To incorporate principles of dimensional similarity, the structural index (P/L^3) has been used, in which P is the compression load and L is the column length. This index may be considered as a measure of loading intensity. Their analysis indicated that at low values of the structural index, columns supported by tension ties offer potential savings of up to 50% of the weight of optimum simple tubular columns. That is because at low values of the structural index, the optimum stress for simple tubular columns is well below the elastic limit of most structural materials.

2.3 Rigidly Connected Crossarm Stayed Columns

In 1970, a set of design-build-test projects⁽³⁾,

assigned to the final year Civil Engineering undergraduates at the Royal Military College of Canada, included the construction and testing of a pin-ended single-crossarm stayed column. The crossarms, instead of being pin-connected to the column as in Chu and Berge's study, were welded to the compression core. The test result was a seven-fold increase in the buckling strength of the column, compared to Chu and Berge's maximum of a four-fold increase. This increase is due to the fact that the crossarm members were firmly fixed to the column, which provided restraint against rotation in addition to the translational restraint existing in Chu and Berge's column.

In 1971, Pearson⁽⁴⁾ examined the behaviour of a pin-ended single-crossarm stayed column with a high slenderness ratio when loaded to its buckling point. This study included experiments in which the stay pretension forces and the stay slopes were varied. The buckling load was affected significantly by both variations in the magnitude of the initial stay tension and changes in the crossarm member length. No relationships were derived to predict analytically the influence of these parameters.

In 1972, another experimental study on a single-crossarm stayed column was carried out by Clarke⁽⁵⁾. The results verified the conclusions made by Pearson. At the same time, some experiments were performed on pin-ended triple-crossarm stayed columns at the Royal Military College of Canada by McCaffrey. Test results obtained

indicated strength increases—ranging from 34 to 45 times that of the Euler buckling load of the unstayed column.

The first analytical study of the rigidly connected crossarm stayed columns appeared in January 1975. Smith, McCaffrey and Ellis⁽⁶⁾ published a paper in which they developed buckling solutions for determining the critical buckling load associated with each of two modes of failure for a pin-ended single-crossarm stayed column. The influence of various stayed column parameters on its buckling behaviour and strength was also demonstrated. A differential calculus approach was adopted to derive the theoretical solutions by assuming the buckled shapes to be of single and double curvature.

In the same year, Khosla⁽⁷⁾ developed the second analytical method based on a finite element approach for determining the buckling loads of stayed columns. This method is extremely flexible and can be applied to any stayed column to get both the critical load and the buckled shape. An alternate approach by Temple⁽⁸⁾ employing stability functions was used to check the finite element procedure.

By using the analytical solutions described above, the problem of determining the maximum buckling load and the corresponding buckled shapes for symmetrical stayed columns was solved. The two analytical studies showed that for a single-crossarm stayed column, two buckling modes or

types of instability are possible. These are represented by a type of triple curvature (symmetrical) and a double curvature (antisymmetrical). These deflected shapes of the column are shown in Fig. 2.1 as Mode I and Mode II respectively.

The study made in this thesis will try, in addition to deriving the relationship between the initial pretension and the corresponding buckling load, to find the analytical basis for the experiments performed by Pearson and verified by Clarke. The influence of the variation of the initial pretension and changes in the crossarm length on the buckling load of a single-crossarm stayed column will be analysed. In addition to this; the influence of changing the stay diameter and modulus of elasticity on both the optimum and minimum effective pretension and the maximum buckling load will be discussed analytically. The maximum buckling load derived by the finite element method will be the basis for the optimum initial pretension required.

CHAPTER 3

ANALYTICAL STUDY OF THE TENSION IN THE STAYS

3.1 General

For stayed columns, the purpose of pretension in the stays is to exert, through the crossarms, certain forces on the column. These forces are the horizontal components of the tension in the stays. Due to symmetry in shape of the stayed column, which implies a symmetry in the pretension, these horizontal forces on the column are in equilibrium and have no direct effect on a vertically applied load until this load reaches the Euler buckling load of the column. At this instant, these horizontal forces will prevent the column from buckling since they constitute a kind of restraint against translation and rotation. By increasing the load, the tension in the stays decreases as will be shown in the next section. At a critical load, which is many times the Euler load, either the tension in the stays becomes zero or they become unable to resist the buckling as will be explained in this chapter. A state of unstable equilibrium is created and the column buckles. In case of a single-crossarm stayed column, if the column has a relatively short crossarm and small stay diameter, the rotational restraint will be high compared to the translational restraint and the column will buckle in a

triple curvature mode, i.e. Mode I buckling. If, on the contrary, the crossarms are relatively long and the stay diameter relatively large, the translational restraint will be larger and the column will buckle according to Mode II, i.e. with a double curvature deflection. Thus, the initial pretension should be large enough to remain effective until the applied load reaches its maximum possible value. At the same time, the pretension should not be too large since the tension in the stays has vertical components which, in addition to the applied load, are parts of the total load tending to cause buckling.

3.2 Basic Assumptions

The following assumptions are made during this analytical study of the tension in the stays:

- 1) The single-crossarm stayed column to be studied is completely symmetrical and ideally concentrically loaded. This means that there is no initial eccentricity or crookedness.
- 2) The connections between the crossarm members and the column are assumed perfectly rigid. The connections between the stays and the column and between the stays and the crossarm members are assumed to be ideal hinges.
- 3) Buckling occurs in one of the two planes containing the stays and the crossarms. In this case, only two stays resist the buckling while in any other case, four stays will resist the buckling.

4) The maximum possible buckling load of the stayed column is assumed to be the load obtained by the finite element method⁽⁷⁾.

5) The axial deformation of the crossarms and of the column have been neglected when deriving the maximum buckling load, but they were taken into consideration when studying the tension in the stays.

3.3 Buckling Load and Pretension Relationships

3.3.1 Definitions

1) Minimum effective pretension: It is the minimum initial pretension of the stays which remains effective until the Euler load has been reached. This means that the pretension in the stays is lost at an applied load less than or equal to the Euler load. At a larger load, the stays become slack and the column buckles since it is no longer reinforced by the set of stays and crossarms. There is no advantage in using stayed columns if the pretension is equal to or less than the minimum effective pretension.

2) Optimum pretension: It is the initial pretension of the stays which disappears completely just after the load of the column reaches its maximum buckling value. This means that the stays remain effective until the maximum critical load of the column has been applied. In the previous work^{(6),(7),(8)}, the pretension was assumed to be optimum. Thus the stayed column was assumed to buckle only

at the highest possible value of the applied load. Theoretically, the optimum pretension is the best value for pretensioning the stays.

3) Maximum possible pretension: It is the initial pretension of the stays which gives vertical components at the ends of the column large enough to cause buckling without any additional applied load. Buckling occurs inspite of the large horizontal components of the tension in the stays which prevent the horizontal translation of the middle of the column. The maximum possible pretension has no practical importance. Its value is required theoretically only, since it is the maximum limit for the pretension and it gives the last point of the buckling load versus pretension curve.

4) Residual pretension: When the initial pretension of the stays is larger than the optimum pretension, the tension in the stays does not go to zero at the instant of buckling as will be shown in the next section. In this case, the residual pretension is the value of the tension remaining in the stays.

3.3.2 Geometrical Analysis*

Only the position of one point and the locus of a second point were known in the relationship between the initial pretension in the stays and the associated buckling

* The first part of this section is similar to that in reference (6).

load of the stayed column. This is illustrated in Fig. 3.1. With zero pretension in the stays, the buckling load is nothing more than the Euler load. It was also known that there is a maximum value for the buckling load which could not be increased whether by increasing or by decreasing the initial pretension.

To derive the relationship between these two limits, consider a pin-ended single-crossarm stayed column with the geometrical properties shown in Fig. 1.1. Let T_i be the initial pretension force in the stays, and α the angle between the stays and the column. If there is no external applied load to the column, then, from the equilibrium of forces in the vertical direction [see Fig. 3.2 (a)], the initial axial force on the column, P_i , induced by the stay pretension, T_i , is:

$$P_i = n_1 T_i \cos \alpha \quad (3.1)$$

in which n_1 = the number of stays connected to the column end. For the cruciform crossarm configuration of the stayed column shown in Fig. 1.1, $n_1 = 4$.

Due to the axial force on the column induced by the pretension, the initial shortening of the column may be expressed as:

$$\Delta L_i = \frac{4T_i L \cos \alpha}{A_c E_c} \quad (3.2)$$

in which A_c = the cross-sectional area of the column, E_c = the modulus of elasticity of the column, and L = the total length of the column.

From the equilibrium of forces in the lateral direction [see Fig. 3.2 (c)], the initial compressive force on the crossarm member, F_i , induced by the initial tension in the stays, T_i , is:

$$F_i = n_2 T_i \sin \alpha \quad (3.3)$$

in which n_2 = the number of stays connected to the end of the crossarm member. For the single-crossarm stayed column $n_2 = 2$.

Due to the compressive force in the crossarm member induced by the initial pretension, the initial shortening of the crossarm member may be written as:

$$\Delta l_{ca} = \frac{2T_i l_{ca} \sin \alpha}{A_{ca} E_{ca}} \quad (3.4)$$

in which l_{ca} = the length of the crossarm member (Fig. 1.1), A_{ca} = the cross-sectional area of the crossarm member, and E_{ca} = the modulus of elasticity of the crossarm member.

Let an axial external load, P_a , be applied to the column. This causes the pretension force in the stays to decrease. The result is a final axial force on the column, P_f , [Fig. 3.2 (b)]. Its magnitude is given by:

$$P_f = P_a + 4T_f \cos \alpha \quad (3.5)$$

in which T_f = the tension in the stays after applying the external load.

In addition, the compressive force on the crossarm member decreases. By considering the equilibrium of forces shown in Fig. 3.2 (d), the final force on the crossarm member, F_f , is given by:

$$F_f = 2T_f \sin \alpha \quad (3.6)$$

Then, as shown in Fig. 3.3, the shortening of the column, Δ_c , from the case of initial axial force, P_i , to the case of final axial force, P_f , can be expressed as:

$$\Delta_c = \frac{L(P_f - P_i)}{A_c E_c} \quad (3.7)$$

By substituting the values of P_f and P_i from Eq. 3.5 and Eq. 3.1, Eq. 3.7 becomes:

$$\Delta_c = \frac{[P_a - 4(T_i - T_f) \cos \alpha]}{K_c} \quad (3.8)$$

in which K_c is the axial stiffness of the column and is given by:

$$K_c = \frac{A_c E_c}{L} \quad (3.9)$$

The magnitude of the elongation of each crossarm member, due to the decrease in its compressive force, is

given by:

$$\Delta_{ca} = \frac{(F_i - F_f)l_{ca}}{A_{ca}E_{ca}} \quad (3.10)$$

Substituting for F_i from Eq. 3.3 and F_f from Eq. 3.6, Eq. 3.10 yields:

$$\Delta_{ca} = \frac{2(T_i - T_f)\sin\alpha}{K_{ca}} \quad (3.11)$$

in which K_{ca} is the axial stiffness of the crossarm member and is given by:

$$K_{ca} = \frac{A_{ca}E_{ca}}{l_{ca}} \quad (3.12)$$

The shortening in the stay length due to the decrease of the tension force in the stays can be expressed as:

$$\Delta_s = \frac{(T_i - T_f)l_s}{A_s E_s} \quad (3.13)$$

in which l_s = the length of the stay (Fig. 1.1), A_s = the cross-sectional area of the stay, and E_s = the modulus of elasticity of the stay.

Eq. 3.13 may be written as:

$$\Delta_s = \frac{T_i - T_f}{K_s} \quad (3.14)$$

in which K_s is the stiffness of the stay given by:

$$K_s = \frac{A_s E_s}{l_s} \quad (3.15)$$

For small deformations, the change in the length of the stay after applying the external load, P_a , is related to the change in the length of the column and to that of the crossarm (Fig. 3.3) by:

$$\Delta_s = \frac{1}{2} \Delta_c \cos \alpha - \Delta_{ca} \sin \alpha \quad (3.16)$$

Substituting for Δ_s from Eq. 3.14, for Δ_c from Eq. 3.8, and for Δ_{ca} from Eq. 3.11 into Eq. 3.16 yields:

$$\frac{T_i - T_f}{K_s} = \frac{[P_a - 4(T_i - T_f) \cos \alpha] \cos \alpha}{2 K_c} - \frac{[2(T_i - T_f) \sin \alpha] \sin \alpha}{K_{ca}} \quad (3.17)$$

Solving Eq. 3.17, the tension force decrease can be expressed in terms of the applied load, P_a , as:

$$T_i - T_f = \frac{P_a \cos \alpha}{2 K_c \left[\frac{1}{K_s} + \frac{2 \sin^2 \alpha}{K_{ca}} + \frac{2 \cos^2 \alpha}{K_c} \right]} \quad (3.18)$$

Since α , K_c , K_s , and K_{ca} are constants for a given single-crossarm stayed column, Eq. 3.18 may be written as:

$$T_i - T_f = P_a C_1 \quad (3.19)$$

$$\text{in which } C_1 = \frac{\cos \alpha}{2 K_c \left[\frac{1}{K_s} + \frac{2 \sin^2 \alpha}{K_{ca}} + \frac{2 \cos^2 \alpha}{K_c} \right]} \quad (3.20)$$

Eq. 3.19 indicates that there is a linear relation between the applied load and the corresponding change in the tension forces in the stays.

The shortening of the column, Δ_c , can be written in terms of the final axial load of the column, P_f , and the initial tension in the stays, T_i , by combining Eq. 3.5 and Eq. 3.8 as follows:

$$\Delta_c = \frac{P_f - 4T_i \cos \alpha}{K_c} \quad (3.21)$$

By substituting for Δ_s from Eq. 3.14, for Δ_c from Eq. 3.21, and for Δ_{ca} from Eq. 3.11, Eq. 3.16 becomes:

$$\frac{T_i - T_f}{K_s} = \frac{[P_f - 4T_i \cos \alpha] \cos \alpha}{2 K_c} - \frac{[2(T_i - T_f) \sin \alpha] \sin \alpha}{K_{ca}} \quad (3.22)$$

Solving Eq. 3.22, the final tension in the stays may be expressed as:

$$T_f = T_i + \frac{(P_f - 4T_i \cos \alpha) \cos \alpha}{2K_c \left(\frac{1}{K_s} + \frac{2\sin^2 \alpha}{K_{ca}} \right)} \quad (3.23)$$

Substituting for T_f from Eq. 3.23 into Eq. 3.5 yields:

$$P_f = P_a + 4 \left[T_i - \frac{(P_f - 4T_i \cos \alpha) \cos \alpha}{2K_c \left(\frac{1}{K_s} + \frac{2\sin^2 \alpha}{K_{ca}} \right)} \right] \cos \alpha \quad (3.24)$$

Solving Eq. 3.24, the applied load, P_a , can be expressed in terms of the initial tension in the stays, T_i , and the final axial load on the column, P_f , as follows:

$$P_a = (P_f - 4T_i \cos \alpha) \left[1 + \frac{2\cos^2 \alpha}{K_c \left(\frac{1}{K_s} + \frac{2\sin^2 \alpha}{K_{ca}} \right)} \right] \quad (3.25)$$

Eq. 3.25 can be simply written in terms of one constant, C_2 , as:

$$P_a = (P_f - 4T_i \cos \alpha) C_2 \quad (3.26)$$

in which $C_2 = 1 + \frac{2\cos^2 \alpha}{K_c \left(\frac{1}{K_s} + \frac{2\sin^2 \alpha}{K_{ca}} \right)}$ (3.27)

The relationship between the initial pretension in the stays and the corresponding buckling load of the single-crossarm stayed column may be divided into three zones:

- 1) A zone associated with an initial pretension smaller than the minimum effective pretension,
- 2) A zone associated with an initial pretension between the minimum effective pretension and the optimum pretension, and
- 3) A zone associated with an initial pretension larger than the optimum pretension.

In the first zone, the initial pretension is so small that it disappears completely when a load is applied that is less than or equal to the Euler load. At the instant the tension in the stays vanishes, the stays become ineffective and the column behaves as an unstayed column. This means that by increasing the load, the column buckles at the Euler load since there is no residual tension in the stays to prevent the column from buckling. This is true for any initial pretension less than the minimum effective pretension. This minimum effective pretension can be calculated from Eq. 3.19. The final tension in the stays, T_f , is zero, while the applied load, P_a , is the Euler load given by:

$$P_E = \frac{\pi^2 EI}{L^2} \quad (3.28)$$

Using the above substitutions, the minimum effective pretension, T_{\min} , can be expressed as:

$$T_{\min} = \frac{\pi^2 E_c I_c C_1}{L^2} \quad (3.29)$$

in which I_c = the moment of inertia of the cross-section of the column, and C_1 = a constant for the stayed column which depends on the geometric properties and materials of the column and is given by Eq. 3.20.

The first zone appears in Fig. 3.4 as a horizontal line, with the Euler load as the buckling load, between zero pretension and the minimum effective pretension.

For the second zone, the pretension is equal to or smaller than the optimum pretension and larger than the minimum effective pretension. In other words, the initial pretension decreases by applying a load on the column, but will not vanish when the Euler load is reached. It will remain effective until reaching a higher load equal to or smaller than the maximum buckling load of the stayed column. This leads to the following criteria used to determine the buckling load corresponding to a given pretension lying in the second zone: the buckling occurs at the load which causes the tension in the stays to vanish. At this instant there is no lateral or rotational restraint to prevent the column from buckling.

Thus, the buckling load can be obtained from Eq. 3.19 expressing the relation between the applied load, P_a , and the corresponding change in the tension in the stays. When the final tension, T_f , goes to zero, the applied load represents the buckling load. Consequently, the governing equation for the buckling load in the second zone can be expressed as:

$$P_{cr} = \frac{T_i}{C_1} \quad (3.30)$$

in which P_{cr} = the buckling load of the stayed column, and C_1 = the constant given by Eq. 3.20.

It is clear from Eq. 3.30 that the relation between the initial pretension and the buckling load is still linear when the pretension lies between the minimum effective pretension and the optimum pretension. Eq. 3.30 can be used to calculate the optimum pretension. When the buckling load, P_{cr} , in Eq. 3.30 reaches its maximum value, the initial pretension, T_i , will be the optimum pretension. Knowing the maximum buckling load from the finite element method⁽⁷⁾, the optimum pretension may be written as:

$$T_{opt} = C_1 P_{max} \quad (3.31)$$

in which T_{opt} = the optimum pretension, P_{max} = the maximum buckling load of the stayed column, and C_1 = the previous constant of proportionality.

The second zone is shown in Fig. 3.4. It consists of a straight line in which the buckling load increases with the increase of the initial pretension until the optimum pretension corresponding to the maximum buckling load.

In the third zone, the initial pretension is greater than the optimum pretension. In this case, the final tension force in the stays, T_f , has a non-zero value. But

this value can not resist the bifurcation of the column if the final load on the column, P_f , reaches its maximum value. The final load is the sum of the applied load and vertical components of the final tension in the stays at the end of the column and is given by Eq. 3.5. Its maximum value is the maximum buckling load of the stayed column, P_{max} .

To compute the residual tension at the instant of buckling, Eq. 3.23 is used and yields:

$$T_r = T_i - (P_{max} - 4T_i \cos \alpha) C_3 \quad (3.32)$$

in which T_r = the residual tension at the instant of buckling, and C_3 = a constant depending on the material properties and geometry of the single-crossarm stayed column, and is given by:

$$C_3 = \frac{\cos \alpha}{2 K_c \left(\frac{1}{K_s} + \frac{2 \sin^2 \alpha}{K_{ca}} \right)} \quad (3.33)$$

The residual tension in the stays represents a part of the load, which in addition to the actual applied load contributes to the buckling load. This means that the larger the initial pretension, the larger the residual tension, and the smaller the applied load. The initial pretension may be large enough to cause buckling by itself without any applied load at all. This is the maximum possible pretension.

The buckling load for the third zone can be

calculated by using Eq. 3.26 which relates the applied load to the final axial load on the column. The applied load will correspond to the buckling load of the column if the final axial load is taken as the maximum buckling load. The governing equation for the buckling load in the third zone can be written as:

$$P_{cr} = (P_{max} - 4T_i \cos \alpha) C_2 \quad (3.34)$$

in which C_2 = a constant which depends on the properties of the materials of the stayed column and its geometry. It is given by Eq. 3.27.

The third zone is shown in Fig. 3.4 as a linear relation in which the buckling load decreases with the increase of the initial pretension. The third zone ends at the maximum possible pretension since a larger pretension means that the stayed column has already buckled. The maximum possible pretension can be calculated from Eq. 3.34 by equating the right hand side to zero yielding:

$$T_{max} = \frac{P_{max}}{4 \cos \alpha} \quad (3.35)$$

The complete effect of the initial pretension on the buckling load of the single-crossarm stayed column is shown in Fig. 3.4, as well as the residual pretension at the instant of buckling.

CHAPTER 4
COMPUTER SOLUTION

4.1 General

A computer program is necessary to solve for the pretension values of a single-crossarm stayed column. The value of the optimum pretension depends on the value of the maximum buckling load of the column which could be obtained by a finite element method that takes advantage of the computer's capability. A computer program has been developed to solve for the effect of the initial pretension on the buckling load of a single-crossarm stayed column. The computer program requires a minimum of data while the output describes completely the analytical relationship between the pretension and the buckling load. The only data required are the length, inner and outer diameter, modulus of elasticity of the column and crossarm, the stay diameter and its modulus of elasticity. The output includes the minimum effective pretension and the corresponding buckling load (i.e. the Euler load), the optimum pretension and the corresponding maximum buckling load, and the maximum possible pretension which corresponds to a zero applied buckling load. The information contained in the output is enough to draw the complete curve describing the relationship between the initial pretension and the buckling load of

the stayed column. It is a simple matter of joining the three points from the output with straight lines as explained in Chapter 3 (see Fig. 3.4). The output also includes the buckling load corresponding to a given initial pretension and the residual pretension at the instant of buckling. The last information in the output is the buckling shape of the stayed column.

The program also includes modifications for the case of a plane single-crossarm stayed column with two crossarms and four stays set in one plane, the plane of buckling, the column being prevented from buckling in any other plane. These modifications were needed for the model column used in the experimental portion of this research as explained in Chapter 6.

4.2 Solution for the Maximum Buckling Load*

The finite element method is used to solve the stability problem of the single-crossarm stayed column. The structure is divided into a number of substructures or finite elements. The elements are assumed to be interconnected at a discrete number of nodal points. The potential energy of each element is written in terms of the displacements of the nodal points. The minimization of the total potential energy of the structure will always result in a stiffness relationship given by

* For more information and details see reference 7.

$$[K]\{\Delta\} = \{F\} \quad (4.1)$$

in which $[K]$ = the stiffness matrix of the complete structure, $\{\Delta\}$ = the vector of nodal displacements, and $\{F\}$ = the vector of loads at the nodes.

Because of the presence of large deflections encountered in the buckling problem, strain-displacement equations contain nonlinear terms which must be included in calculating the stiffness matrix. Including the appropriate nonlinear terms in the strain-displacement relations results in a stiffness matrix $[K]$ comprised of two components. That is,

$$[K] = [K_E] + [K_G] \quad (4.2)$$

in which $[K_E]$ = the conventional elastic stiffness matrix, and $[K_G]$ = the geometric stiffness matrix.

For the typical beam column element and end displacements shown in Fig. 4.1, the elastic stiffness matrix in the local coordinate system is given by

$$[k_E] = \begin{bmatrix} u_1 & v_1 & \theta_1 & u_2 & v_2 & \theta_2 \\ EA/L_1 & & & & & \text{SYM} \\ 0 & 12EI/L_1^3 & & & & \\ 0 & 6EI/L_1^2 & 4EI/L_1 & & & \\ -EA/L_1 & 0 & 0 & EA/L_1 & & \\ 0 & -12EI/L_1^3 & -6EI/L_1^2 & 0 & 12EI/L_1^3 & \\ 0 & 6EI/L_1^2 & 2EI/L_1 & 0 & -6EI/L_1^2 & 4EI/L_1 \end{bmatrix} \quad (4.3)$$

in which E = the modulus of elasticity of the element, A = the cross-sectional area of the element, I = its moment of inertia, and L_1 = the length of the element.

The geometric stiffness matrix of the beam column element in the local coordinate system is given by

$$[\tilde{k}_G] = P_{in} \begin{bmatrix} 0 & & & & & & \\ 0 & 6/5L_1 & & & & & \\ 0 & 1/10 & 2L_1/15 & & & & \\ 0 & 0 & 0 & 0 & & & \\ 0 & -6/5L_1 & -1/10 & 0 & 6/5L_1 & & \\ 0 & 1/10 & -L_1/30 & 0 & -1/10 & 2L_1/15 & \end{bmatrix} \quad (4.4)$$

in which P_{in} = the initial loading at which the geometric stiffness matrix is calculated.

The elastic stiffness matrix is independent of load level. The geometric stiffness matrix depends not only on the geometry but also on the initial internal force existing in the member at the start of the loading step. This matrix represents the effect of the axial load on the flexural stiffness.

As a second step in determining the buckling load, after dividing the structure into the suitable number of elements, the elastic and geometric stiffness matrices are calculated for each element of the stayed column. Then, the master elastic and the master geometric stiffness matrices are assembled for the possible nodal displacements.

The axial load in the column can be expressed as

$$P = \lambda P^* \quad (4.5)$$

in which λ is a constant and P^* represents the relative magnitude of the applied loads which can be conveniently taken as unity. Also, the geometric stiffness matrix which is proportional to the internal forces at the start of the loading step, may be written as

$$[K_G] = \lambda [K_G^*] \quad (4.6)$$

in which $[K_G^*]$ = the geometric stiffness matrix for a unit value of the applied forces. Hence, Eq. 4.1 can be written as

$$[K_E + \lambda K_G^*] \{\Delta\} = \{F\} \quad (4.7)$$

At the buckling load, no external disturbances are required to displace the structure. Hence,

$$[K_E + \lambda K_G^*] \{\Delta\} = \{0\} \quad (4.8)$$

Since $\{\Delta\}$ cannot be zero at the critical load, then the determinant of the stiffness matrix is zero. Thus,

$$|K_E + \lambda K_G^*| = 0 \quad (4.9)$$

In this typical eigenvalue problem, the lowest value of λ gives the buckling load for the stayed column if P^* is chosen as unity. The eigenvector associated with this eigenvalue gives the relative value of the displacement

components, that is, the buckled shape.

Because of the singularity of the geometric stiffness matrix, Eq. 4.9 should be multiplied by $[K_E]^{-1}/\lambda$ to read

$$|\gamma [I] + [K_E]^{-1}[K_G^*]| = 0 \quad (4.10)$$

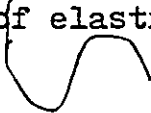
in which $[I]$ = unit matrix, and $\gamma = 1/\lambda$

Subroutine NROOT, from the IBM SYSTEM/360 Scientific Subroutine Package⁽¹⁰⁾, calculates the eigenvalues of the matrix $[K_E]^{-1}[K_G^*]$ which are γ . To obtain the buckling load, the largest value of γ is inverted to obtain the smallest eigenvalue λ .

4.3 Description of Computer Program

The computer program, written to handle the calculations required to find the maximum buckling load and the main pretension values, consists of approximately 400 cards. The program is written in FORTRAN IV. A complete listing of the program is contained in Appendix I. The program consists of a main program and five subroutines. The steps of the program can be summarized as follows:

- 1) Read Data. Only three cards are needed. Each card contains the necessary informations for one of the three components of the stayed column. The column length, its outer diameter, its inner diameter and its modulus of elasticity are read on the first card. On the second card, there is the same data for the crossarm. The diameter of the stays and the modulus of elasticity are read on the



third card.

2) Calculate the properties of the stayed column.

These properties include the areas and moments of inertia of the column, crossarms and stays, as well as the stay length. The Euler load of the column is also calculated.

3) Using these properties, call subroutine SCCMEK to calculate the master elastic stiffness matrix for the stayed column. The stayed column is divided into ten elements: the column is divided into four elements and each crossarm or stay is considered as one element. The moments of inertia for the stays, which are subjected to axial tensile forces only, are taken as zero since they do not possess bending stiffness. The elastic stiffness matrix for each element is calculated and transformed to the global coordinate system using a standard transformation matrix. The master stiffness matrix is set up for the assumed node displacements using a "Variable Correlation Scheme". The finite elements and the assumed possible node displacements taken into consideration are shown in Fig. 4.2.

4) Knowing the column length, call subroutine SCCMGK to calculate the master geometric stiffness matrix of the stayed column. The element geometric stiffness matrix is only calculated for the four elements of the column since the initial axial forces in the crossarms are very small compared to its buckling load. The master geometric stiffness matrix is assembled for the assumed possible displacements.

5) Subroutine ARRAY from IBM System/360 is used to put the master elastic and geometric stiffness matrices in a vector form to suit the use of subroutine NROOT.

6) Then, subroutines NROOT and EIGEN are used to calculate the eigenvalues of $[K_E]^{-1}[K_G^*]$. The reciprocal of the largest eigenvalue gives the lowest eigenvalue of $[K_G^*]^{-1}[K_E]$ which corresponds to the maximum buckling load for the single-crossarm stayed column. The eigenvector corresponding to this eigenvalue gives the relative values of the buckled shape corresponding to the maximum buckling load.

7) The constants relating the pretension values to the buckling loads and residual pretension are calculated either for the space or plane single-crossarm stayed column.

8) The output includes the geometrical properties of the column, the minimum effective, the optimum and maximum possible pretension, and the corresponding buckling loads. The relative shape of buckling, as well as, the residual pretension and expected buckling load for a given initial pretension are also included.

4.4 Limitations of Computer Program

The computer program calculate the necessary pretension values and the corresponding buckling loads required to draw the complete initial pretension-buckling load curve. Unfortunately, it is subjected to the following limitations:

- 1) The stayed column must be of the single-crossarm

type.

2) The column end restraints must be hinged.

3) The column and the crossarms must have a tubular section. The cross-sectional properties of the column must be the same for the full length of the column. Also, the properties of the crossarms must not change through its length.

4) The number of crossarms must be four arranged in a cruciform manner or two set in one plane. The corresponding number of stays must be eight or four.

5) Each of the crossarms, as well as the stays, must have the same length and properties.

CHAPTER 5

EFFECT OF STAYED COLUMN PARAMETERS

5.1 General

In this chapter, the pretension-buckling relationships are applied to a numerical example in order to gain insight into the effects that various stayed column parameters have on the optimum pretension and the corresponding maximum buckling load of a pin-ended single-crossarm stayed column. The effect of these parameters on the minimum effective pretension is also demonstrated. The three parameters which were varied are the crossarm member length, the stay diameter, and the stay modulus of elasticity. The computer program written in Chapter 3, after only a slight change, was used to obtain the results required to study the effect of the various parameters. The results indicate that the required optimum pretension was significantly altered by the changes in any of the three parameters studied.

5.2 Numerical Example

The following numerical example is used to demonstrate the influence of the various stayed column parameters on the optimum and minimum effective pretension, and the maximum buckling load. The column and crossarm members are

assumed to be circular tubes with an outside diameter of 2.25 in. and an inside diameter of 1.75 in. The modulus of elasticity of the steel tubing, either for the column or the crossarms, was taken to be 29.6×10^6 psi. The length of the column was selected to be 20 ft. To explore the influence of crossarm member length on the pretension-buckling behaviour, the ratio of half column length, l , to crossarm member length, l_{ca} , is varied from ten to one. To examine the influence of stay diameter on the optimum and minimum effective pretension and the corresponding buckling load, the stay diameter is changed from $3/16$ in. to $7/8$ in. with an increment of $1/16$ in. The modulus of elasticity of the stays is varied from 9.4×10^6 psi to 29.6×10^6 psi to demonstrate its effect on the required pretension values and buckling load.

5.3 Effect of Crossarm Member Length

The analytical results which demonstrate the effect of the crossarm member length on the optimum and minimum effective pretension and the corresponding buckling load are shown in Fig. 5.1 to Fig. 5.7. These figures reveal that by varying the crossarm member length the optimum pretension follows the shape of the buckling load curve. It increases with the increase of the buckling load and decreases with its decrease. This is due to the fact that the constant of proportionality between the pretension and the buckling load, C_1 , does not change greatly with the

change of the crossarm length. Examining Eq. 3.20, the increase of the crossarm length, and consequently the angle α between the stays and the column, causes a decrease in K_s , K_{ca} , $\cos \alpha$ and an increase in $\sin \alpha$. The result is a gradual decrease in the value of C_1 . In this example, C_1 decreases to approximately half its value by increasing the crossarm member length ten times.

At large ratios of l to l_{ca} , the minimum effective pretension does not vary with the change in the crossarm member length. It decreases only at low values of l to l_{ca} . This variation is governed by Eq. 3.29. Since the term $\pi^2 EI/L^2$ on the right hand side of the equation is constant, the change in the minimum effective pretension with the increase of the crossarm member length represents also the change in C_1 .

Fig. 5.1 represents the optimum and minimum effective pretension, and the corresponding buckling load as a function of l to l_{ca} ratio for a stay diameter of $3/16$ in and stay modulus of elasticity of 9.4×10^6 psi. It shows that for large ratios of l to l_{ca} , instability is controlled by Mode I, the type of triple curvature buckling mentioned in Chapter 2 (see Fig. 2.1). As the ratio of l to l_{ca} decreases, a rapid increase in the maximum buckling load and consequently the optimum pretension occur. For small ratios of l to l_{ca} , Mode II, the type of double curvature mentioned in Chapter 2 (Fig. 2.1), becomes the controlling instability mode at bifurcation. The result of decreasing

the ratio of l to l_{ca} is a decrease in the maximum buckling load accompanied by a rapid decrease of the optimum pretension. This is due to the fact that C_1 gets smaller rapidly. This behaviour is expected since the increase in the crossarm member length leads to the decrease of the rotational restraint and to the increase of the translational restraint of the column at the crossarm level. The maximum possible buckling load, and consequently the maximum optimum pretension, is in the vicinity of the intersection of the two buckling modes curves.

Figs. 5.1, 5.2 and 5.3 illustrate the influence of the crossarm member length on the optimum and minimum effective pretension, and the corresponding buckling load at a small stay diameter and various values of stay modulus of elasticity. From these figures, it is apparent that as the modulus of elasticity of the stays is increased, for a constant small stay diameter, the maximum possible buckling load and maximum optimum pretension occur at a large ratio of l to l_{ca} . In this case, the buckling load is slightly increased while the corresponding increase in the optimum pretension is very large. The use of steel rods having a modulus of elasticity of 29.6×10^6 psi instead of steel wire ropes having a modulus of elasticity of 9.4×10^6 psi causes a 7% increase in the buckling load and more than 300% increase in the required pretension. The reason for this increase can be obtained by again inspecting Eq. 3.20. The increase in the stay modulus of elasticity leads to an

increase in K_s and hence a large increase in C_1 .

Figs. 5.4, 5.5 and 5.6 represent the effect of crossarm member length on the maximum buckling load, the optimum and minimum effective pretension at a medium sized stay diameter and various values of stay modulus of elasticity. These figures show that the previous observations for a small stay diameter are still valid for medium sized stay diameter. In case of a medium sized stay diameter, the maximum possible buckling load and the corresponding maximum optimum pretension occur at a larger ratio of l to l_{ca} . These maximum values occur at a ratio slightly larger than ten in case of a stay modulus of elasticity of 19.5×10^6 psi and at a much larger ratio in case of a stay modulus of elasticity of 29.6×10^6 psi. As the stay diameter increases, a small increase in the value of the maximum buckling load and a larger increase in the value of the corresponding optimum pretension occur. This is again due to the increase in K_s and consequently the relatively large increase in the constant of proportionality C_1 .

The effect of the crossarm member length on the buckling load, the optimum and minimum effective pretension at a large stay diameter and various values of modulus of elasticity is illustrated in Fig. 5.7. Only Mode II controls the buckling since Mode I governs only at a ratio of l to l_{ca} much larger than ten. As the stay modulus of elasticity changes, no appreciable difference can be obtained in the value of the maximum buckling load while

the optimum pretension changes considerably. The decrease in the values of the maximum buckling load and of the corresponding optimum pretension is small at large ratios of l to l_{ca} and is large at small ratios.

5.4 Effect of Stay Diameter

It has already been pointed out that the increase in the stay diameter is accompanied by an appreciable increase in the constant of proportionality C_1 . If this is the case it would be expected that the optimum pretension would also increase. This is illustrated in Figs. 5.8 to 5.14. These figures indicate that, by varying the stay diameter, the optimum pretension curves do not follow the shape of the maximum buckling load curves as was the case in the previous section. As the stay diameter is increased, both the optimum and minimum effective pretension increase continuously, even without an increase in the corresponding buckling load. This can be explained by considering the constant of proportionality C_1 in Eq. 3.20. In this equation K_s is proportional to the square value of the stay diameter. Thus an increase in the stay diameter has a considerable effect on the increase of K_s and C_1 . Consequently, the optimum and minimum effective pretension increase even at constant buckling load.

Fig. 5.8 illustrates the curves of optimum and minimum effective pretension, and the corresponding buckling load as a function of the stay size. The ratio of l to l_{ca}

is ten and the stay modulus of elasticity is 9.4×10^6 psi. For small stay diameters, Mode I buckling is the controlling mode. In this case, the increase in the stay diameter leads to a rapid increase in the maximum buckling load and a similar increase in the optimum pretension. For large stay diameters, the buckling is controlled by Mode II. In this case, the increase in the maximum buckling load, due to an increase in the stay diameter, is slow. But the optimum pretension continues to increase with the same rapid rate as in Mode I zone because of the rapid increase in C_1 . The modes of buckling controlling the instability were anticipated because the translational restraint of the column at the crossarm level increases with the increase of the stay diameter.

Figs. 5.8, 5.9 and 5.10 illustrate the influence of the stay diameter on the buckling loads and the corresponding pretensions at a large ratio of l to l_{ca} for various values of stay modulus of elasticity. These figures show the effect of the stay modulus of elasticity, at a large ratio of l to l_{ca} (ten), on the point of intersection of the two buckling mode curves at which both Mode I and Mode II buckled configurations are equally possible. As the stay modulus of elasticity is increased, the point of intersection occurs at a smaller diameter yielding a slightly larger maximum buckling load. This means that the increase in the stay modulus of elasticity leads to an

increase in the maximum buckling load, the optimum and minimum effective pretension. This is true for various stay diameters. At large stay diameters, the increase in the optimum pretension is always quite large compared to the corresponding increase in the maximum buckling load. This is due to the increase of both the area and modulus of elasticity of the stay which greatly affect the value of C_1 .

Figs. 5.11, 5.12 and 5.13 confirm the validity of the observations mentioned above when the ratio of l to l_{ca} becomes smaller, six instead of ten. In this case, the point of intersection of Mode I and Mode II curves occurs at a smaller stay diameter and a slightly smaller maximum buckling load. This is obvious because the increase in the crossarm member length causes the decrease of the rotational restraint and the increase of the translational restraint of the column at the crossarm level. In case of a ratio of l to l_{ca} of six, the decrease in the optimum pretension, as well as the minimum effective pretension, is much larger than the decrease in the maximum buckling load at the point of intersection of the two buckling mode curves. This is clearer at a large stay modulus of elasticity. In case of steel rods with a modulus of elasticity of 29.6×10^6 psi, the optimum pretension decreases from 1.5 kips to less than 0.5 kips while the maximum buckling load decreases from 30.2 kips to 28.9 kips. This is due to the large decrease in C_1 when the ratio of l to l_{ca} falls from ten to six

causing a decrease of $\cos \alpha$, K_s and K_{ca} in Eq. 3.20.

Probably the most interesting results are obtained in Fig. 5.14 in which the diameter and modulus of elasticity of the stay vary while the ratio of l to l_{ca} is kept constant at one. The variation of these parameters has a very significant effect on the optimum and minimum effective pretension while the maximum buckling load remains approximately the same. As the stay diameter and modulus of elasticity are increased, the maximum buckling load increases very slowly. This is because Mode II is the controlling mode of buckling far away from the point of its intersection with Mode I buckling which does not occur at a practical stay diameter. At the same time, the increase of the stay diameter and modulus of elasticity causes a large increase in K_s and consequently C_1 as seen from Eq. 3.20. The result is a considerable increase of the optimum and minimum effective pretension. As the stay diameter is increased from $3/16$ in. to $7/8$ in., the increase in the optimum pretension is over 1200%. The use of steel rods with a modulus of elasticity of 29.6×10^6 psi instead of steel wire ropes with a modulus of elasticity of 9.4×10^6 psi cause an increase in the required optimum pretension from 200%, in case of $7/8$ in. stay diameter, to 400%, in case of $3/16$ in. stay diameter. Approximately the same percentage increase applies in the case of minimum effective pretension, while the maximum buckling load remains approxi-

mately constant in all the cases considered.

5.5 Effect of Stay Modulus of Elasticity

The effect of varying the stay modulus of elasticity from 9.4×10^6 psi to 29.6×10^6 psi on the maximum buckling load, the optimum and minimum effective pretension was investigated theoretically. The results are shown in Figs. 5.15 to 5.21. As is the case when the stay diameter is varied, the pretension curves do not follow the shape of the buckling load curves. As the stay modulus of elasticity is increased, both the optimum and minimum effective pretension tend to increase continuously at approximately a constant rate. But the buckling load increases rapidly when controlled by Mode I buckling, and slowly when controlled by Mode II buckling. Equations 3.14, 3.20 and 3.31 give an explanation to this difference in behaviour between the buckling loads and the corresponding pretensions. As the stay modulus of elasticity is increased, K_s and consequently the constant of proportionality C_1 increase. The large increase of C_1 counteracts the effect of the slow increase of the buckling load when controlled by Mode II buckling, hence the optimum pretension keeps its constant rate of increase.

Fig. 5.16 shows the influence of the stay modulus of elasticity at a constant stay diameter, 7/16 in., and a ratio of l to l_{ca} of ten. At small values of stay modulus of elasticity, instability is controlled by Mode I buckling.

This mode is always accompanied by a rapid increase in the buckling load when the stay modulus of elasticity increases. At large values of stay modulus of elasticity, instability is controlled by Mode II buckling. In this case, as the stay modulus of elasticity is increased, the increase in the buckling strength is slow. Mode II governs at large values of stay modulus of elasticity because of the increase in the stiffness of the stay members. This increase in the stiffness means an increase in the translational restraint of the column at the crossarm level. As explained previously, the optimum and minimum effective pretension increase rapidly both in the zone controlled by Mode I buckling and in the zone controlled by Mode II buckling.

Figs. 5.15, 5.16 and 5.17 represent the effect of stay modulus of elasticity on the maximum buckling load, the optimum and minimum effective pretension at a constant ratio of l to l_{ca} of ten and different values of stay diameter. It can be seen that at small stay diameters and large ratios of l to l_{ca} , Mode I controls the bifurcation. For medium sized stay diameters, Mode I governs at small moduli of elasticity while Mode II governs at large moduli of elasticity. At large stay diameters, only Mode II is the governing buckling shape. Thus, the point of intersection of the two buckling mode curves occurs at a very large stay modulus of elasticity as the stay diameter

decreases from $7/16$ in. to $3/16$ in. As the diameter increases to $7/8$ in., the point of intersection occurs at a relatively small value of stay modulus of elasticity. Again, the reason for this behaviour is that both the area of the stay and its modulus of elasticity affect the stiffness of the stay members, and consequently the translational restraint of the column at the level of the crossarms. The change in the values of the maximum buckling load is always small when instability is controlled by Mode II buckling, and significant when Mode I governs. This means that there is no appreciable gain in the strength of the column when the stay diameter or modulus of elasticity is increased in the Mode II zone. As the stay modulus of elasticity increases, there is a large increase in the optimum pretension whether Mode I or Mode II governs.

The influence of the stay modulus of elasticity on the maximum buckling load, the optimum and minimum effective pretension is affected by the change in the ratio of l to l_{ca} . The effect of decreasing the ratio of l to l_{ca} from ten to six is shown in Figs. 5.18, 5.19 and 5.20. Fig. 5.18 reveals that the governing mode for various values of stay modulus of elasticity at a stay diameter of $3/16$ in. is Mode I buckling. Mode II is the controlling mode of buckling for both $7/16$ in. and $7/8$ in. stay diameters. This means that as the ratio of l to l_{ca} is

decreased, the point of intersection of the two buckling mode curves occurs at a smaller stay modulus of elasticity. This is due to the fact that as the crossarm member length is increased, the translational restraint increases and the rotational restraint decreases at the level of the crossarm member. There is an appreciable increase in the maximum buckling load in the zones which were controlled by Mode I at a ratio of l to l_{ca} of ten. The change in the optimum and minimum effective pretension is not significant in case of decreasing the ratio of l to l_{ca} to six.

Fig. 5.21 illustrates the effect of the stay modulus of elasticity on the buckling load, the optimum and minimum effective pretension at a ratio of l to l_{ca} of one and various values of stay diameter. In all the cases, Mode II is the governing mode. The buckling load does not change significantly with the change of any of these parameters. Only the optimum and minimum effective pretension are considerably affected. They increase continuously with the increase of the stay modulus of elasticity. This increase occurs with approximately the same rate for any of the stay diameters. There is also an appreciable increase in the optimum and minimum effective pretension with the increase of the stay diameter. In both cases, K_s and consequently C_1 increase and lead to a large increase in the required pretension for a constant buckling load. Thus, it is not preferable to increase the stay modulus of elasticity or

stay diameter at a small ratio of l to l_{ca} . There will be no gain in the buckling strength of the column while the required optimum pretension will increase considerably.

CHAPTER 6

EXPERIMENTAL PROCEDURE AND RESULTS

6.1 General

A series of tests were conducted on a single-crossarm stayed column model to verify the theoretical relationships between the initial pretension and the corresponding buckling load derived in Chapter 3. The tested model had only two crossarms and four stays set in one plane as shown in Fig. 6.1. The buckling was confined to that plane. The tested column properties are given in the following section. This section includes the geometrical and material properties of the column. Then, the experimental equipment and procedure are outlined. Finally, the results are summarized at the end of this chapter.

6.2 Tested Column Properties

6.2.1 Geometric Properties

The plane single-crossarm stayed column model was preferred over a conventional space single-crossarm stayed column model. The advantages of the first type of stayed column may be summarized in the following:

- 1) Its buckling occurs in one confined plane, the plane of the crossarms and stays, while for a space column buckling may occur in one of the two planes containing

crossarms and stays. Therefore, its buckling is easier to control.

2) It needs less material since the space column contains four crossarms and eight stays compared to two crossarms and four stays in case of plane stayed column. Thus, half the material for the stayed elements is used.

3) The plane column takes less effort to set up, uses less equipment and requires fewer readings during the experiment without any loss of accuracy or efficiency.

The choice of the plane type model was accompanied by a theoretical modification in the predicted relationship between the initial pretension and the corresponding buckling load. This modification was necessary to suit the decrease in the number of stays at each end of the column. It is derived in the next chapter.

The length of the column was chosen according to the space available in the laboratory, and at the same time as close as possible to the practical length of a stayed column. A length of ten feet was satisfactory. The diameters of the column, crossarms, and stays were chosen such that the maximum buckling load could be applied conveniently in the laboratory. The cross-sections of the column and the crossarm have the same dimensions and properties. The outer diameter of the tube, from which the column and crossarms were cut, is 1.50 in. and the inner diameter is 1.00 in. The stay diameter was governed by the available load cells

that can measure the force in the stays, and was taken as 1/8 in. An emphasis on the accuracy, both in cross-sectional dimensions and longitudinal straightness, was required.

6.2.2 Material Properties

Both the column and the crossarm members were cut from a cold drawn round seamless steel mechanical tube MT-1015. Commercial steel rods were used for stays. Several tests were carried out on specimens to determine the necessary properties of the tube and rods. The tube was found to have an ultimate stress of 70 ksi. The yield stress was 49 ksi which was satisfactory since the theoretical axial stress at the maximum buckling load was 22 ksi. The modulus of elasticity of the tube was 29.1×10^3 ksi. Tests on the steel rods indicated that the modulus of elasticity was 29.3×10^3 ksi while the ultimate stress was 89 ksi. Thus the ultimate force taken by the wire was 1080 lbs while the theoretical optimum pretension was 240 lbs.

6.3 Experimental Equipment

A set of four ring load cells were chosen to be placed with the four stay members. Each ring load cell consists of an aluminum ring beam and two strain gages. The ring beam has an outer diameter of 2.0 in., an inner diameter of 1.5 in., and a thickness of 0.375 in. Two holes located along one of its diameters are slightly more than 1/8 in. diameter, which fit the stay diameter. Two strain gages are placed on the inner and outer diameter of the

ring beam to give an indication of the deflection of the ring beam and consequently the axial force acting along the two holes. These load cells were used to fulfill two functions. They had to measure the tension in the stays by their strain gages. At the same time, they were used to introduce the pretension in the stays through nuts and threads as shown in Fig. 6.2. Thus, there was no need for turnbuckles.

A Universal Flat load cell was used to measure the, applied compressive load of the column. It has a maximum capacity of 25 kips compared to the maximum theoretical buckling load of 21.5 kips. A small groove was machined on the top of the load cell to fit an end ball of the column as shown in Fig. 6.3.

A hydraulic jack used to apply the axial load of the column is shown in Fig. 6.4. In addition to a separate base, the jack was mounted by a connection part having a hollow tube to fit the cylindrical piston of the jack and a rectangular top to fit the base of the flat load cell.

The strain indicators used to measure the strain in the strain gages are shown in Fig. 6.5. Fourteen channels of information that read deformations were needed during the tests: one for each ring beam load cell and ten for gages applied on the column and crossarms. These channels were provided by the two identical strain indicators. Another strain indicator was used for the flat load cell calibration.

Two dial gages were used to measure the lateral

deflection at the mid-height of the column.

6.4 Experimental Procedure

The calibration of the two types of load cells, the column preparation and testing to get the buckling load for different initial pretension are outlined in this section. An important precaution was necessary to be able to use the same column for the different tests. This precaution is explained at the end of this section.

6.4.1 Equipment Preparation

A calibration of the flat load cell was made on a Universal Testing Machine by applying a compressive load in increments of 500 lbs up to the maximum load of 25,000 lbs. The readings of the connected strain indicator were used to prepare the linear calibration chart of the load cell.

A calibration of the four ring load cell was made by hanging weights vertically along the two holes in increments of 20 lbs. The weights representing the axial force in the stays were increased up to 400 lbs which is a 160 lbs over the theoretical optimum pretension of the stayed column model. The two strain gages on each ring beam were connected to their proper position in the strain indicator in a half bridge connection. The average reading of each increment of load was used to plot one curve for all the ring load cells. This curve, which was found to be a straight line, represents the calibration chart relating the axial force along the two holes to the reading of the strain

in each ring load cell.

6.4.2 Column Preparation

After determining the important properties of the materials used in the model column, the tube was cut into the required lengths for the column and crossarms. The crossarms were machined to fit the column at one end of each crossarm, and at the other end, two inclined threaded holes were drilled to hold the stays. Then, the crossarms were welded in place to satisfy the requirement that they be rigidly attached to the column.

Two bases for the column were machined as shown in Fig. 6.6 such that they fit the two ends of the column. Each base had a groove that fit a small ball which represented the hinged support. Each base was welded to one end of the column to transmit axially the compressive load. Another function of these bases was to hold the stays through inclined threaded holes which suit the inclination of the stays to the column. Fig. 6.3 shows the base during the experiment.

Six strain gages were applied at three positions on the column. Four others were applied at the middle of the crossarms. These gages were applied at opposite sides in the plane of buckling. A sketch of the positions of the strain gages is shown in Fig. 6.7. They were used to measure the strains during the experiment.

The stays were cut and threaded to be joined to the

ends of the column and crossarms, and, at the same time, to hold the ring load cells through nuts.

A small groove was machined in a thick plate to fit the top end ball of the column. Two holes were drilled in the plate so that it could be firmly attached to the girder of a frame in the laboratory. This top plate is shown fixed in its position in Fig. 6.8. The base of the hydraulic jack was welded to the floor with its center exactly under the center of the groove of the top plate. Thus, the welding ensured that the applied load passed through the axis of the column during all the tests.

The column was set in its place using two end balls of 1.0 in. diameter each. Hence, the column could rotate easily at each end which represented the assumed hinged ends of the stayed column. The column was bound by the top plate and the girder at the top, and by the flat load cell and the hydraulic jack at the bottom.

To confine the buckling in the plane of the crossarms and stays, two sets of lateral supports, each consisting of two bars welded to two angles, were prepared. Two square tubes were clamped to these lateral supports as shown in Figs. 6.9 and 6.1. Thus, the movement of the column in the direction perpendicular to the plane of the crossarms and stays was prevented with a minimum amount of friction.

Two dial gages were installed at each end of the crossarms. They were used to determine the lateral deflection of the column at the level of the crossarms under the

effect of the applied load during the tests.

6.3.4 Column Testing

First, the column was tested without stays. The aim of this test was to ensure that the buckling load of the column is the Euler load. This was considered as a proof that the two sets of lateral supports confining the buckling in one plane had a negligible effect on the buckling load.

Then, a series of tests was conducted with different initial pretensions. They cover the three zones described in the analytical derivation of the relationships between the initial pretension and the corresponding buckling load. In general, each test began by introducing equal pretensions in the four stays. The pretensions were gradually applied so that neither the column nor the crossarms bent under the forces in the stays. This was done by tightening the nuts along the threads of the stays at the ring load cells in reasonable increments and in order until reaching the required initial pretension. The value of pretension at each increment was controlled by using the strain indicator and calibration chart. Then, the column was loaded in increments until buckling. The load was axially applied using the hydraulic jack. Its value was known from the strain indicator reading and the calibration chart of the flat load cell. The two end balls served to keep the load axial and to allow the rotation of the ends of the column. After each increment of load, the readings of the dial gages

were taken to get the horizontal deflection of the column at the level of crossarms. The readings of the strain gages on the column and crossarms were used to check the applied load and the straightness of the crossarms during the experiment. The readings of the strain gages on the ring load cells were recorded to give a measurement of the remaining tension in the stays after each increment of load.

The upper limit of the applied load differed from test to test according to the position of the initial pretension of the test in the theoretical curve of buckling load versus initial pretension. In the first zone, the load was slightly increased above the Euler load which was considered as the buckling load. In the second zone, the observed buckling load was taken as the load at which the tension in two stays on one side of the column vanished. The applied load was slightly increased above that load. In the third zone, the observed buckling load was taken as the load at which a considerable increase in the horizontal deflection of the column at the level of crossarms occurred without a significant increase in load. In this case, the tension did not vanish in any stay. Any attempt to increase the applied load beyond this limit led to the failure of the two stays resisting the deflection of the column.

6.4.4 An Important Precaution

Only one column was tested several times at different initial pretensions until buckling. To ensure the

elasticity of the column after buckling each time, a maximum allowable deflection at the level of crossarms had to be determined. This deflection was calculated such that it kept all the fibers of the column below the elastic limit under the applied load. The critical load after which the extreme fibers exceed the elastic range can be calculated using the well-known formula:

$$\sigma = \frac{P}{A} \pm \frac{Mc}{I} \quad (6.1)$$

Eq. 6.1 may be written for the stayed column in terms of the allowable deflection Δ_a as:

$$\sigma_y = \frac{P_a}{A_c} + \frac{P_a \Delta_a D_o}{2 I_c} \quad (6.2)$$

in which σ_y = the yield stress of the material of the column, and D_o = the outer diameter of the column.

Eq. 6.2 may be arranged to yield the following expression for the maximum allowable deflection under the applied load:

$$\Delta_a = \frac{2 I_c \sigma_y}{P_a D_o} - \frac{2 I_c}{A_c D_o} \quad (6.3)$$

This means that the deflection allowed at the end of each test depended on the amount of the applied load. A further precaution was that this deflection should not cause the failure of the stays on the convex side of the column.

6.5 Experimental Results

For each test, the load-deflection curve was drawn. On the same graph, the tension in each stay is plotted against the applied load. Figs. 6.10 and 6.11 illustrate the curves of load versus deflection and tension in the stays for an initial pretension less than the minimum effective pretension. The results for tests starting with an initial pretension between the minimum effective pretension and the optimum pretension are shown in Figs. 6.12 to 6.16. Figs. 6.17 to 6.20 show the effect of an initial pretension equal to and greater than the optimum pretension on the buckling load and the residual pretension. The results of the experimental buckling loads and residual pretensions compared to the theoretical values are shown in Fig. 6.21. The analysis of these results is presented in the next chapter.

CHAPTER 7

ANALYSIS OF EXPERIMENTAL RESULTS

7.1 General

To compare the experimental results with the theoretical values, the analytical relationships between the initial pretension and the corresponding buckling load should be modified. The reduction in the number of stays at the ends of the plane stayed column should be taken into account. This modification is presented in the next section. Another difference between the theoretical treatment of the stays as made of one homogeneous material and the actual elements used as stays in the model should be considered. This is due to the existence of the ring load cells in the stay elements which caused the change of the stiffness of these elements from that of stays made of steel rods only. The equivalent stay modulus of elasticity that should be used to predict the theoretical buckling load for each test is derived in this chapter. Finally, the experimental results are compared with the predicted values based on the above modifications.

7.2 Analytical Relationships between Buckling Load and Pretension for a Plane Single-Crossarm Stayed Column

A plane single-crossarm stayed column has only two

stays at each end of the column compared to four in the case of a space stayed column. For a plane column, the value of n_1 in Eq. 3.1 is two, and the initial axial force on the column induced by the initial pretension, T_i , may be expressed as:

$$P_i = 2 T_i \cos \alpha \quad (7.1)$$

After applying an axial external load, P_a , the expression of the final axial force on the column given by Eq. 3.5 is changed to:

$$P_f = P_a + 2 T_f \cos \alpha \quad (7.2)$$

By substituting the new values of P_f and P_i from Eq. 7.2 and Eq. 7.1, Eq. 3.7 becomes:

$$\Delta_c = \frac{[P_a - 2(T_i - T_f) \cos \alpha]}{K_c} \quad (7.3)$$

Substituting for Δ_s from Eq. 3.14, for Δ_{ca} from Eq. 3.11, and for Δ_c from Eq. 7.3 into Eq. 3.16 yields:

$$\frac{T_i - T_f}{K_s} = \frac{[P_a - 2(T_i - T_f) \cos \alpha] \cos \alpha}{2 K_c} - \frac{[2(T_i - T_f) \sin \alpha] \sin \alpha}{K_{ca}} \quad (7.4)$$

Solving Eq. 7.4, the decrease in the pretension force, $T_i - T_f$, may be written as:

$$T_i - T_f = \frac{P_a \cos \alpha}{2 K_c \left[\frac{1}{K_s} + \frac{2 \sin^2 \alpha}{K_{ca}} + \frac{\cos^2 \alpha}{K_c} \right]} \quad (7.5)$$

The shortening of the column can be written in terms of the final axial load, P_f , by combining Eqs. 7.2 and 7.3 as follows:

$$\Delta_c = \frac{P_f - 2 T_i \cos \alpha}{K_c} \quad (7.6)$$

Comparing Eq. 7.6 with Eq. 3.21, it is obvious that Eq. 3.23 should be substituted by:

$$T_f = T_i - \frac{(P_f - 2 T_i \cos \alpha) \cos \alpha}{2 K_c \left(\frac{1}{K_s} + \frac{2 \sin^2 \alpha}{K_{ca}} \right)} \quad (7.7)$$

Substituting for T_f from Eq. 7.7 into Eq. 7.2 yields:

$$P_f = P_a + 2 \left[T_i - \frac{(P_f - 2 T_i \cos \alpha) \cos \alpha}{2 K_c \left(\frac{1}{K_s} + \frac{2 \sin^2 \alpha}{K_{ca}} \right)} \right] \cos \alpha \quad (7.8)$$

Solving Eq. 7.8, the applied load, P_a , can be expressed in terms of the final axial load of the column, P_f , and the initial tension in the stays, T_i , as follows:

$$P_a = (P_f - 2 T_i \cos \alpha) \left[1 + \frac{2 \cos^2 \alpha}{K_c \left(\frac{1}{K_s} + \frac{2 \sin^2 \alpha}{K_{ca}} \right)} \right] \quad (7.9)$$

These modifications lead to the following relationships relating the initial pretension to the corresponding buckling load for a plane single-crossarm stayed column. In the first zone, the Euler load given by Eq. 3.28 is considered as the buckling load since the tension in the stays becomes zero under the applied load. The minimum effective pretension can be calculated from the following expression:

$$T_{\min} = \frac{\pi^2 E_c I_c C_i}{L^2} \quad (7.10)$$

in which C_i is a constant of proportionality given by:

$$C_i = \frac{\cos \alpha}{2 K_c \left(\frac{1}{K_s} + \frac{2 \sin^2 \alpha}{K_{ca}} + \frac{\cos^2 \alpha}{K_c} \right)} \quad (7.11)$$

In the second zone, the governing equation for the buckling load can be written as:

$$P_{cr} = \frac{T_i}{C_i} \quad (7.12)$$

The maximum pretension in the second zone is the optimum pretension given by:

$$T_{opt} = C_i P_{\max} \quad (7.13)$$

in which P_{\max} is the maximum buckling load of the stayed column that is the same for the plane or space column.

The buckling load in the third zone is governed by the following equation:

$$P_{cr} = (P_{max} - 2 T_i \cos \alpha) C_2 \quad (7.14)$$

in which C_2 is a constant of proportionality given by:

$$C_2 = 1 + \frac{\cos^2 \alpha}{K_c \left(\frac{1}{K_s} + \frac{2 \sin^2 \alpha}{K_{ca}} \right)} \quad (7.15)$$

The residual pretension should be equal to zero in the first and second zone, while in the third zone it has a value given by:

$$T_r = T_i - (P_{max} - 2 T_i \cos \alpha) C_3 \quad (7.16)$$

in which C_3 is the same constant given by Eq. 3.33.

7.3 Equivalent Stay Modulus of Elasticity

In the plane stayed column model, a stay was composed of steel rods and a ring beam load cell. The modulus of elasticity of the stay was not directly taken as the rod modulus of elasticity, but it was calculated according to the actual stiffness of the stay and load cell.

The deflection of the ring beam due to a tension force in the rods was calculated using Castigliano's theorem. The calculation is outlined in Appendix II. The value of the deflection of a ring beam of mean radius, R , under a tension force T in the rods is given by:

$$\delta_b = \frac{\pi TR}{4 E_b A_b} + \frac{\pi TR}{4 G_b A_b} + \frac{TR^3}{4 E_b I_b} \left(\pi - \frac{\pi}{8} \right) \quad (7.17)$$

in which E_b = the modulus of elasticity of the ring beam, A_b = the cross-sectional area of the ring beam, I_b = its moment of inertia, and G_b = its modulus of rigidity.

Due to the tension force T , the elongation of the actual length of the steel rods used in the stay was calculated from the well-known formula:

$$\Delta_r = \frac{T l_r}{E_r A_r} \quad (7.18)$$

in which l_r = the actual length of rods used in one stay, E_r = the modulus of elasticity of the rods, and A_r = the cross-sectional area of the rods.

The actual stiffness of the stay was taken as:

$$S = \frac{T}{\delta_b + \Delta_r} \quad (7.19)$$

Accordingly, an equivalent stay modulus of elasticity was used in the computer program to predict the theoretical buckling load for each test. Its value was taken as:

$$E_e = \frac{S l_t}{A_r} \quad (7.20)$$

in which l_t = the theoretical length of the stay calculated

in the computer program.

7.4 Comparison of Observed and Predicted Buckling Loads and Residual Tension in the Stays

7.4.1 Case of Initial Pretension Less than the Minimum Effective Pretension

The theoretical minimum effective pretension was found to be 44 lbs. The results of two tests carried out at an initial pretension less than this value are represented in Figs. 6.10 and 6.11. It can be seen that the column can support a load larger than the Euler load which is considered the theoretical buckling load. This is due to the increasing tension force in the two stays on the convex side of the column. This force prevented the completion of buckling. But as the tension force in the other two stays approached zero, they became ineffective, and consequently the column was no longer considered to be a stayed column. This was taken as the buckling of the column. According to this point of view, the experimental buckling load in Fig. 6.11 appears slightly higher than the theoretical buckling load. This is probably due to the temporary residual strain in the load cell after the disappearance of the tension in the rods.

Generally, the tension in all the stays did not decrease at the same rate under the application of a load as was considered in the theoretical approach. This is due to the imperfection of the column. In all the tests, the

tension in the two stays on the side of the initial imperfection began to decrease less than that in the other two stays under the applied load. Then, as the load was increased, the tension started to increase in the two stays on the convex side of the column. This increase usually occurred in the vicinity of the buckling load.

7.4.2 Case of Initial Pretension between the Minimum Effective and the Optimum Pretension

The theoretical optimum pretension was found to be 240 lbs and the corresponding buckling load was 21.5 kips. Taking the experimental buckling load as that load at which the tension in any stay vanished, Figs. 6.12 to 6.14 show good agreement between experimental and theoretical values of buckling load. The tension in the two stays on the convex side of the column decreased less than that in the other two stays up to the vicinity of the buckling load. Then, it began to increase due to the increasing deflection at the crossarm level.

At a buckling load higher than 13.5 kips, the experimental results became much less than the theoretical values, as shown in Figs. 6.15 to 6.17. This can be explained by the effect of the initial imperfection of the column which increases appreciably with the increase in the value of the buckling load. The imperfection caused a higher rate of decrease in the tension in the two stays on the concave side of the column at high values of applied load.

7.4.3 Case of Initial Pretension Greater than the Optimum Pretension

Figs. 6.18 to 6.20 illustrate the experimental and theoretical values of buckling load for an initial pretension greater than the optimum pretension. In this case, the theoretical buckling load is slightly less than the maximum value, while the experimental results indicated approximately the same buckling load. Thus, the difference between the theoretical and experimental values remains high because of the imperfection as stated before. The initial imperfection had the same effect on the value of the residual pretension which was taken as the remaining tension in the two stays assisting the buckling at the instant of buckling. The residual pretension was appreciably less than its theoretical value at these high values of buckling load. On the other hand, the tension in the other two stays was considerably larger than the theoretical value because of the large deflection at the level of crossarms.

Fig. 6.21 illustrates a comparison of the theoretical and experimental values of buckling load in the three zones. The theoretical and experimental residual pretension at the instant of buckling are also shown on the same figure.

CHAPTER 8

CONCLUSIONS AND RECOMMENDATIONS

8.1 General

This thesis was concerned with the study of pretension for a single-crossarm stayed column. A geometrical analysis was used to predict the effect of the initial pretension in the stays on the buckling load of the column. A computer program was written to obtain the basic pretension values and the corresponding buckling loads for a given space or plane single-crossarm stayed column. The influence of three stayed column parameters on the optimum and minimum effective pretension, and the maximum buckling load was demonstrated. Experimental results for the buckling load at different initial pretensions were obtained by testing a plane single-crossarm stayed column. The results were compared to the theoretical values.

8.2 Conclusions

The following conclusions may be drawn on the basis of this study:

- 1) The relation between the initial pretension and the corresponding buckling load is controlled by three values: the minimum effective pretension below which there is no increase in the buckling load of the column over its

Euler load, the optimum pretension which is associated with the maximum buckling load of the column, and the maximum possible pretension which causes buckling without any external applied load.

2) An initial pretension less than or equal to the minimum effective pretension does not affect the buckling load of the column.

3) The relation between the initial pretension and the corresponding buckling load will be linear if the initial pretension is between the minimum effective and the optimum pretension. As the initial pretension is increased, the buckling load increases.

4) The relation between the initial pretension and the corresponding buckling load will continue to be linear if the initial pretension is greater than the optimum pretension. In this case, as the initial pretension is increased, the buckling load decreases.

5) The effect of the crossarm length on the buckling load and the optimum pretension depends on the values of the stay diameter and its modulus of elasticity. At small ratios of l to l_{ca} , the buckling load and the optimum pretension increase rapidly with the increase of the crossarm length. At large ratios of l to l_{ca} , as the crossarm length is increased, the buckling load and the optimum pretension decrease. The ratio of l to l_{ca} is considered large or small according to the values of stay diameter and modulus of elasticity.

6) At large ratios of l to l_{ca} , the minimum effective pretension remains approximately constant with the change of the crossarm length. At small ratios of l to l_{ca} , as the crossarm length is increased, the minimum effective pretension slowly decreases.

7) The increase in the stay diameter causes an increase in the buckling load and the optimum pretension. The increase is rapid when the buckling load is controlled by Mode I buckling. When controlled by Mode II buckling, the increase in the buckling load is very slow, but the increase in the optimum pretension continues to be rapid.

8) The minimum effective pretension increases continuously with the increase in the stay diameter.

9) The increase in the stay modulus of elasticity leads to a rapid increase in the optimum pretension and to a continuous increase in the minimum effective pretension. The buckling load increases rapidly when controlled by Mode I buckling and slowly when controlled by Mode II buckling. At small ratios of l to l_{ca} , the increase in the buckling load with the increase in the stay modulus of elasticity is insignificant.

10) Economical design of stayed columns may be obtained by choosing the proper stay diameter and modulus of elasticity. In some regions governed by Mode II buckling, the increase in the stay diameter or stay modulus of elasticity does not significantly affect the buckling load.

11) The experimental verification of the relationship between the initial pretension and the corresponding buckling load showed two points. For the values of initial pretension lying in the first and half of the second zone in the theoretical relationship, there is good agreement between the observed and predicted buckling loads. For larger values of initial pretension, the effect of the imperfection of the column led to an experimental buckling load lower than the predicted value.

8.3 Future Research

The theoretical approach used in this study to predict the effect of pretension on the buckling load of stayed columns is limited to space or plane single-crossarm stayed columns. Further studies should extend to double-, triple-crossarm and other types of stayed columns.

The single-crossarm stayed column under consideration is loaded by an axial force. Other types of loads, such as lateral loads, could be studied.

Stayed columns may buckle after the yielding of the extreme fibers of the columns. The inelastic buckling of stayed columns should be researched.

The geometrical approach used for the single-crossarm stayed column may be complicated for other types of stayed columns. Other methods, such as the energy method, could be used.

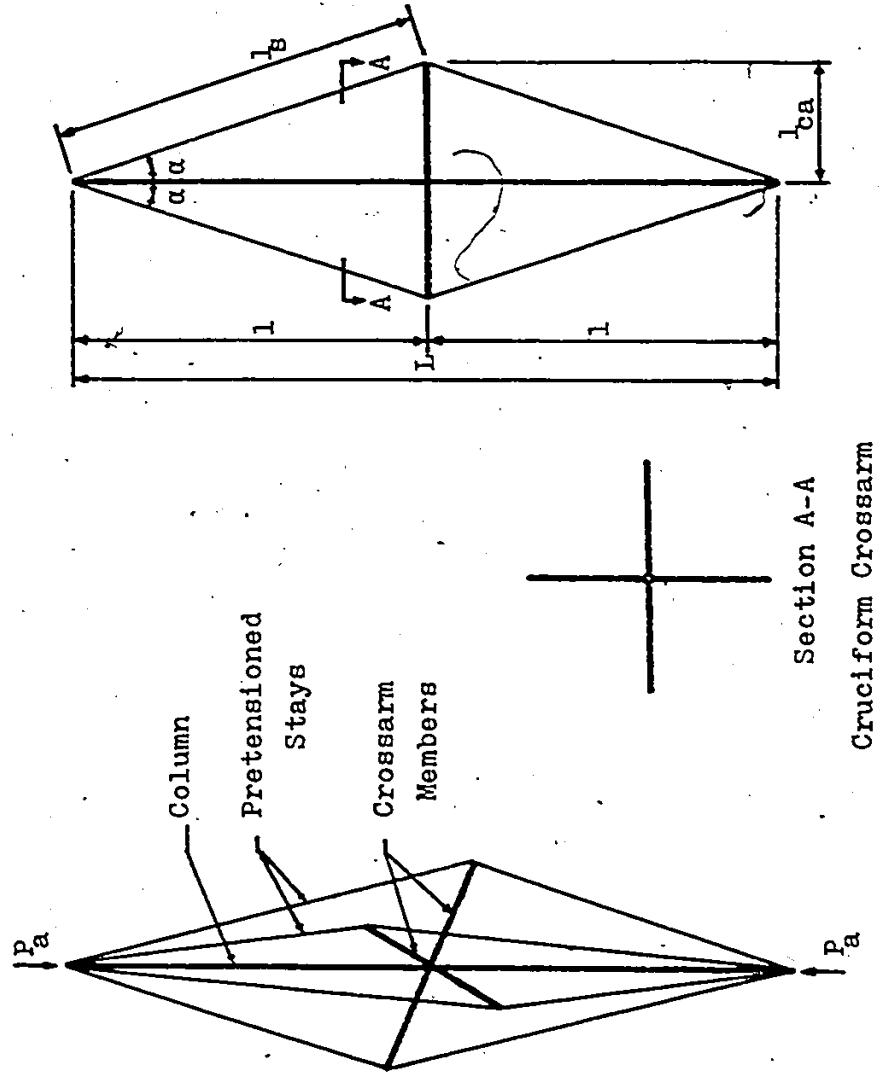
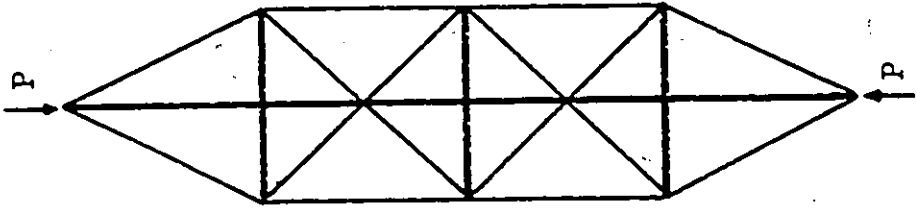
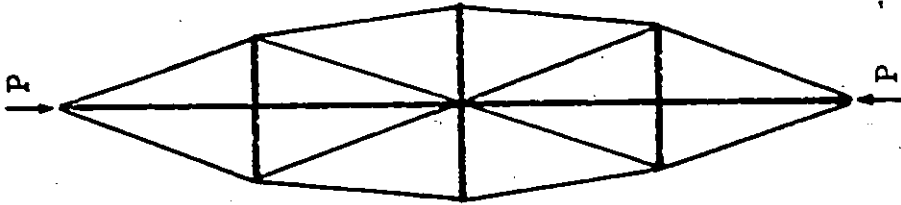


Fig. 1.1.1 Single-Crossarm Stayed Column.



Triple-Crossarm



Double-Crossarm

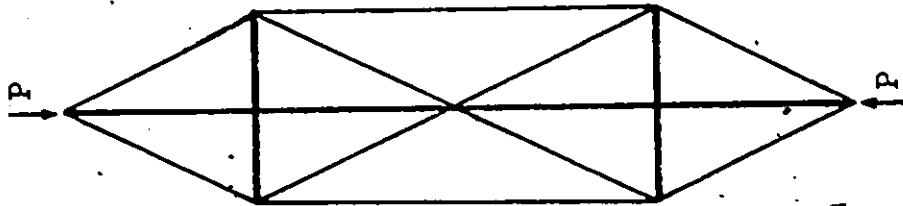
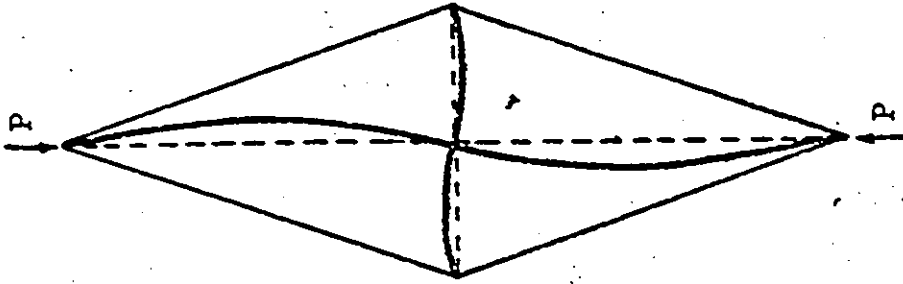
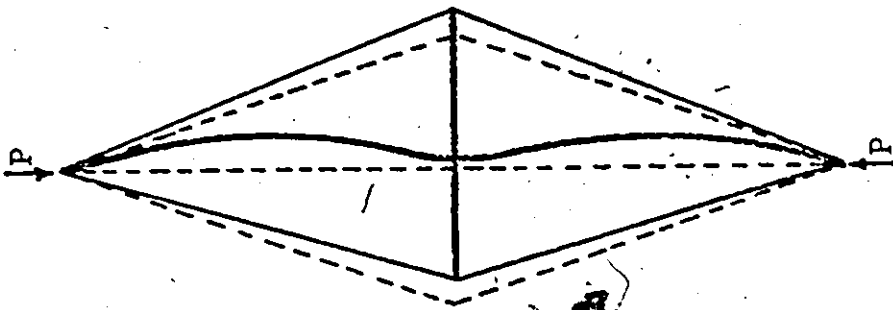


Fig. 1.2 Double- and Triple-Crossarm Stayed Columns.



MODE II



MODE I

Fig. 2.1 Buckling Modes of Pin-ended Single-Crossarm Stayed Column.

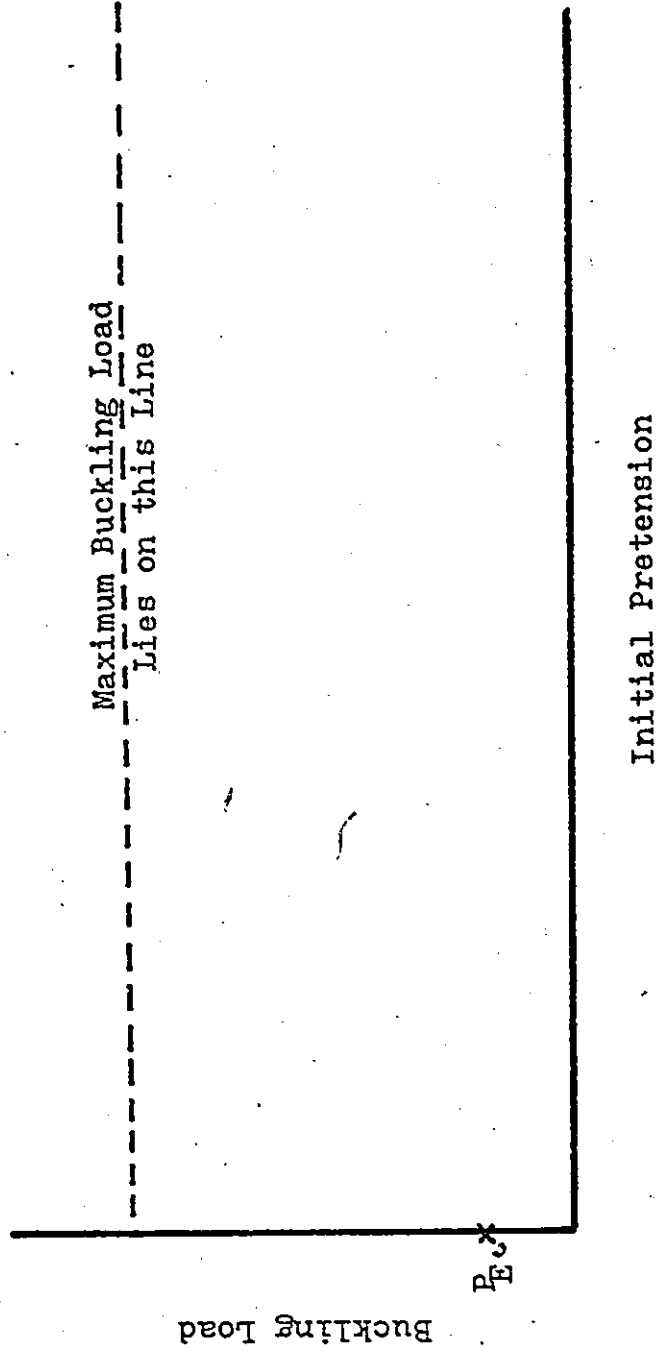


Fig. 3.1 Known Limits.

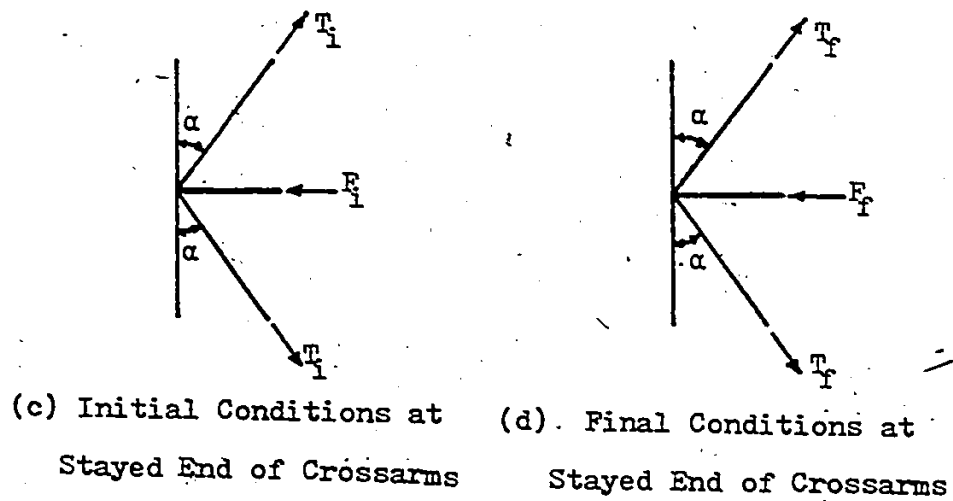
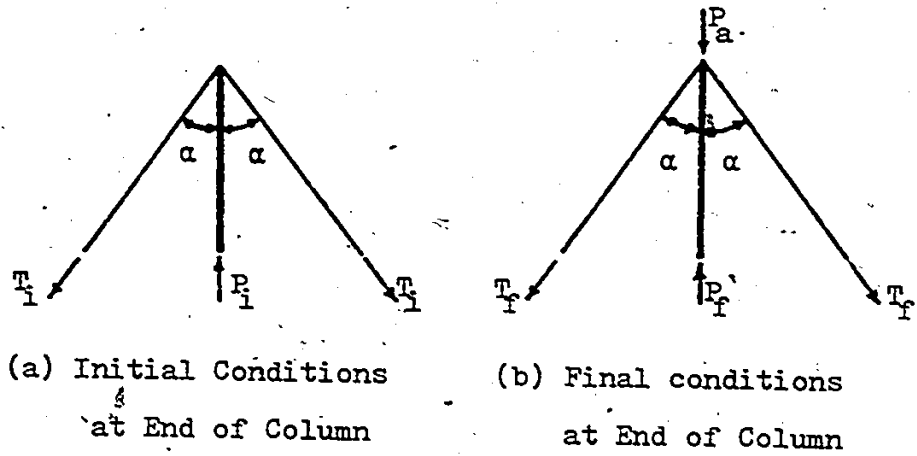


Fig. 3.2 Equilibrium Force Systems of Stayed Column.

(After Smith, McCaffrey, and Ellis)

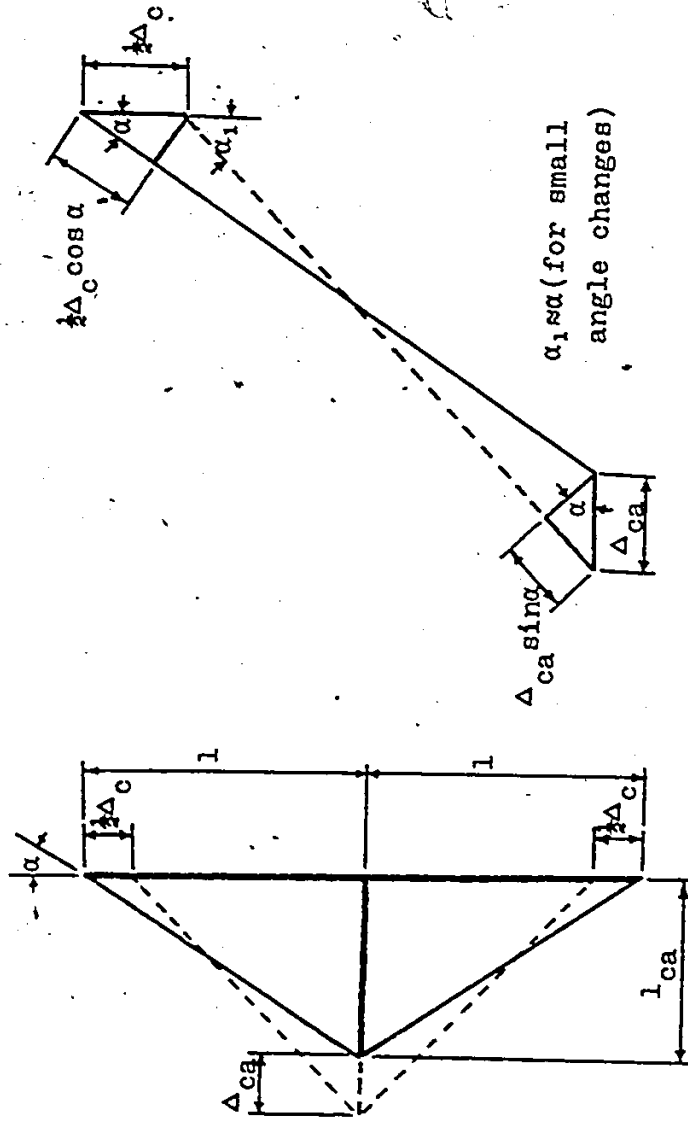


Fig. 3.3 Change in Length of Stays Due to Axial Deformation.

(After Smith, McCaffrey, and Ellis)

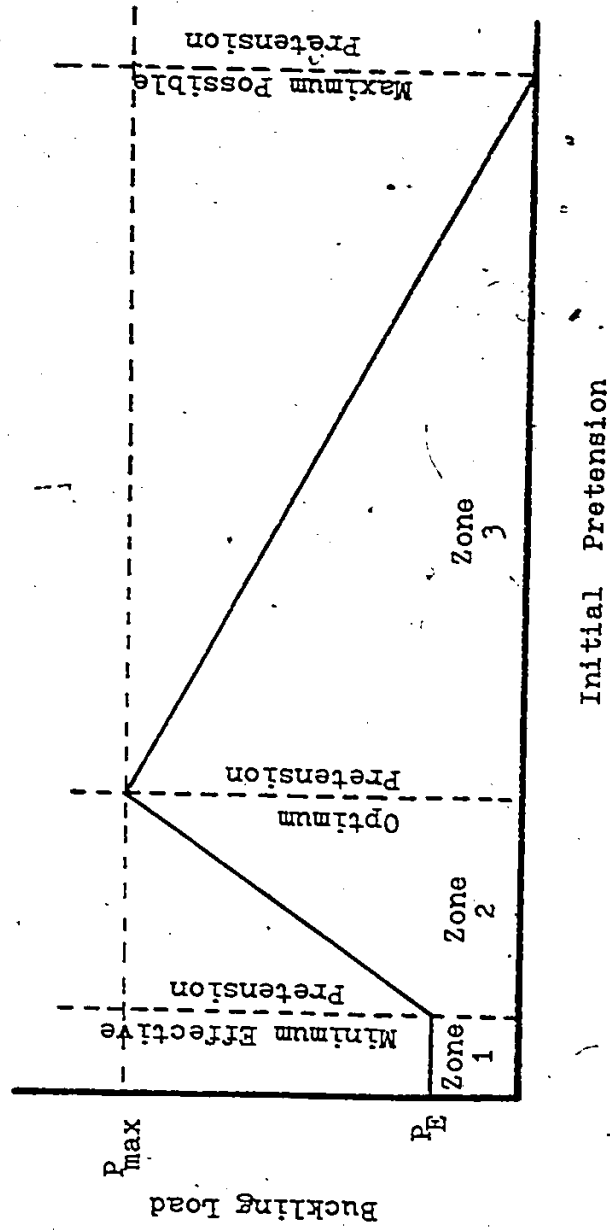


Fig. 3.4 Initial Pretension versus Buckling Load.

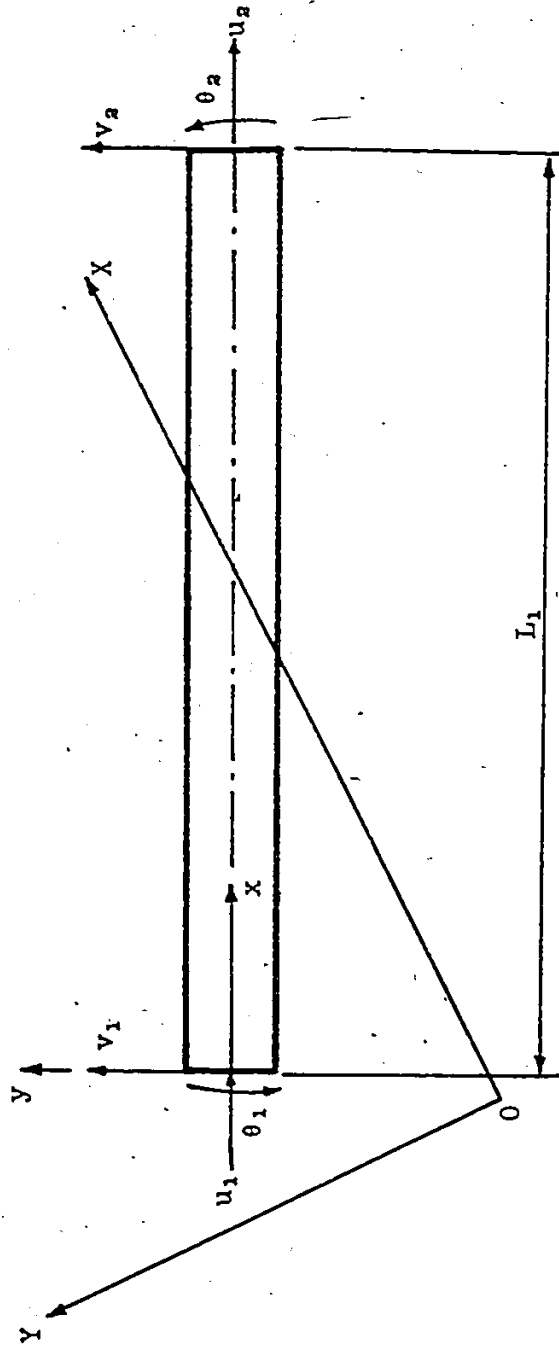


Fig. 4.1 Beam Element for Two-Dimensional Structures.

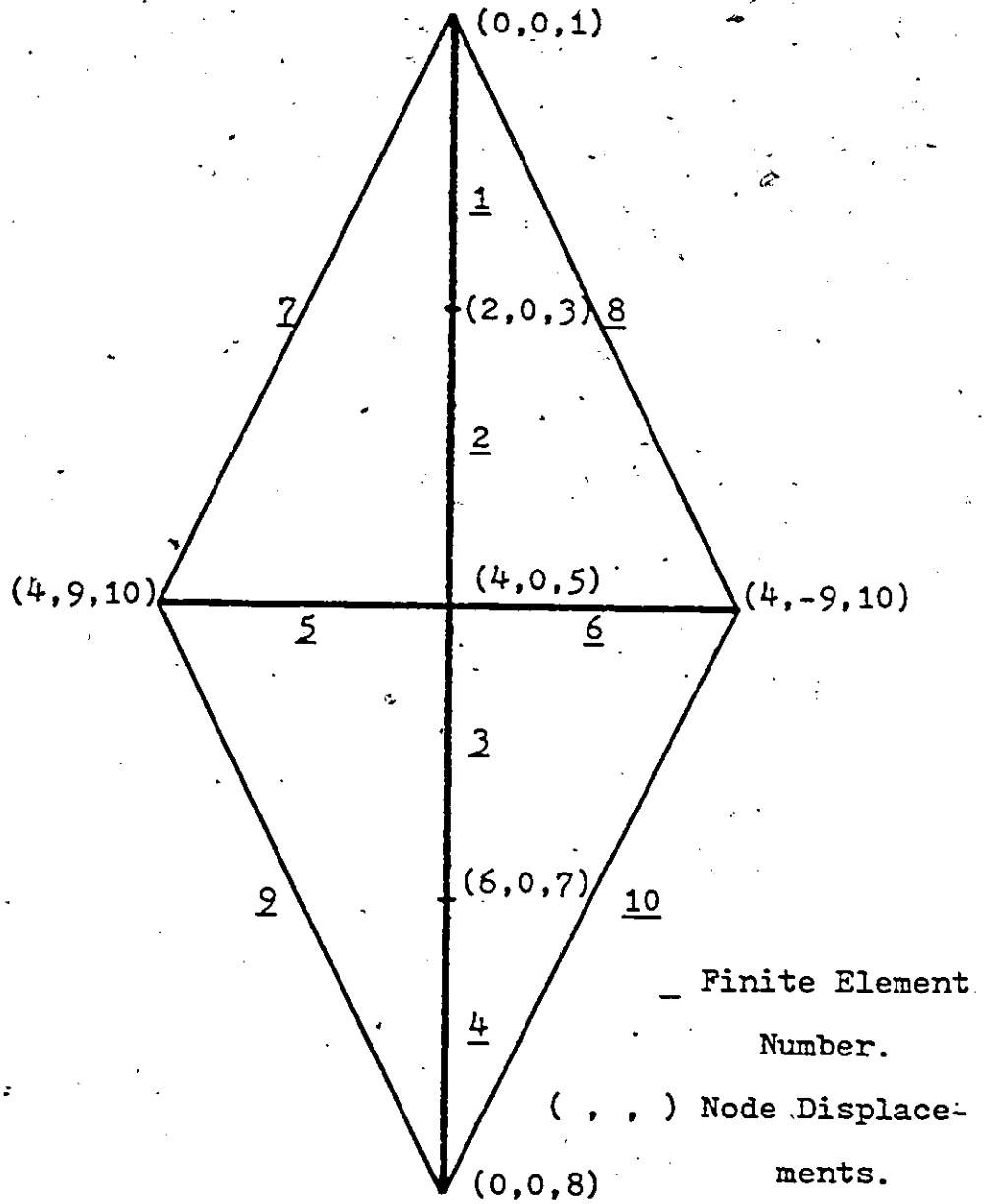


Fig. 4.2 Finite Elements and Assumed Possible Node Displacements for a Single-Crossarm Stayed Column.

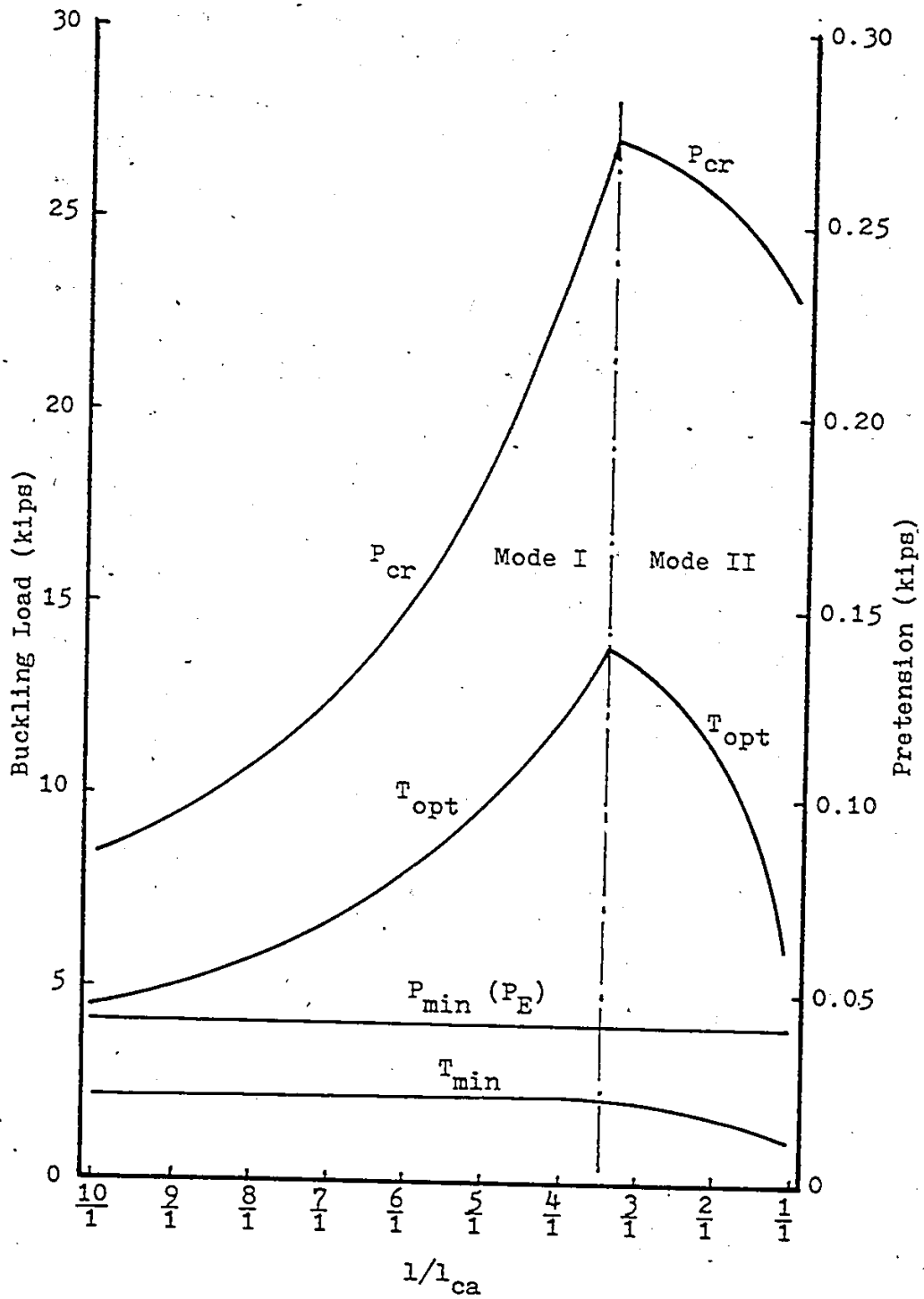


Fig. 5.1 Effect of Crossarm Length for a Stay Diameter of $3/16$ in. and Modulus of Elasticity of 9400 ksi.

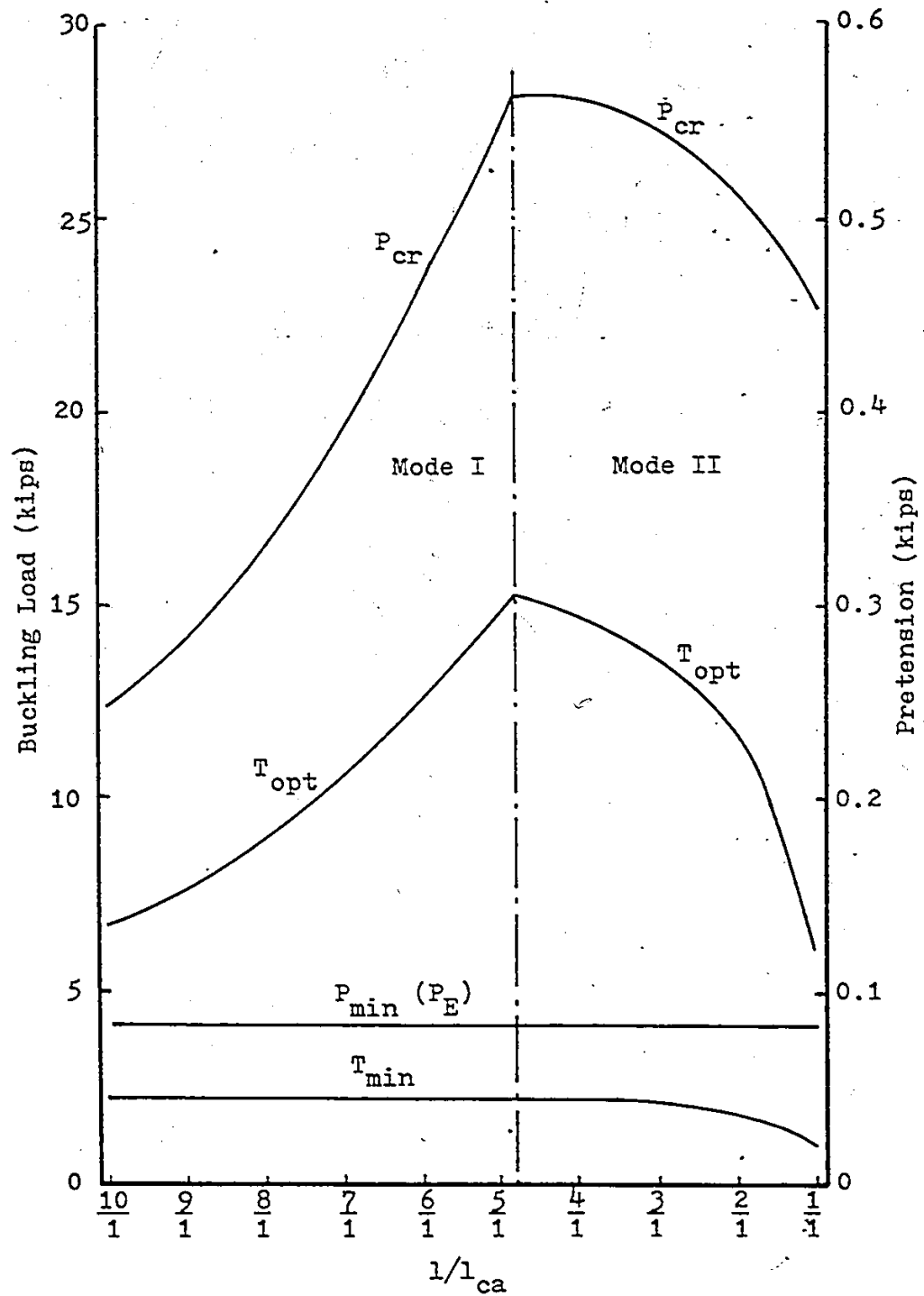


Fig. 5.2 Effect of Crossarm Length for a Stay Diameter of $\frac{3}{16}$ in. and Modulus of Elasticity of 19500 ksi.

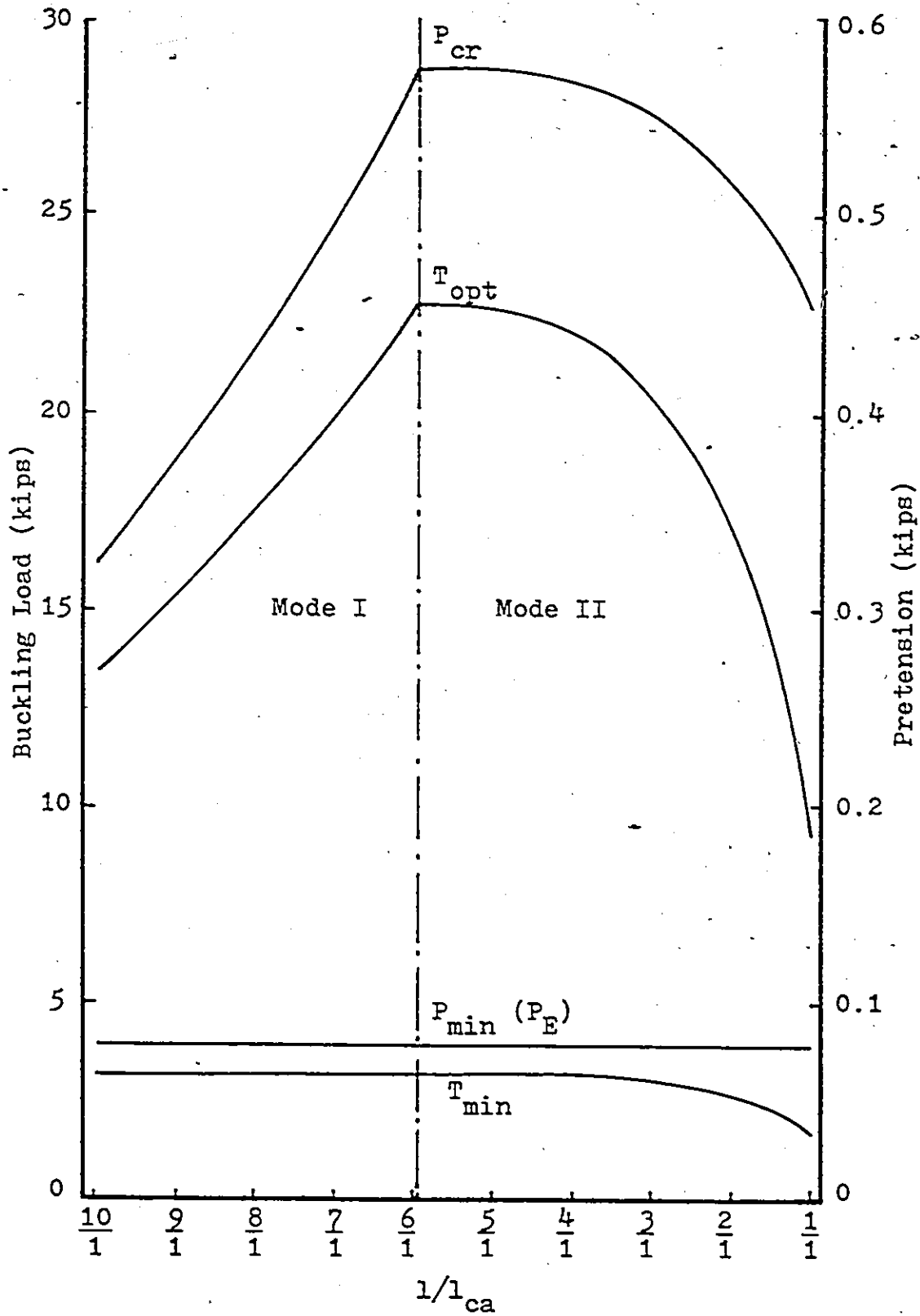


Fig. 5.3 Effect of Crossarm Length for a Stay Diameter of $3/16$ in. and Modulus of Elasticity of 29600 ksi.

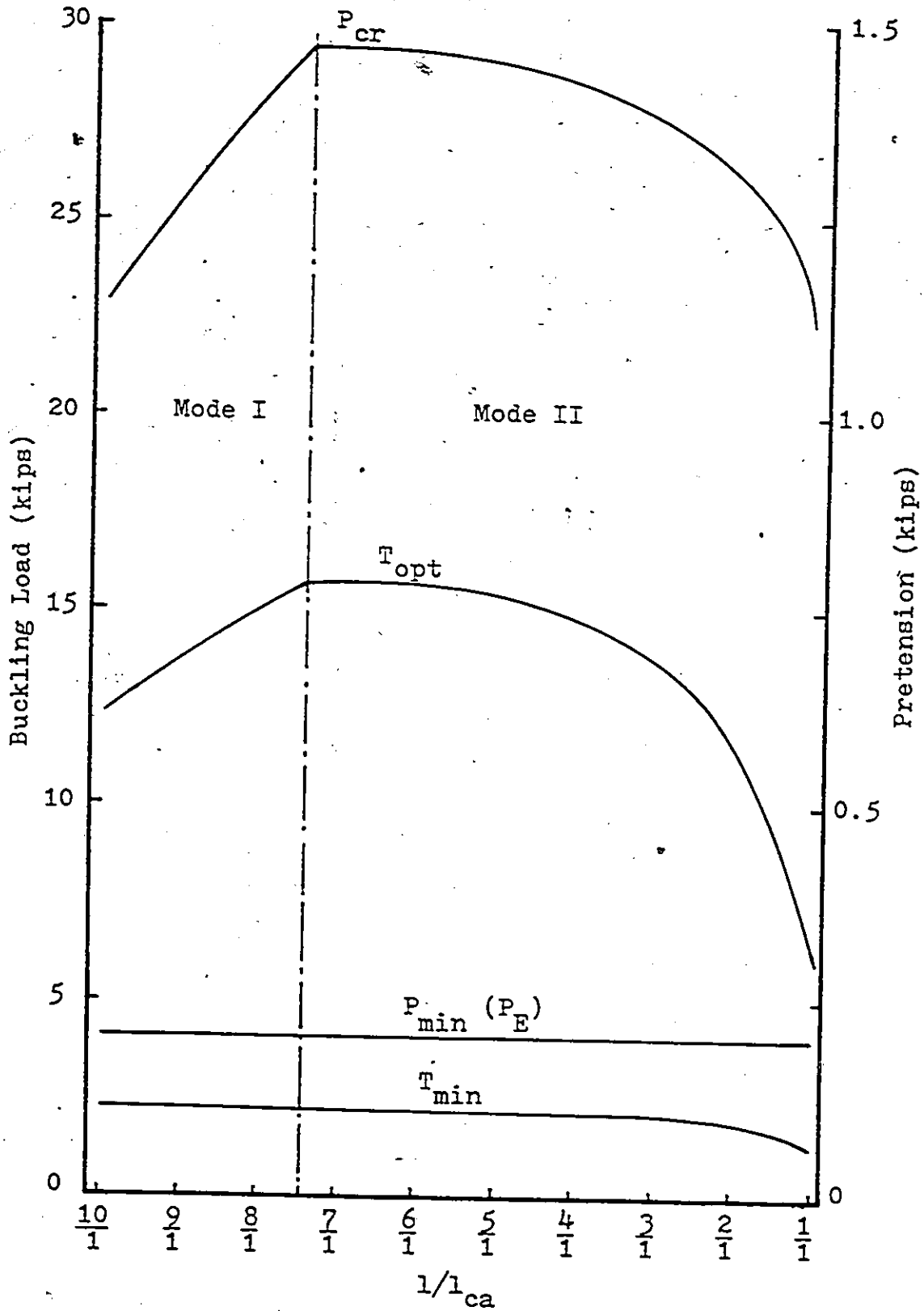


Fig. 5.4 Effect of Crossarm Length for a Stay Diameter of 7/16 in. and Modulus of Elasticity of 9400 ksi.

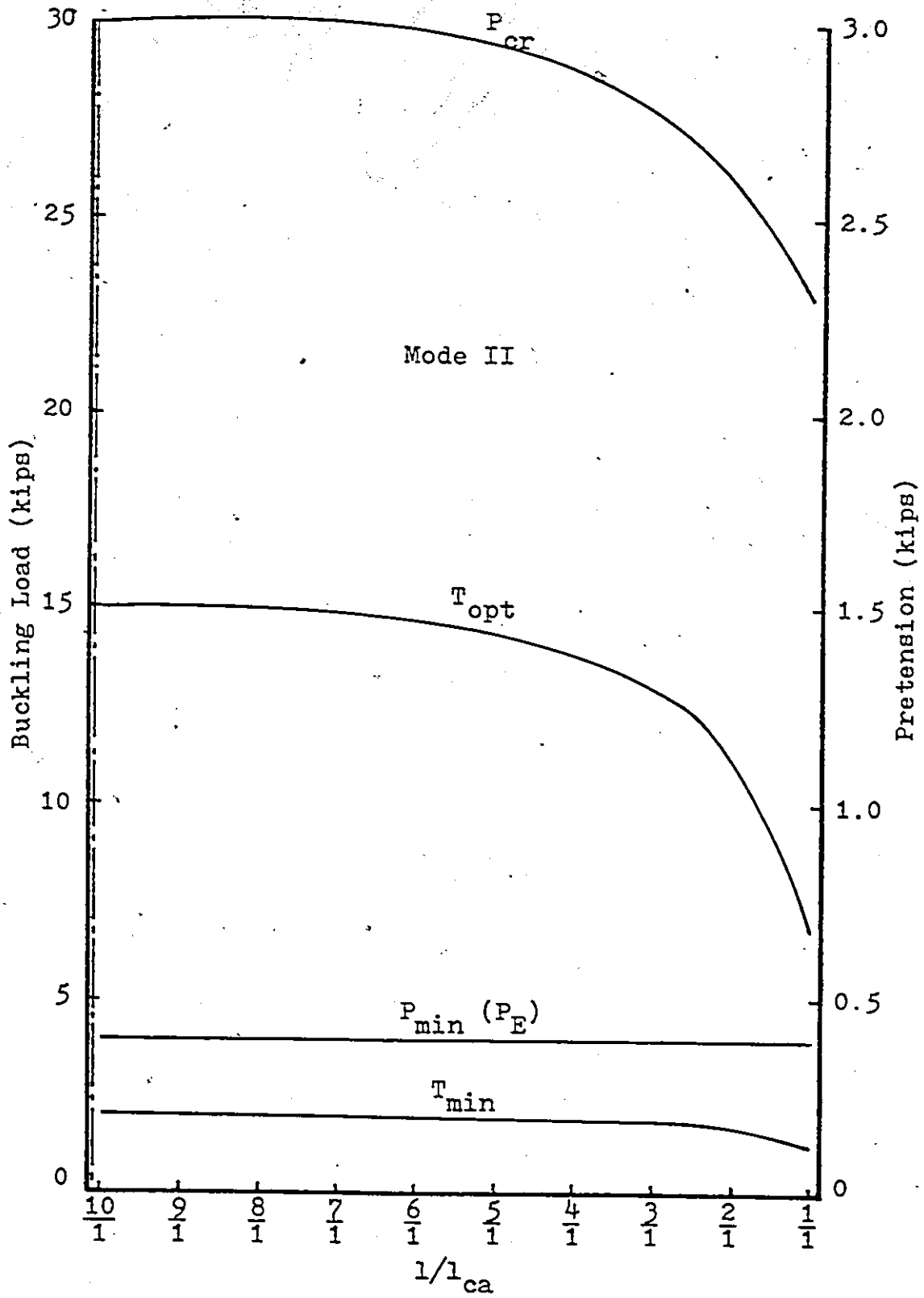


Fig. 5.5 Effect of Crossarm Length for a Stay Diameter of 7/16 in. and Modulus of Elasticity of 19500 ksi.

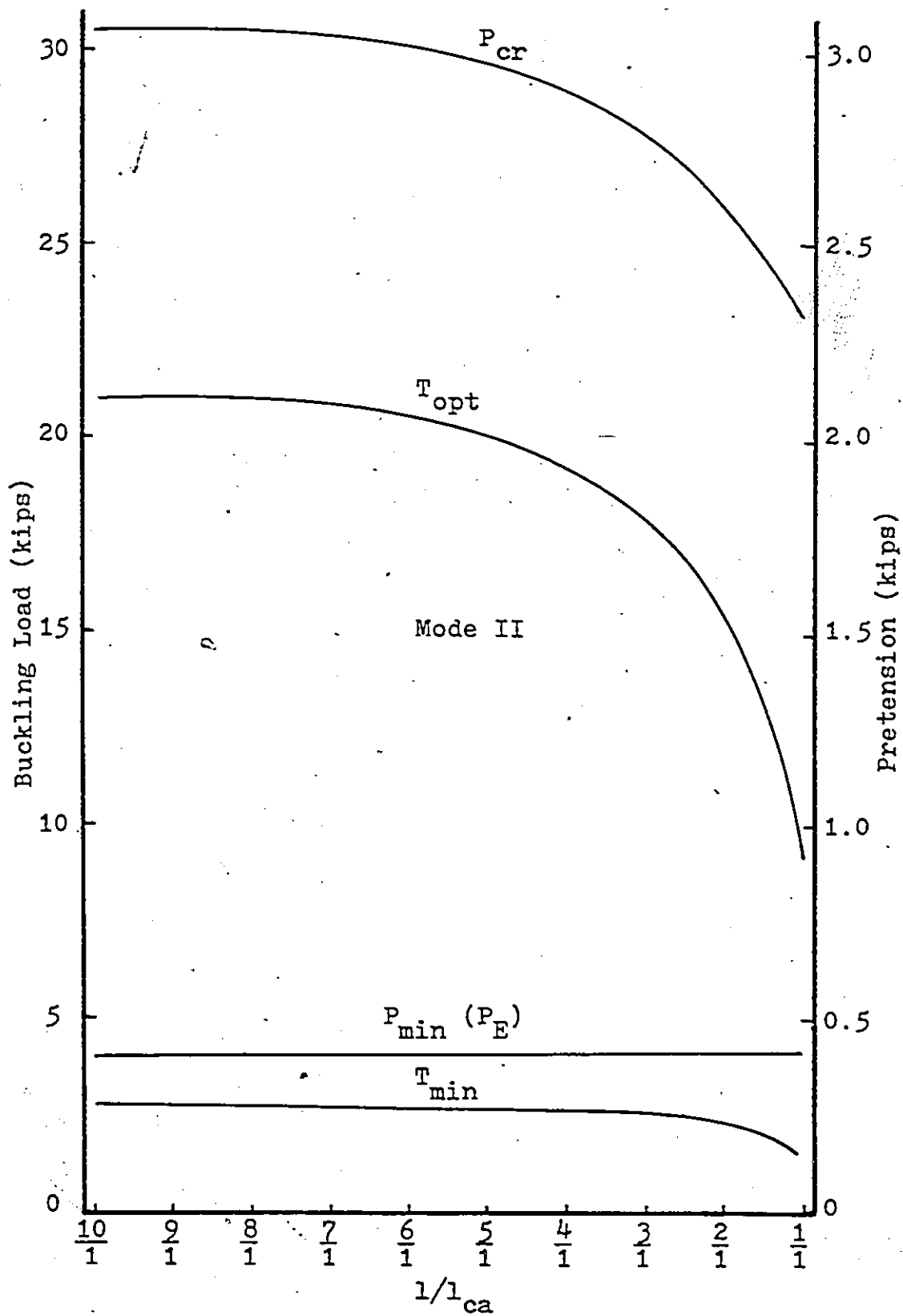


Fig. 5.6 Effect of Crossarm Length for a Stay Diameter of 7/16 in. and Modulus of Elasticity of 29600 ksi.

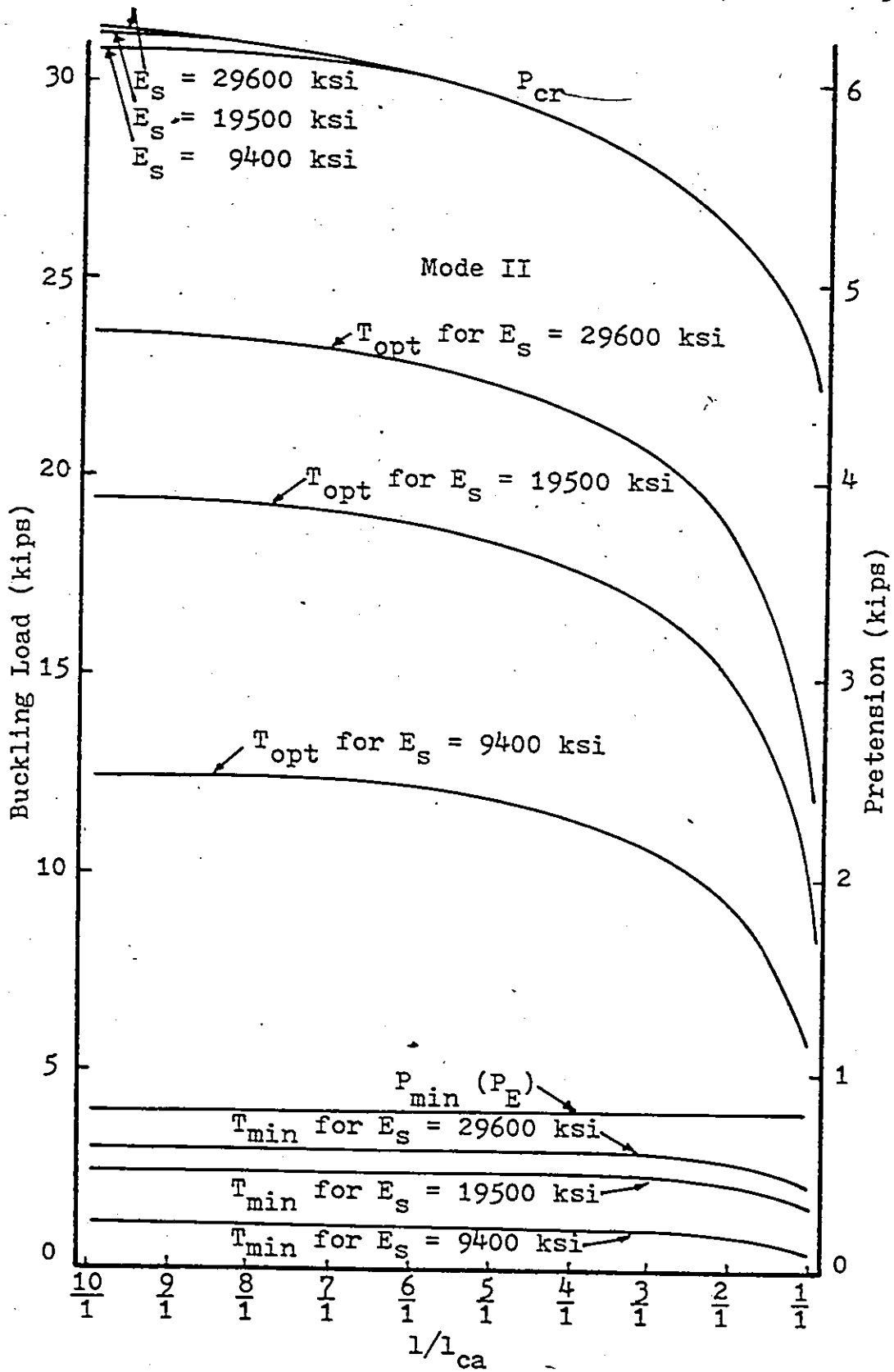


Fig. 5.7 Effect of Crossarm Length for a Stay Diameter of 7/8 in. and Various Values of Stay Modulus of Elasticity.

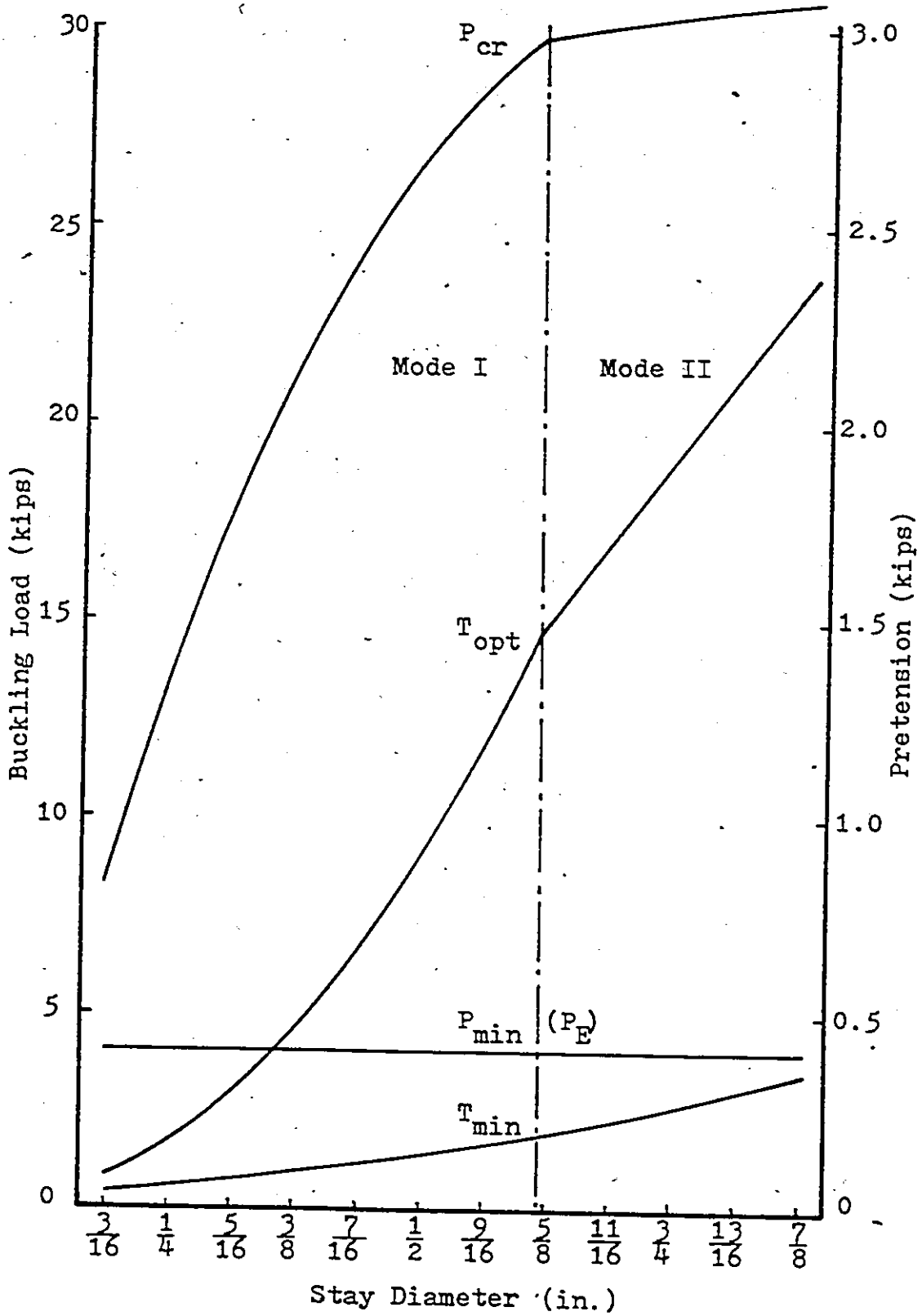


Fig. 5.8 Effect of Stay Diameter for a Ratio of $1/1_{ca}$ of Ten and Stay Modulus of Elasticity of 9400 ksi.

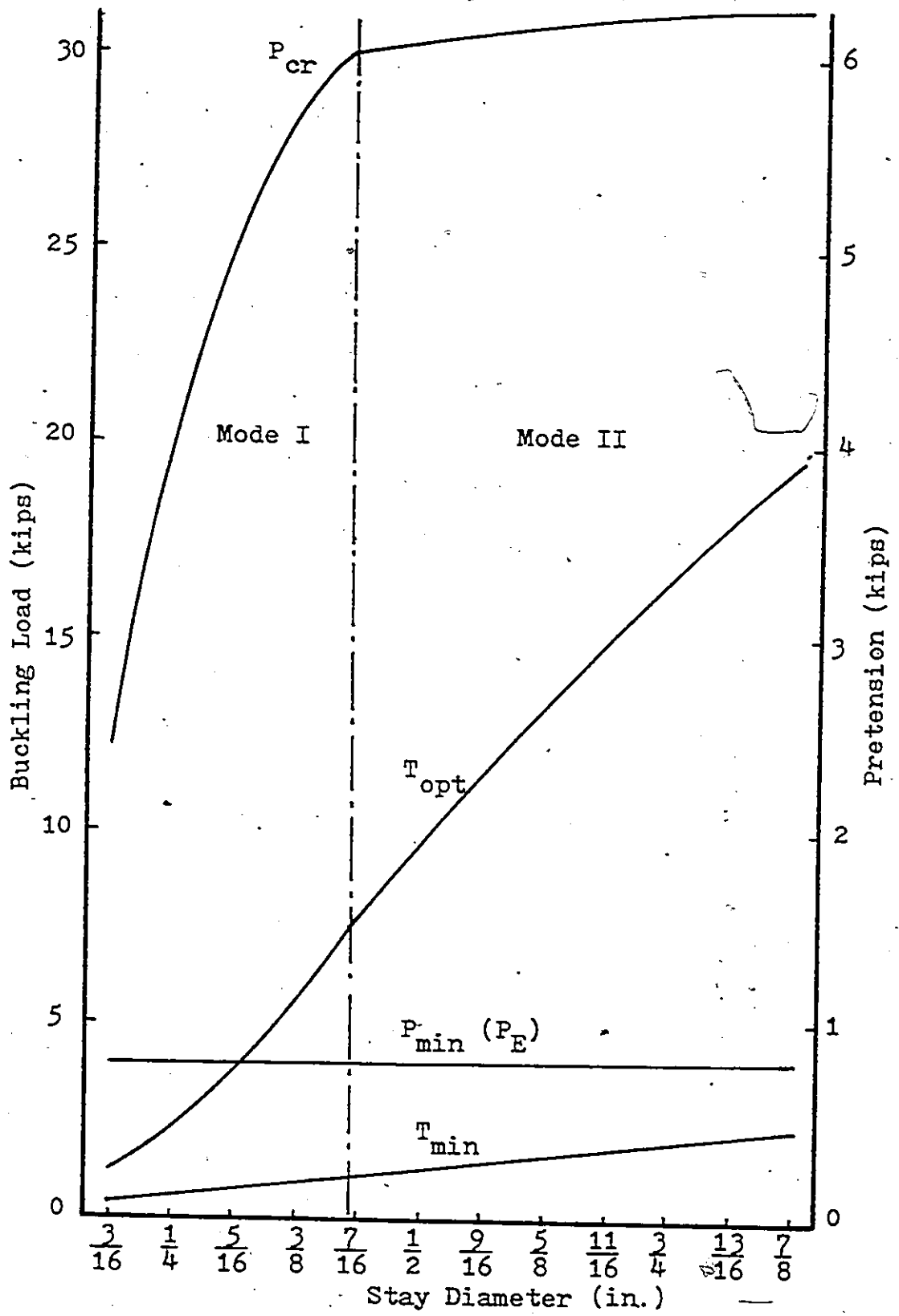


Fig. 5.9 Effect of Stay Diameter for a Ratio of $1/l_{ca}$ of Ten and Stay Modulus of Elasticity of 19500 ksi.

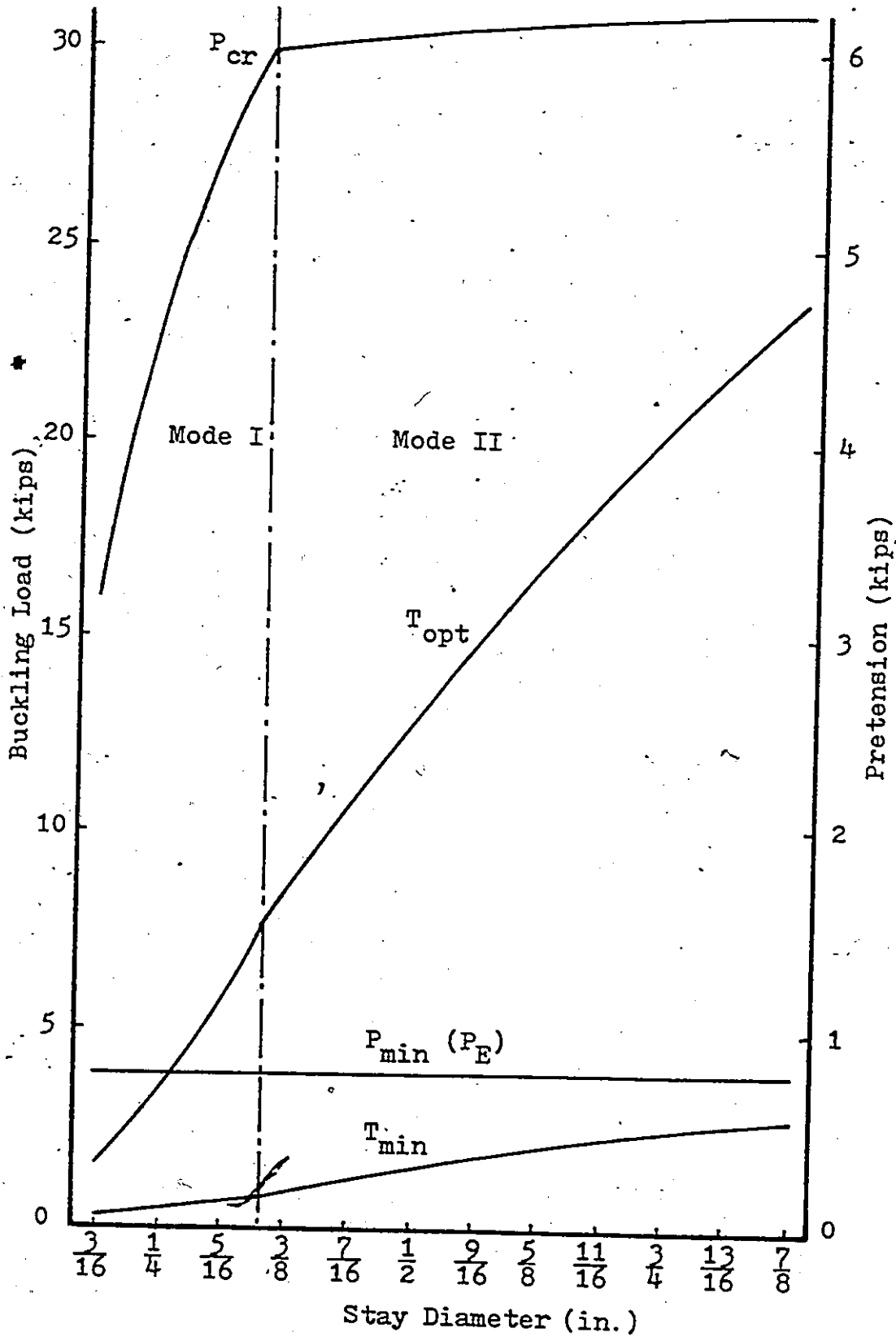


Fig. 5.10 Effect of Stay Diameter for a Ratio of $1/l_{ca}$ of Ten and Stay Modulus of Elasticity of 29600 ksi.

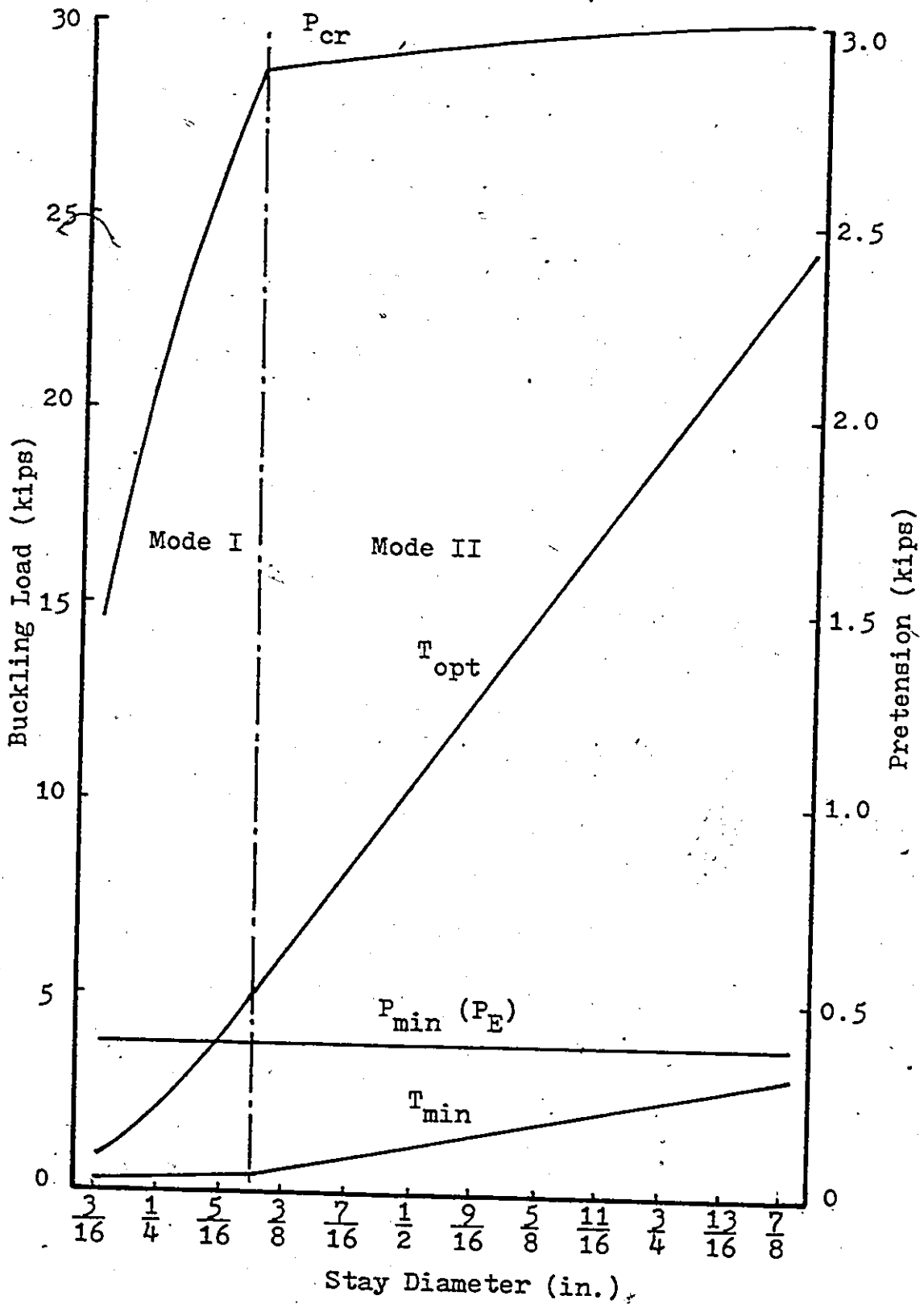


Fig. 5.11 Effect of Stay Diameter for a Ratio of l/l_{ca} of Six and Stay Modulus of Elasticity of 9400 ksi.

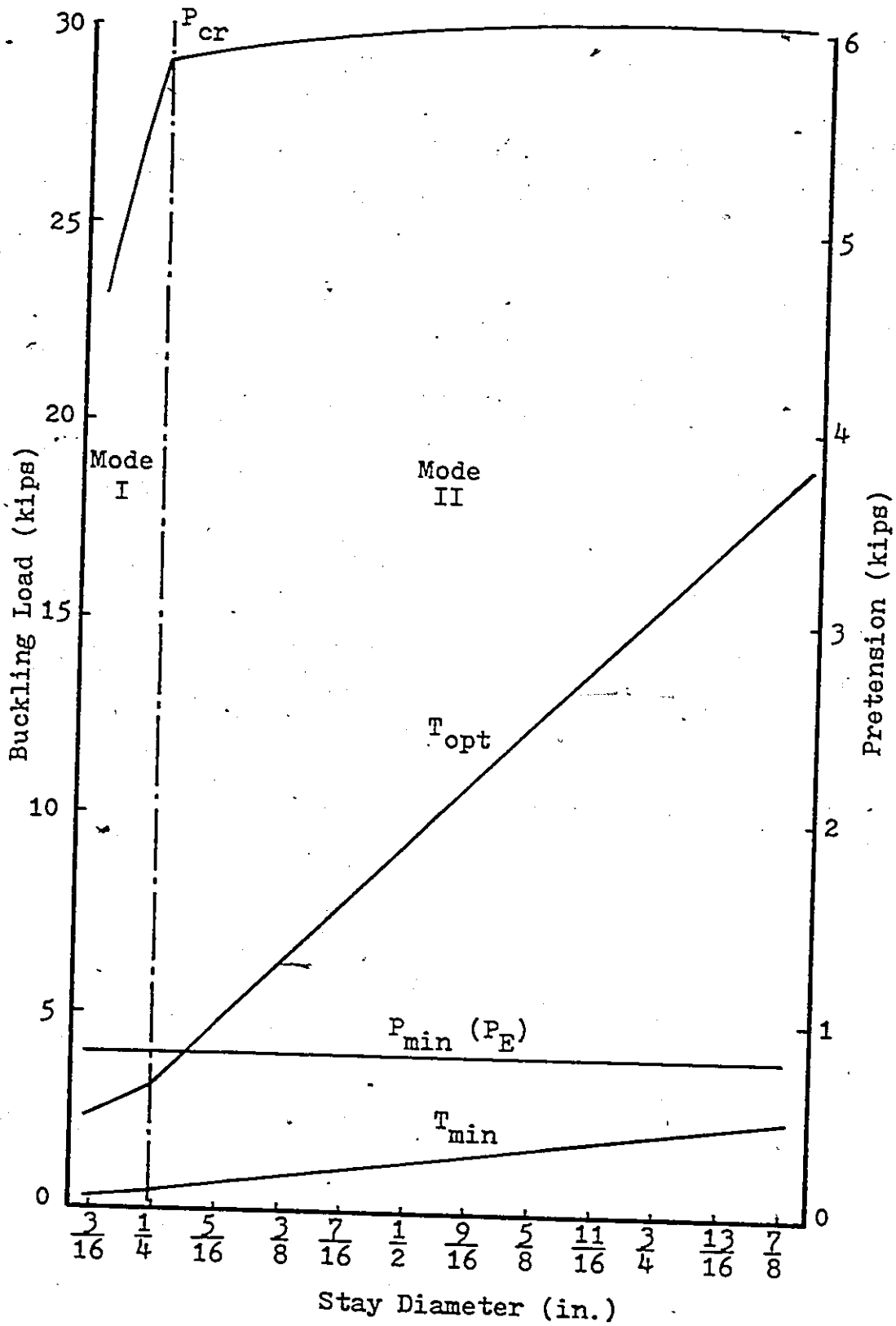


Fig. 5.12 Effect of Stay Diameter for a Ratio of l/l_{ca} of Six and Stay Modulus of Elasticity of 19500 ksi.

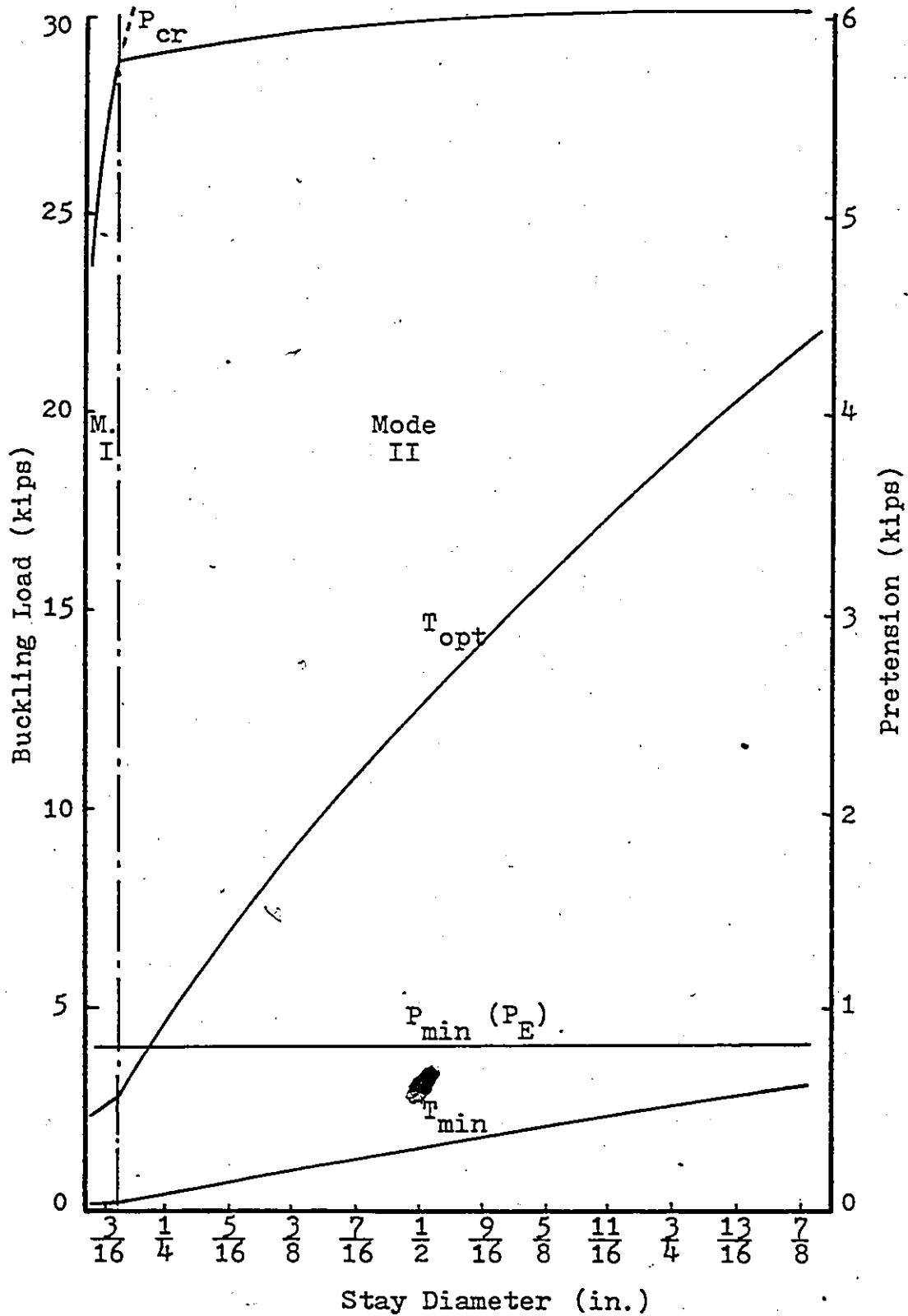


Fig. 5.13 Effect of Stay Diameter for a Ratio of $1/l_{ca}$ of Six and Stay Modulus of Elasticity of 29600 ksi.

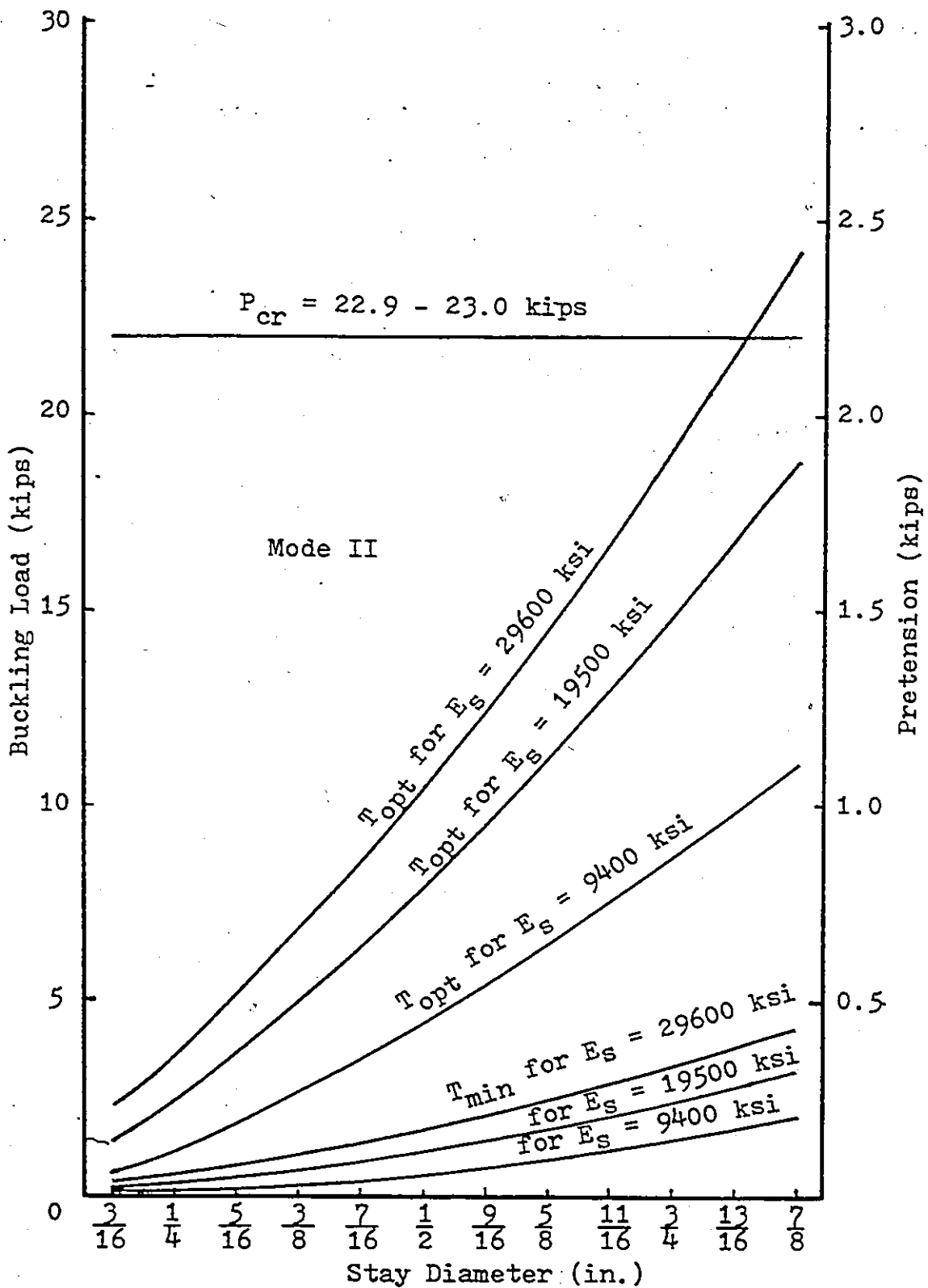


Fig. 5.14 Effect of Stay Diameter for a Ratio of $1/l_{ca}$ of One and Various Values of Stay Modulus of Elasticity.

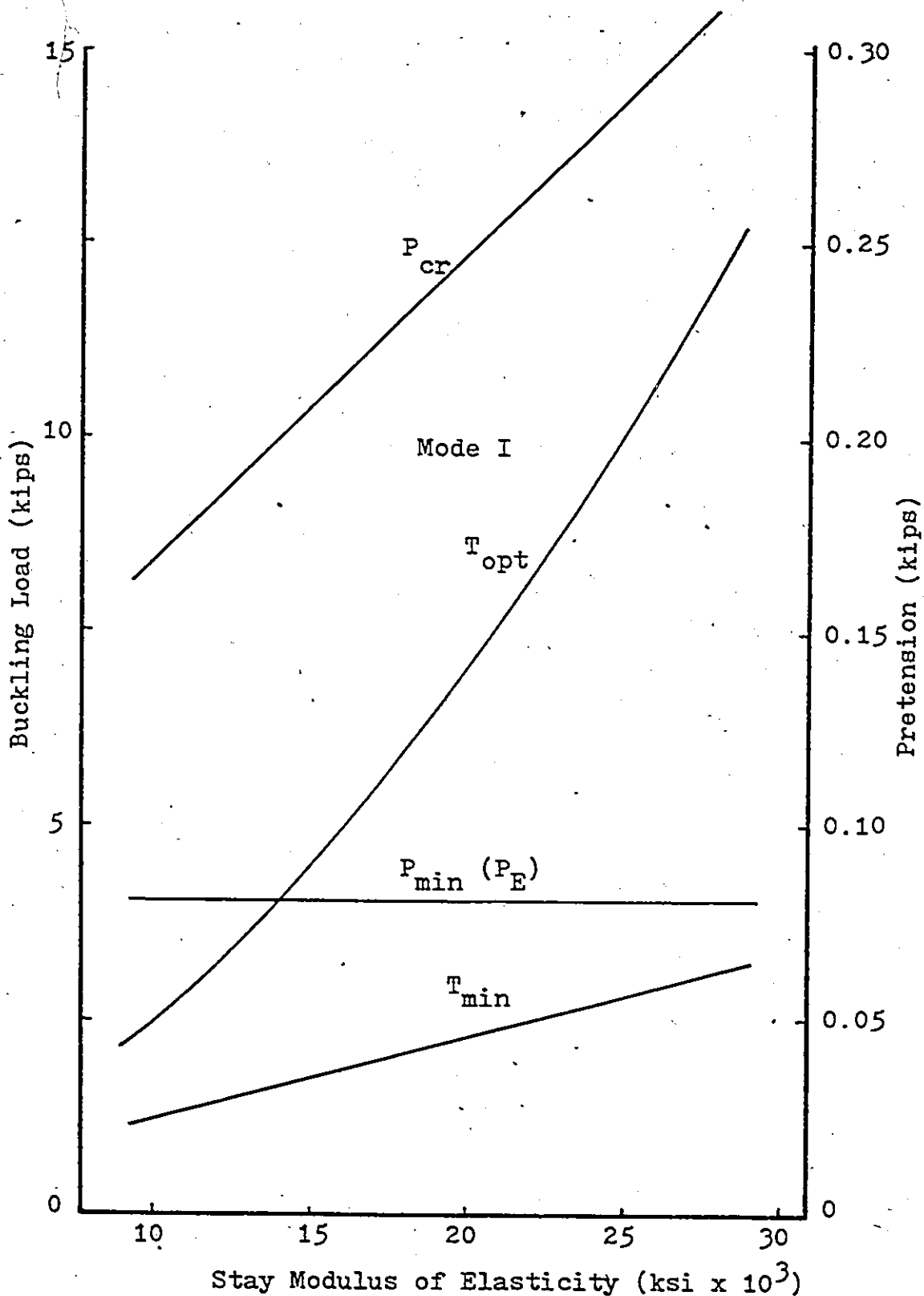


Fig. 5.15 Effect of Stay Modulus of Elasticity for a Ratio of l/l_{ca} of Ten and Stay Diameter of 3/16 in.

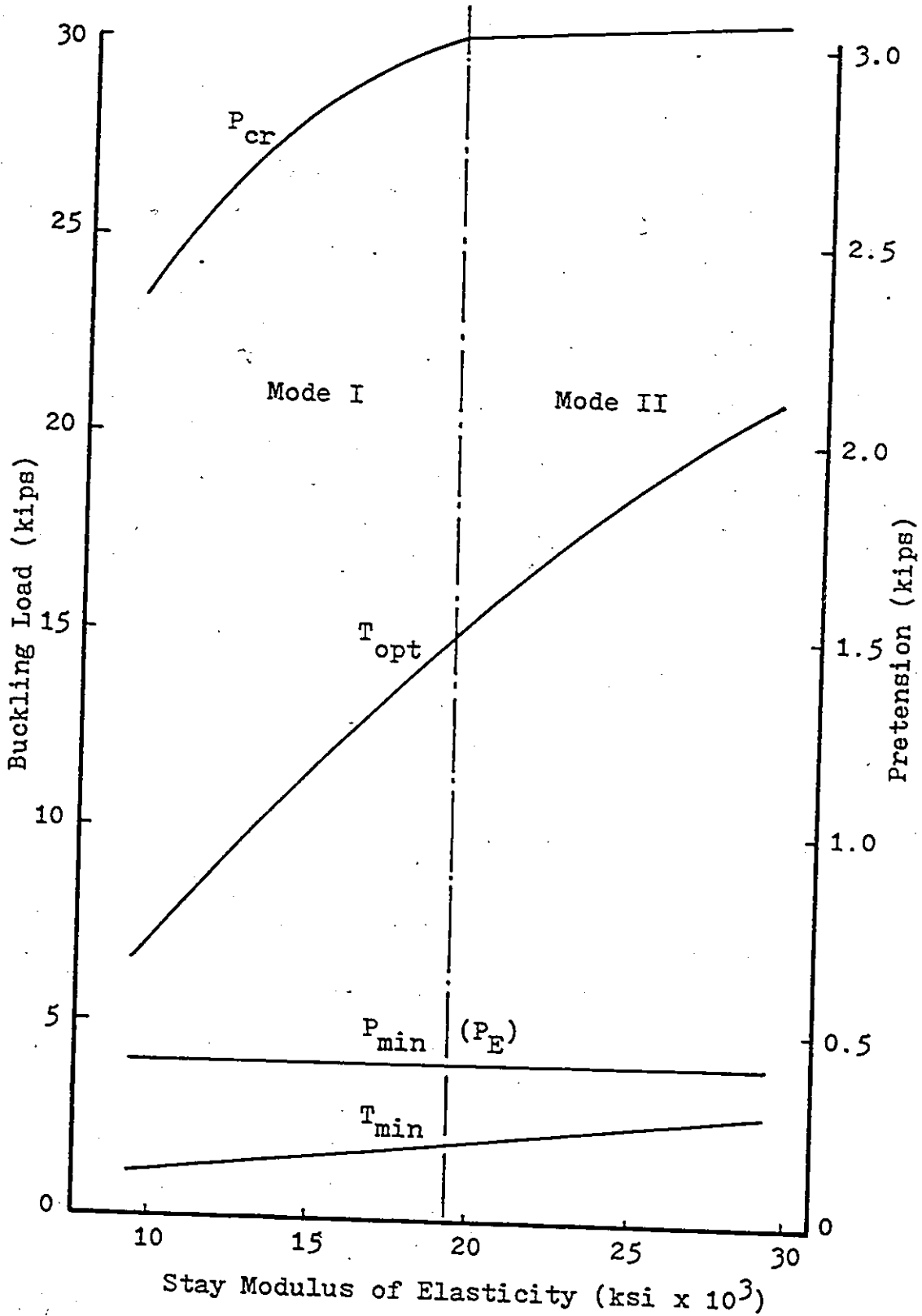


Fig. 5.16 Effect of Stay Modulus of Elasticity for a Ratio of l/l_{ca} of Ten and Stay Diameter of 7/16 in.

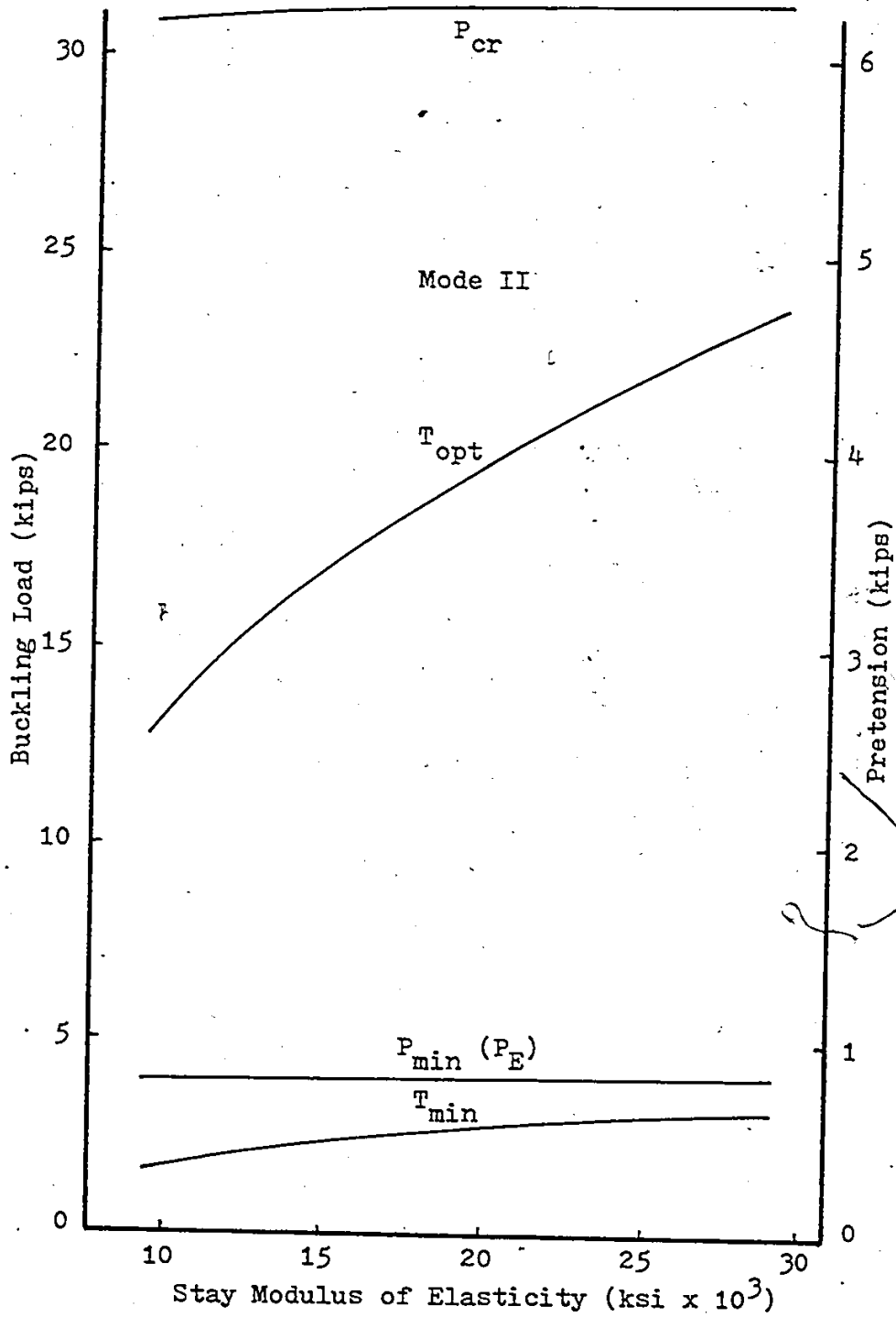


Fig. 5.17 Effect of Stay Modulus of Elasticity for a Ratio of l/l_{ca} of Ten and Stay Diameter of 7/8 in.

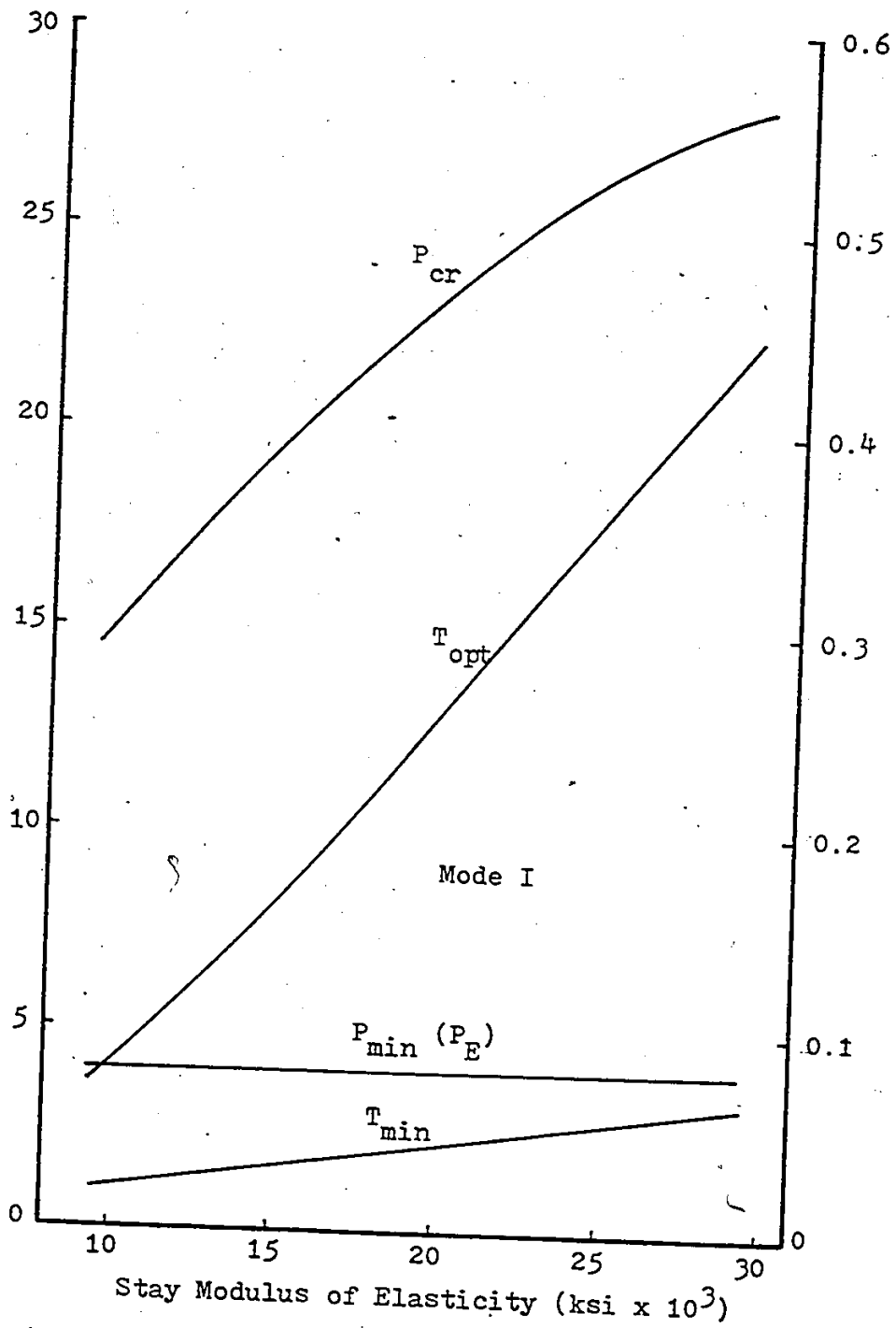


Fig. 5.18 Effect of Stay Modulus of Elasticity for a Ratio of l/l_{ca} of Six and Stay Diameter of 3/16 in.

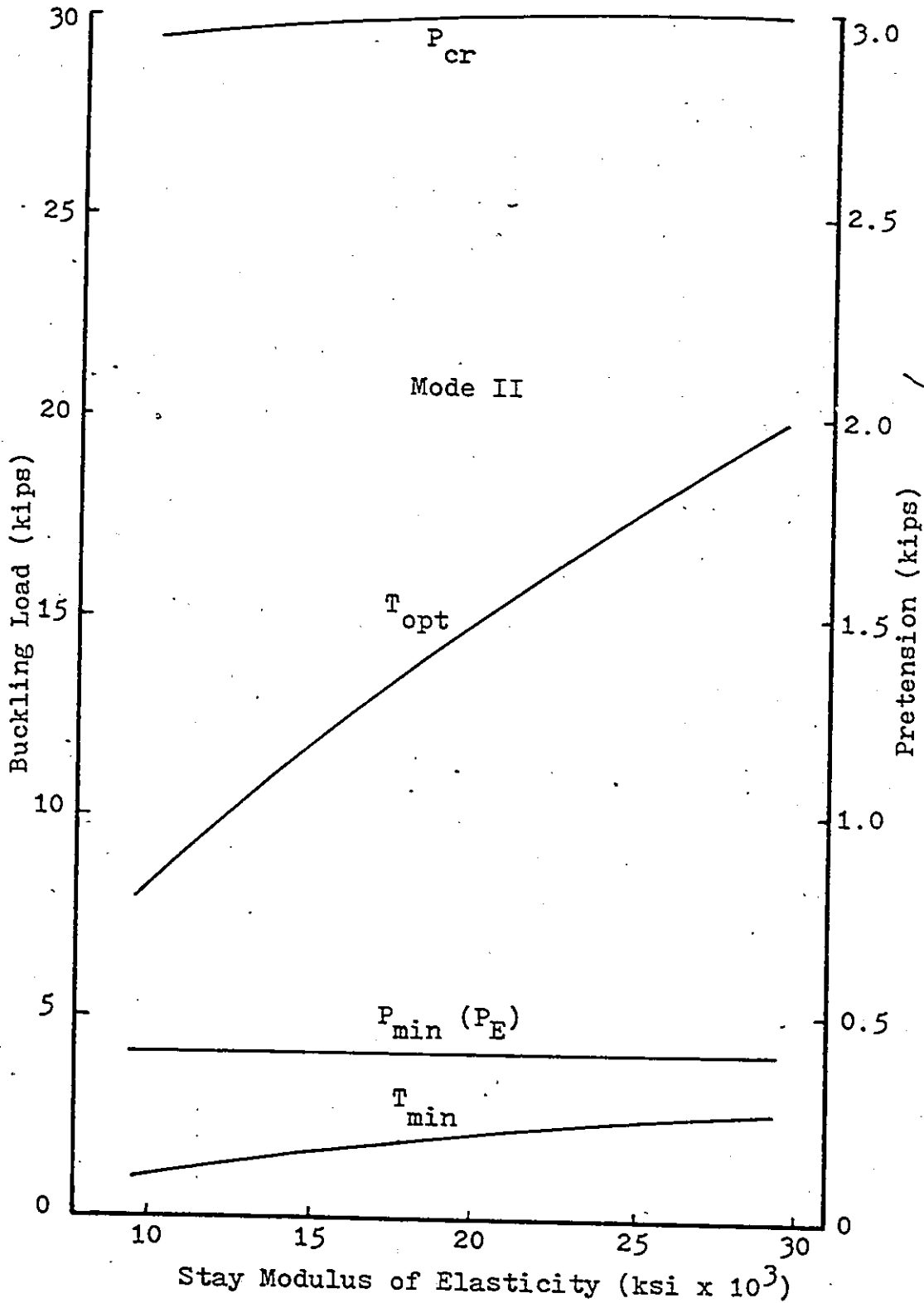


Fig. 5.19 Effect of Stay Modulus of Elasticity for a Ratio of l/l_{ca} of Six and Stay Diameter of 7/16 in.

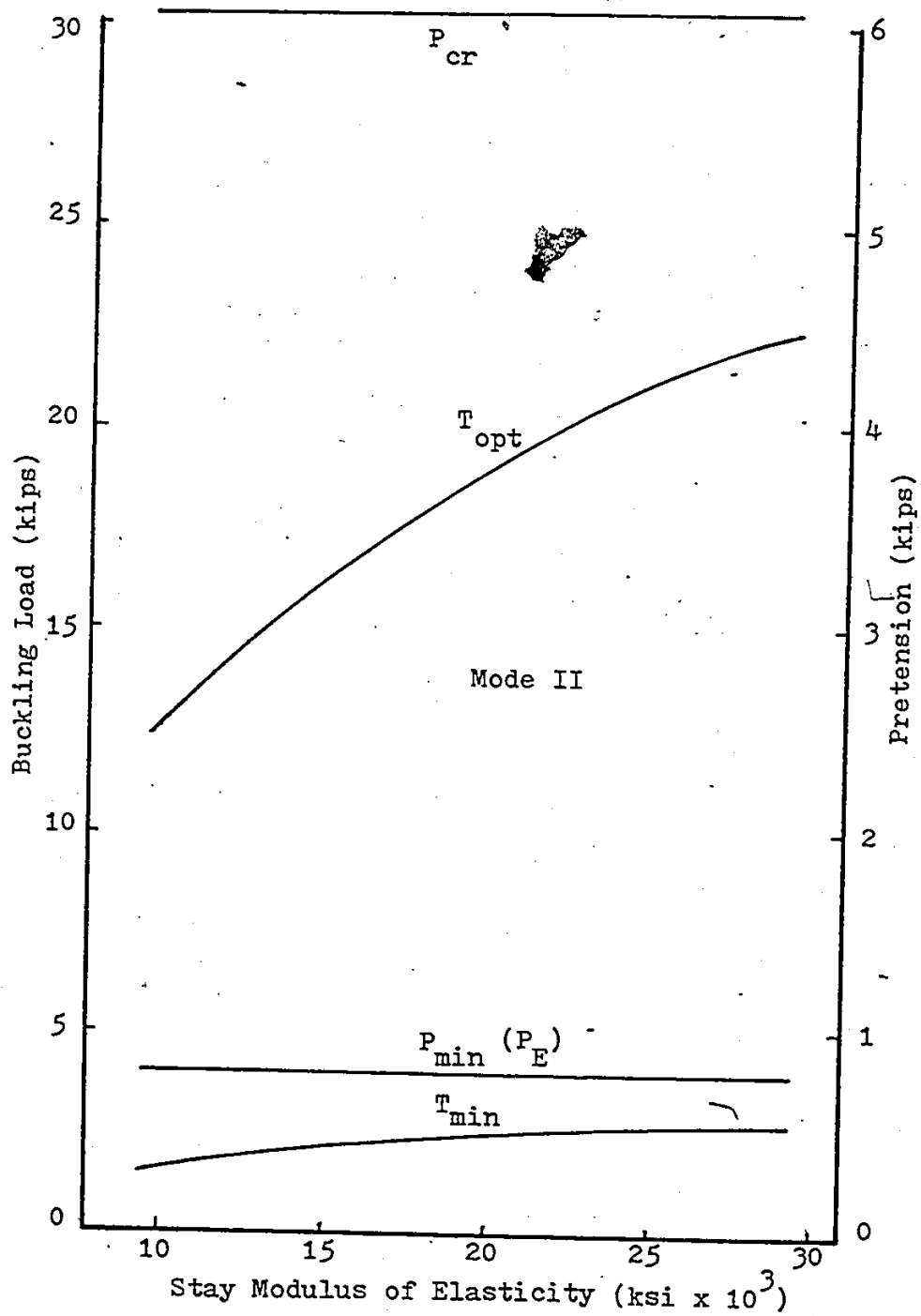


Fig. 5.20 Effect of Stay Modulus of Elasticity for a Ratio of l/l_{ca} of Six and Stay Diameter of 7/8 in.

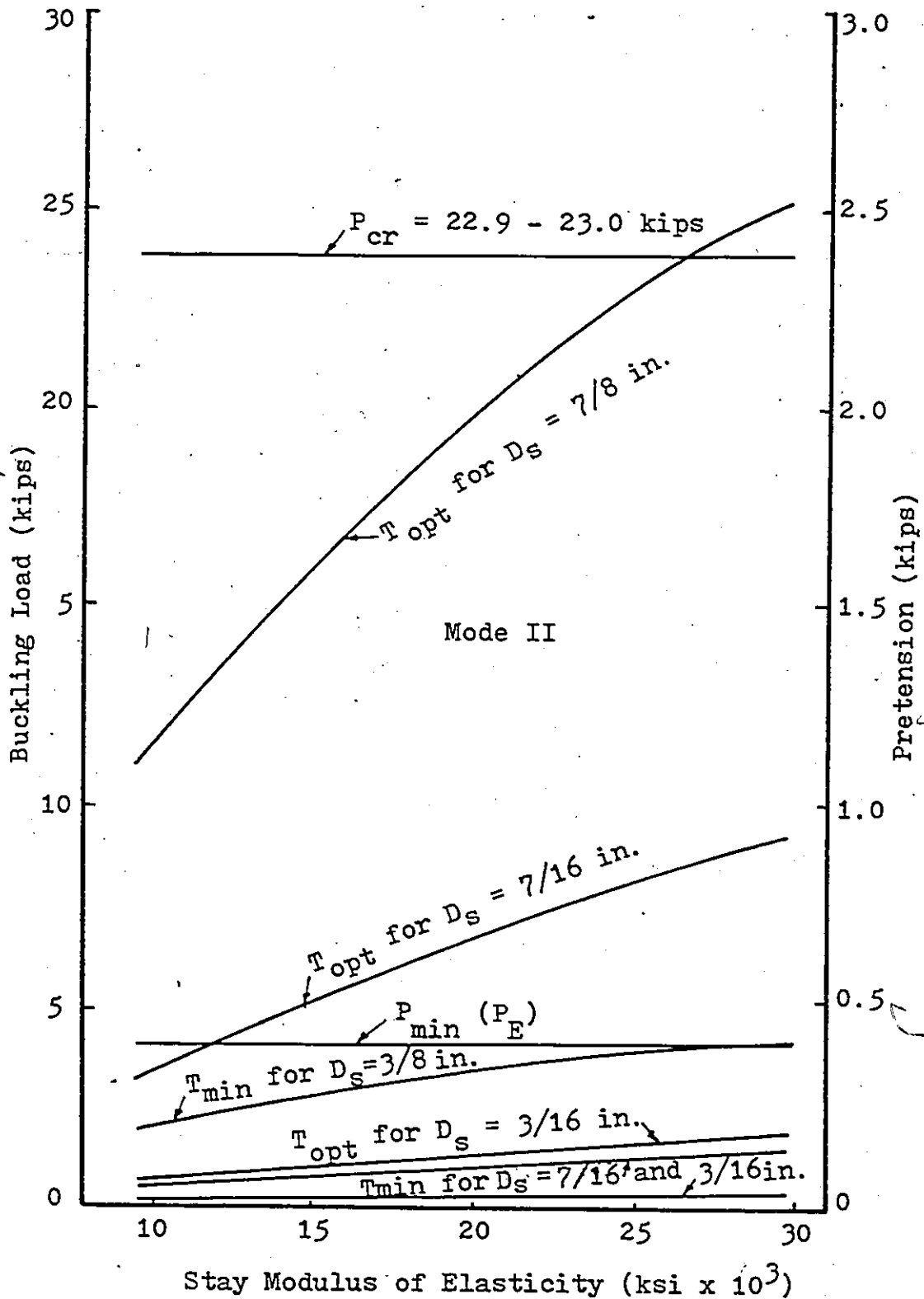


Fig. 5.21 Effect of Stay Modulus of Elasticity for a Ratio of l/l_{ca} of One and Various Values of Stay Diameter.

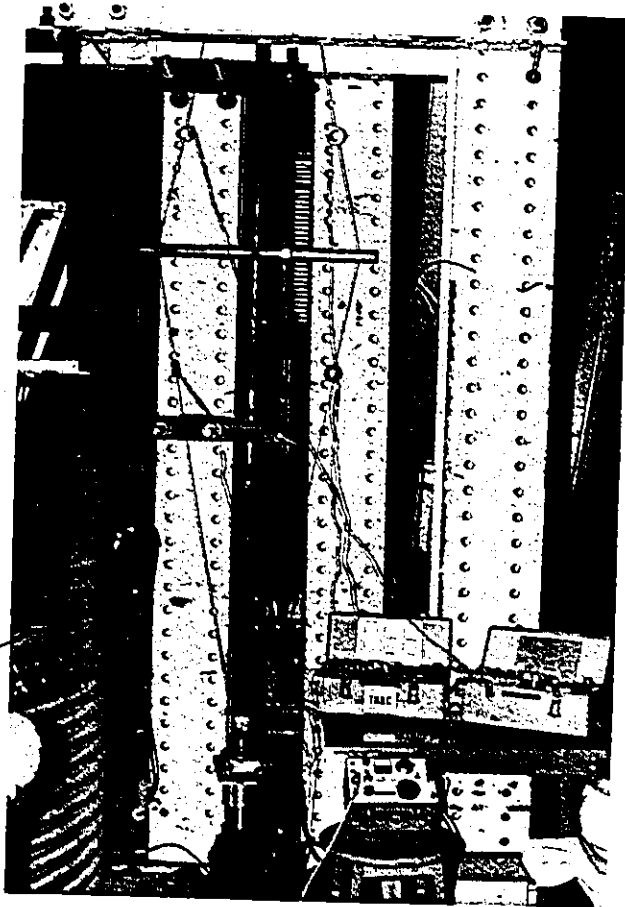


Fig. 6.1 Plane Single-Crossarm Stayed Column.

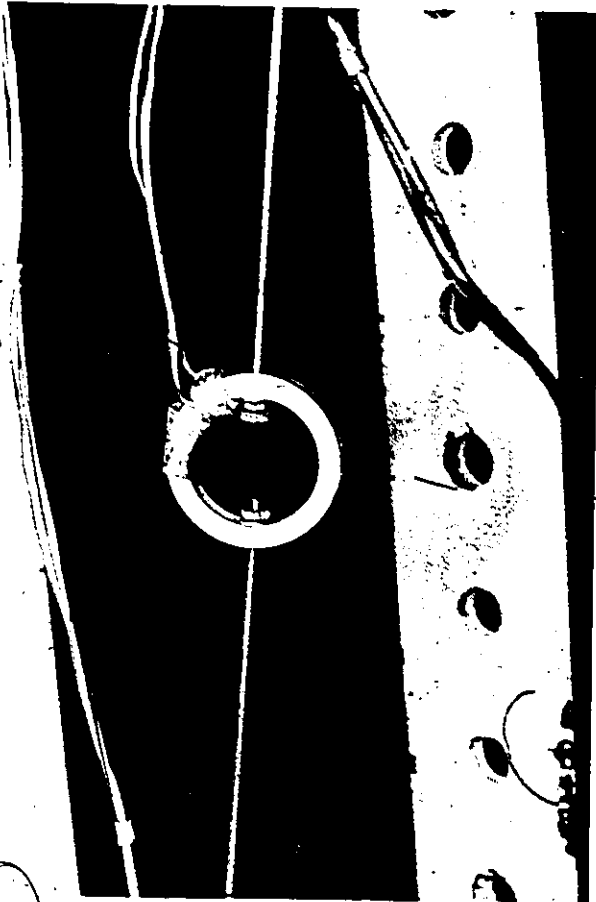


Fig. 6.2 Ring Beam Load Cell.



8
Fig. 6.3 Universal Flat Load Cell.

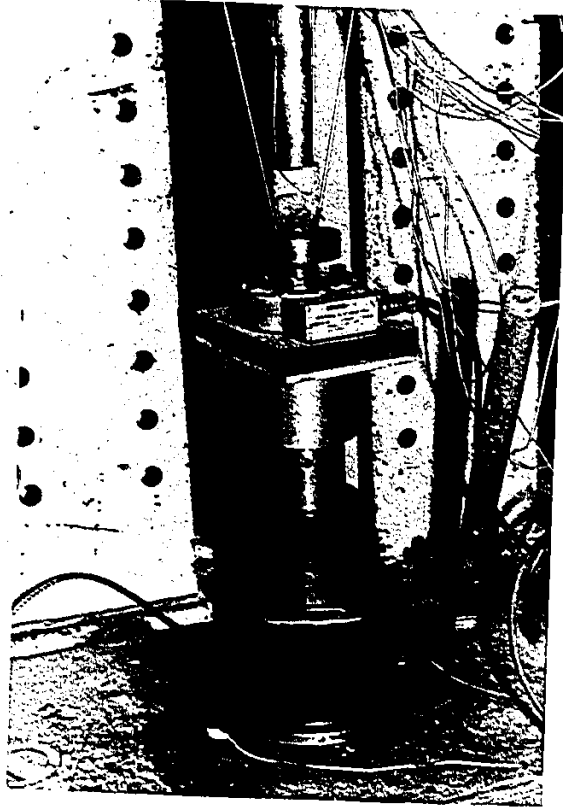


Fig. 6.4 Hydraulic Jack.

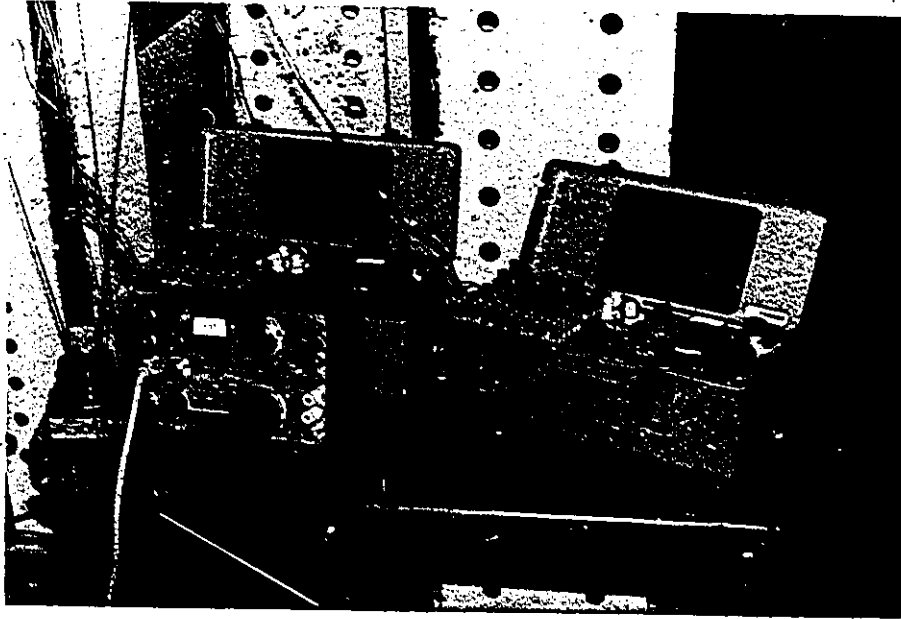


Fig. 6.5 Strain Indicators.

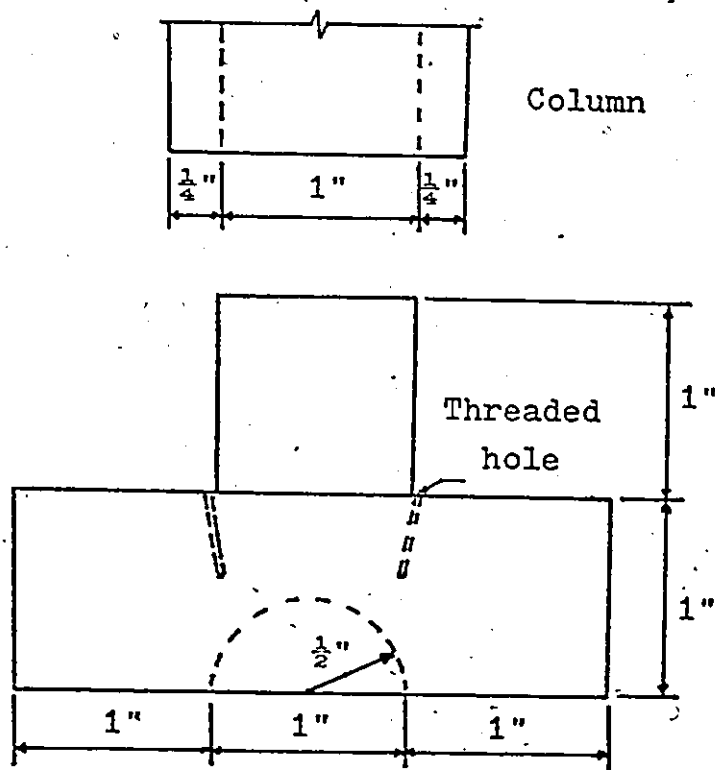


Fig. 6.6 Column Base.

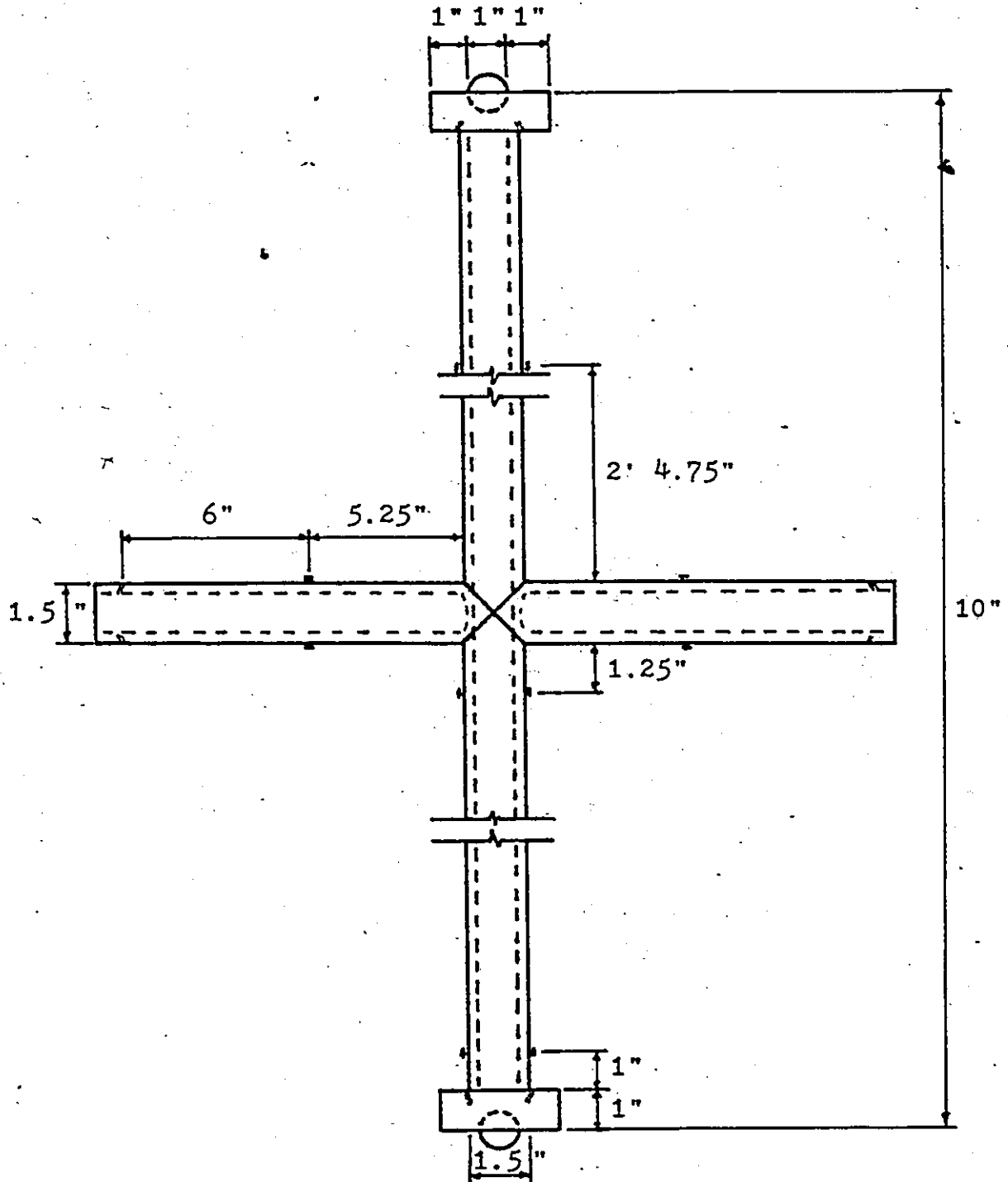


Fig. 6.7 Positions of Strain Gages on the Stayed Column.

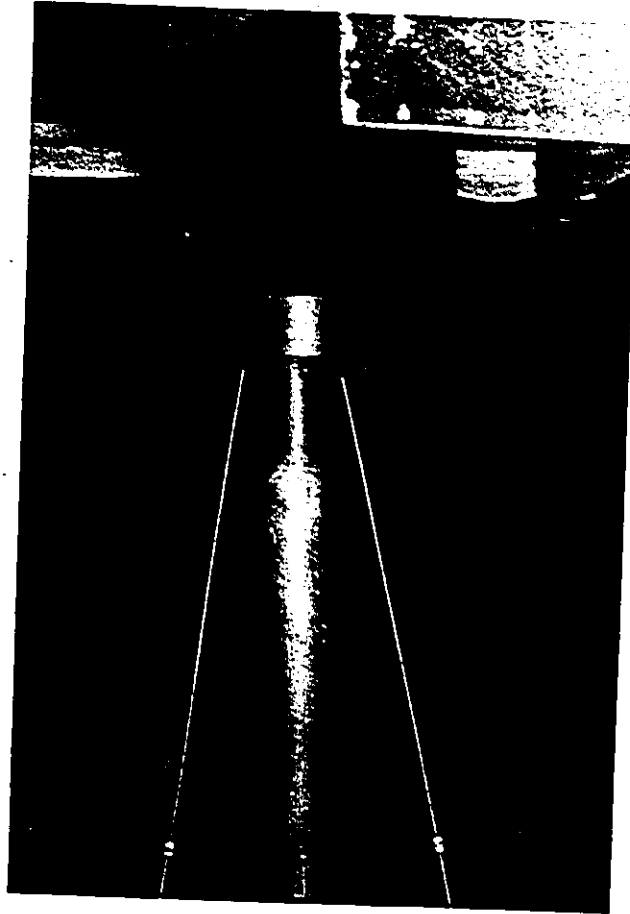


Fig. 6.8 Top Plate of the Column.

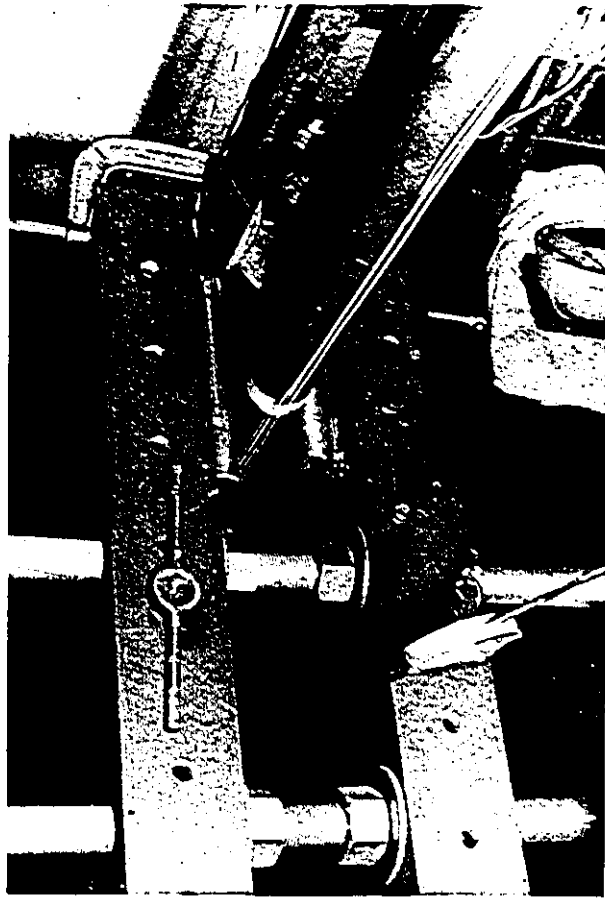


Fig. 6.9 Lateral Support of the Column.

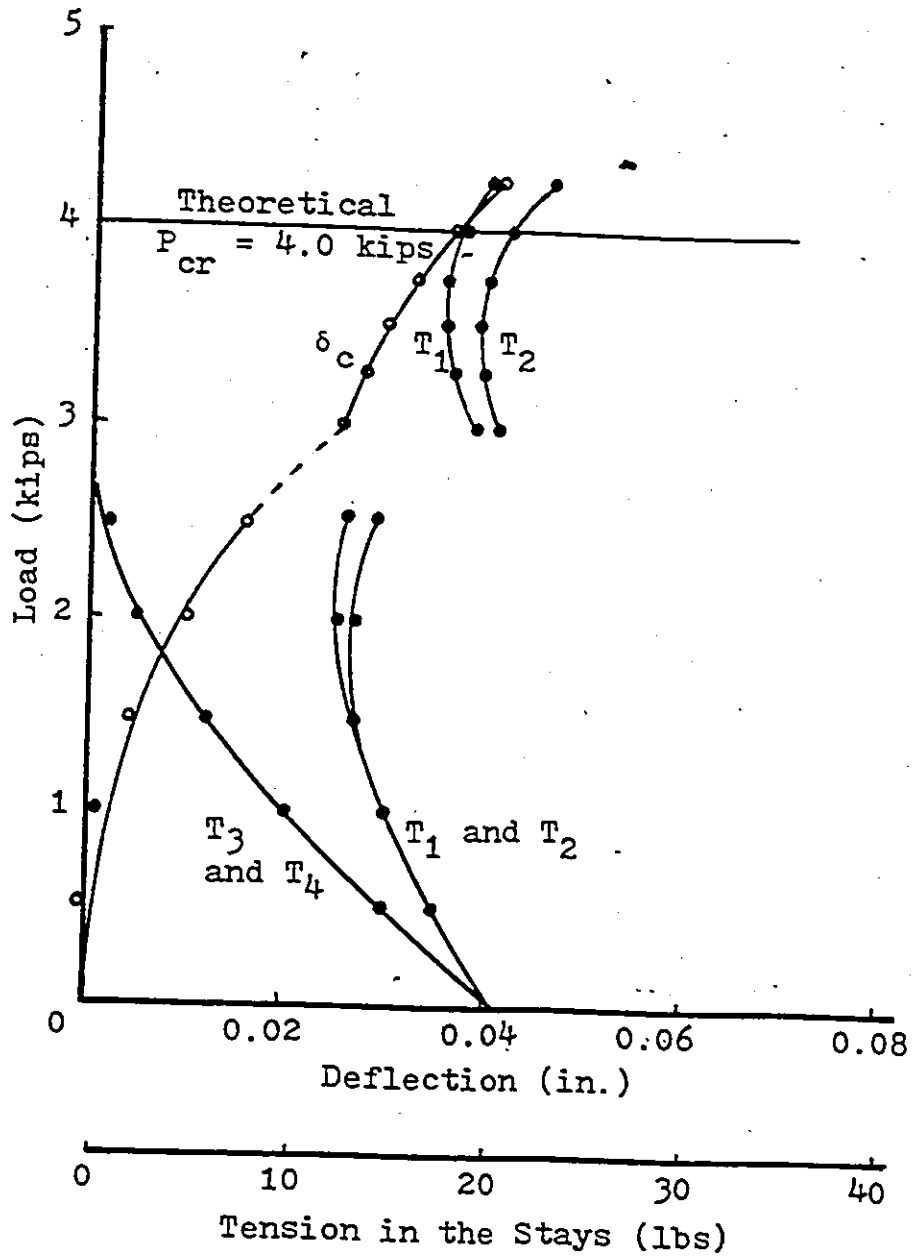


Fig. 6.10 Load versus Deflection and Tension in the Stays for an Initial Pretension of 20 lbs.

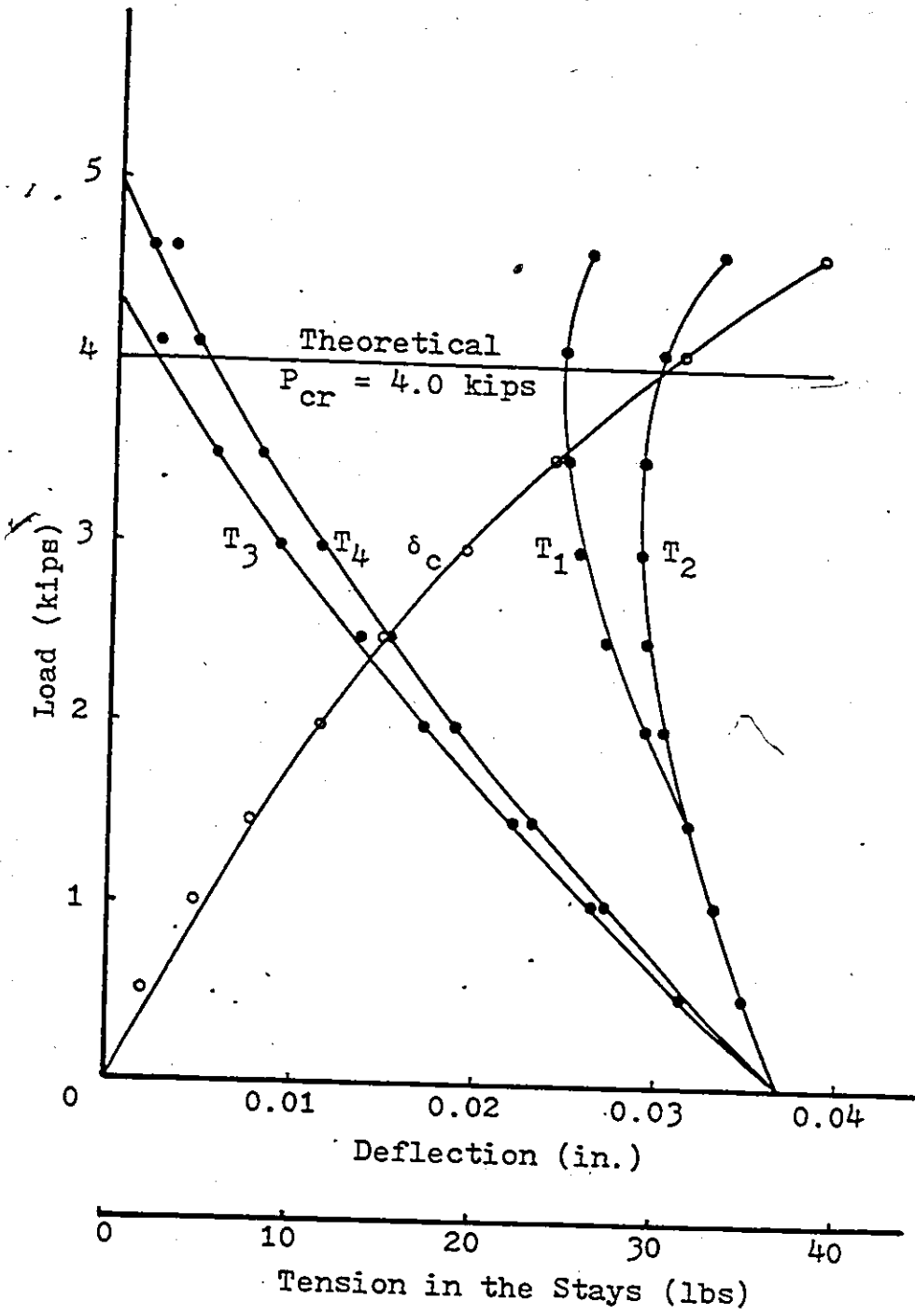


Fig. 6.11 Load versus Deflection and Tension in the Stays for an Initial Pretension of 37 lbs.

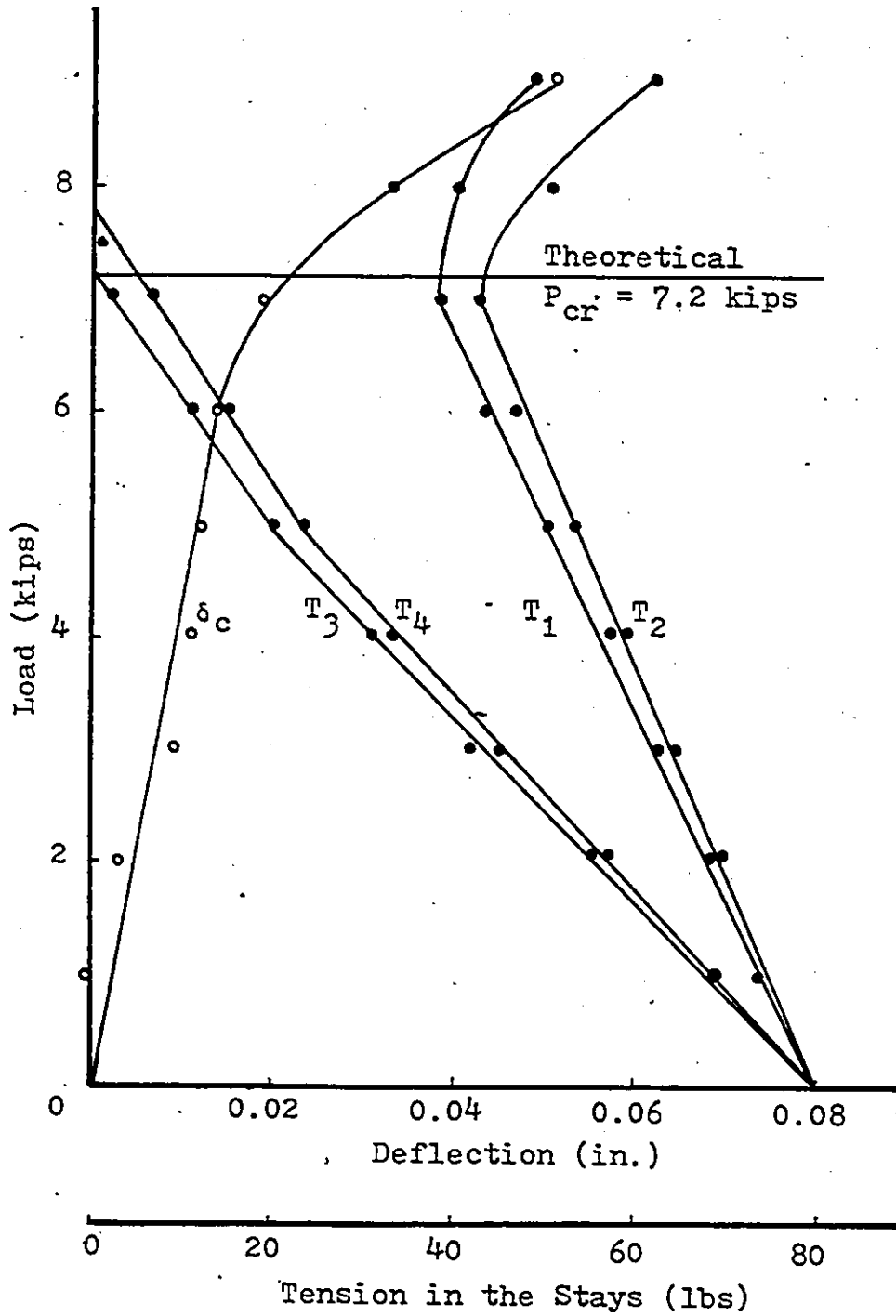


Fig. 6.12 Load versus Deflection and Tension in the Stays for an Initial Pretension of 80 lbs.

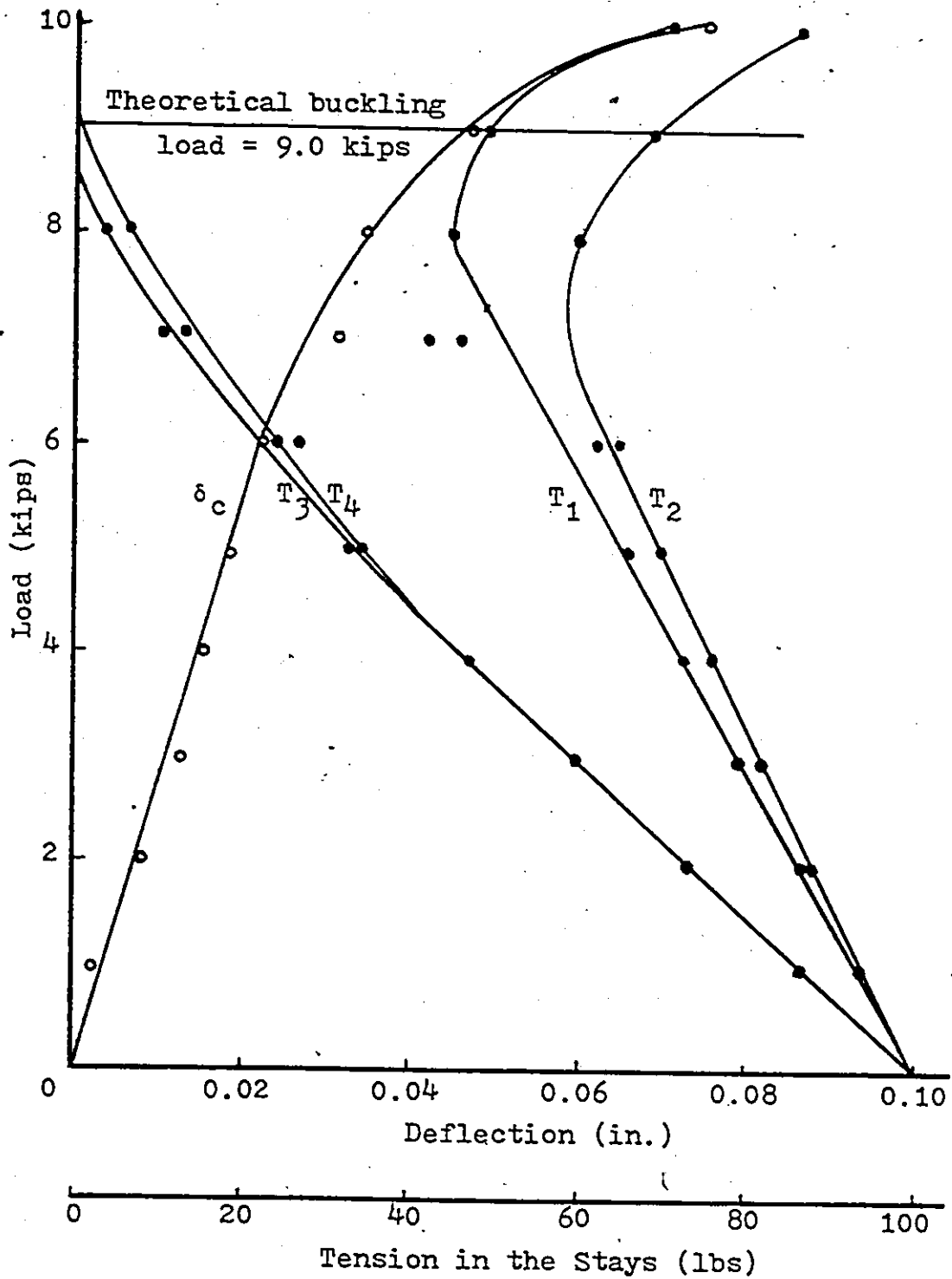


Fig. 6.13 Load versus Deflection and Tension in the Stays for an Initial Pretension of 100 lbs.

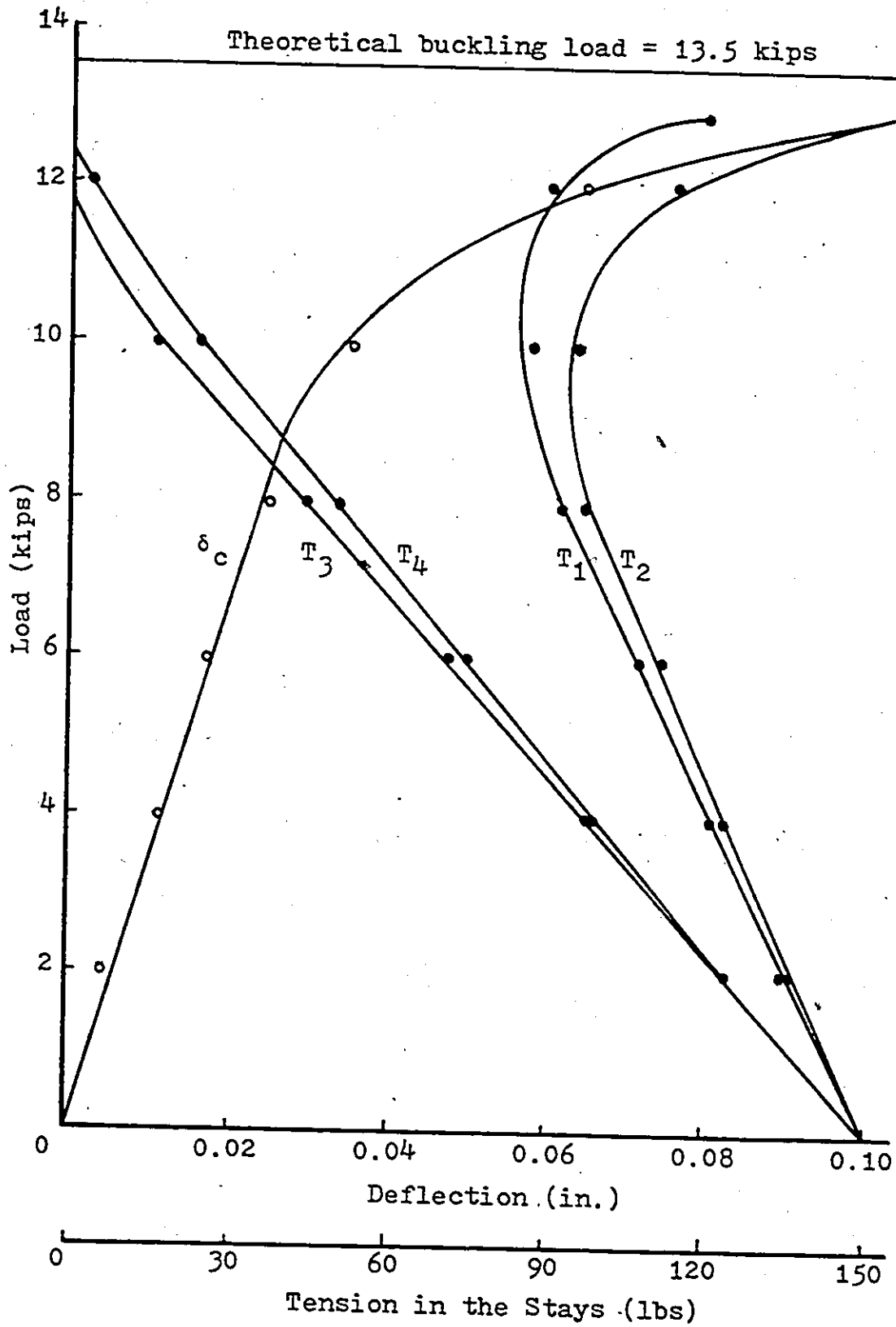


Fig. 6.14 Load versus Deflection and Tension in the Stays for an Initial Pretension of 150 lbs.

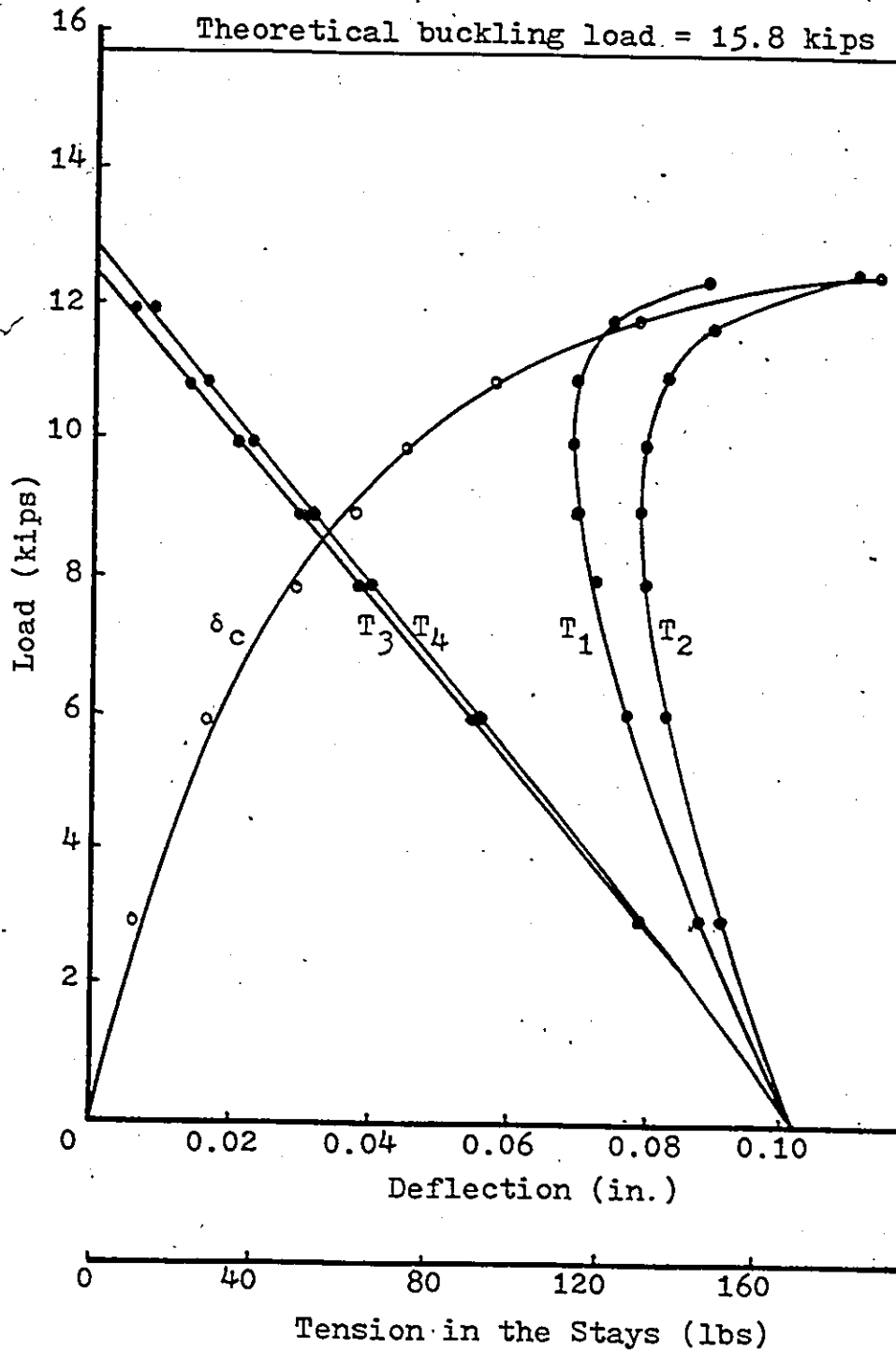


Fig. 6.15 Load versus Deflection and Tension in the Stays for an Initial Pretension of 175 lbs.

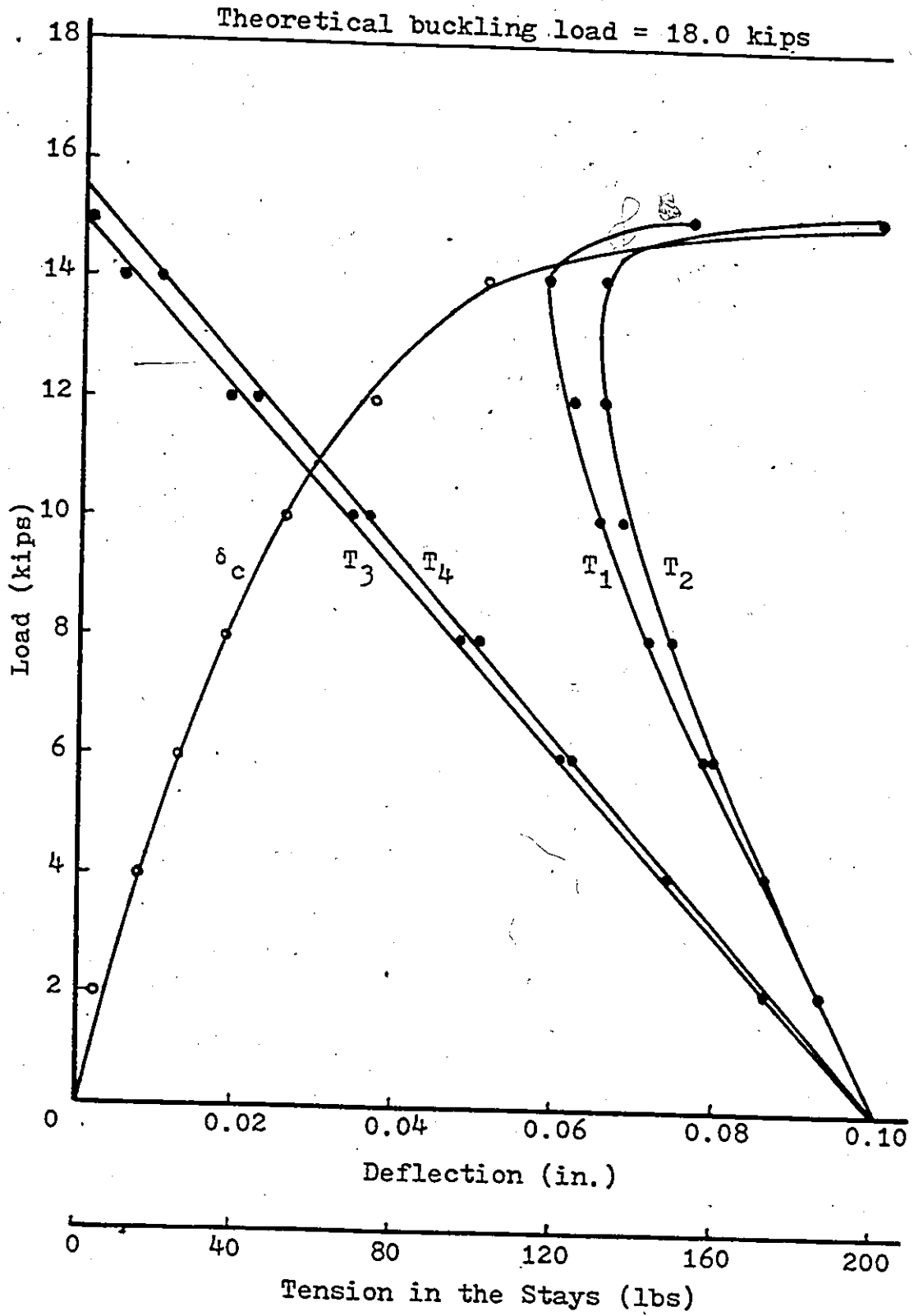


Fig. 6.16 Load versus Deflection and Tension in the Stays for an Initial Pretension of 200 lbs.

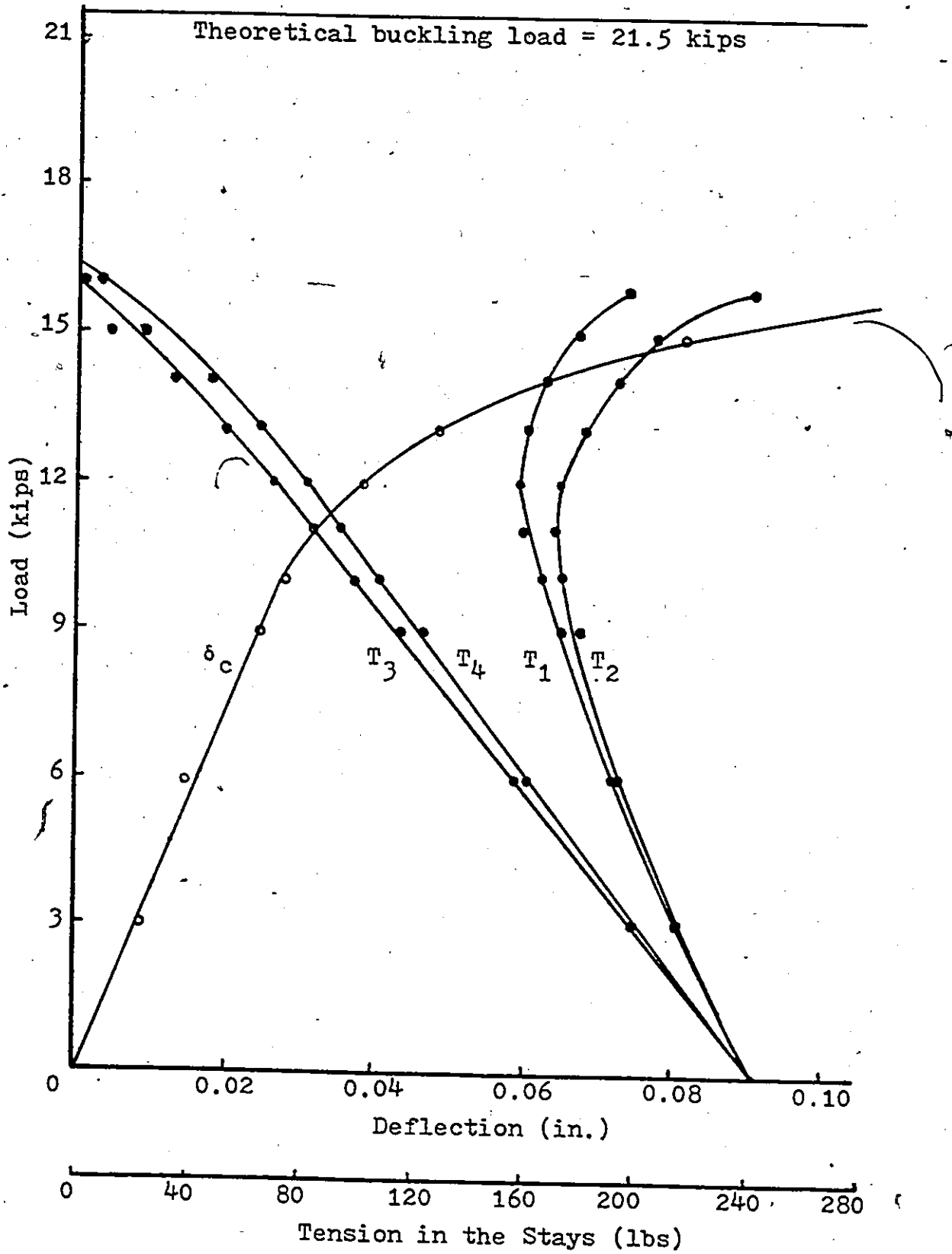


Fig. 6.17 Load versus Deflection and Tension in the Stays for an Initial Pretension of 240 lbs.

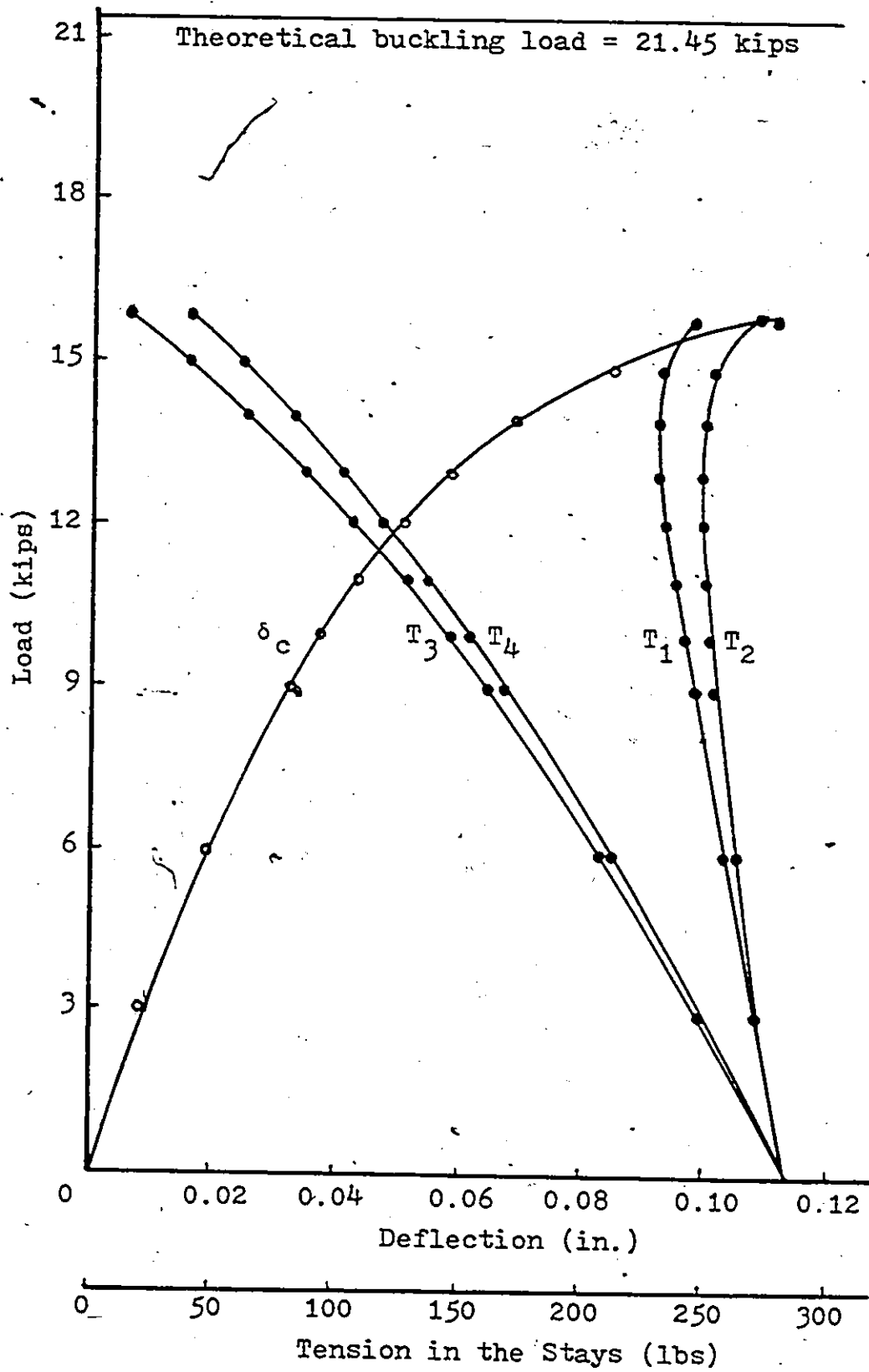


Fig. 6.18 Load versus Deflection and Tension in the Stays for an Initial Pretension of 280 lbs.

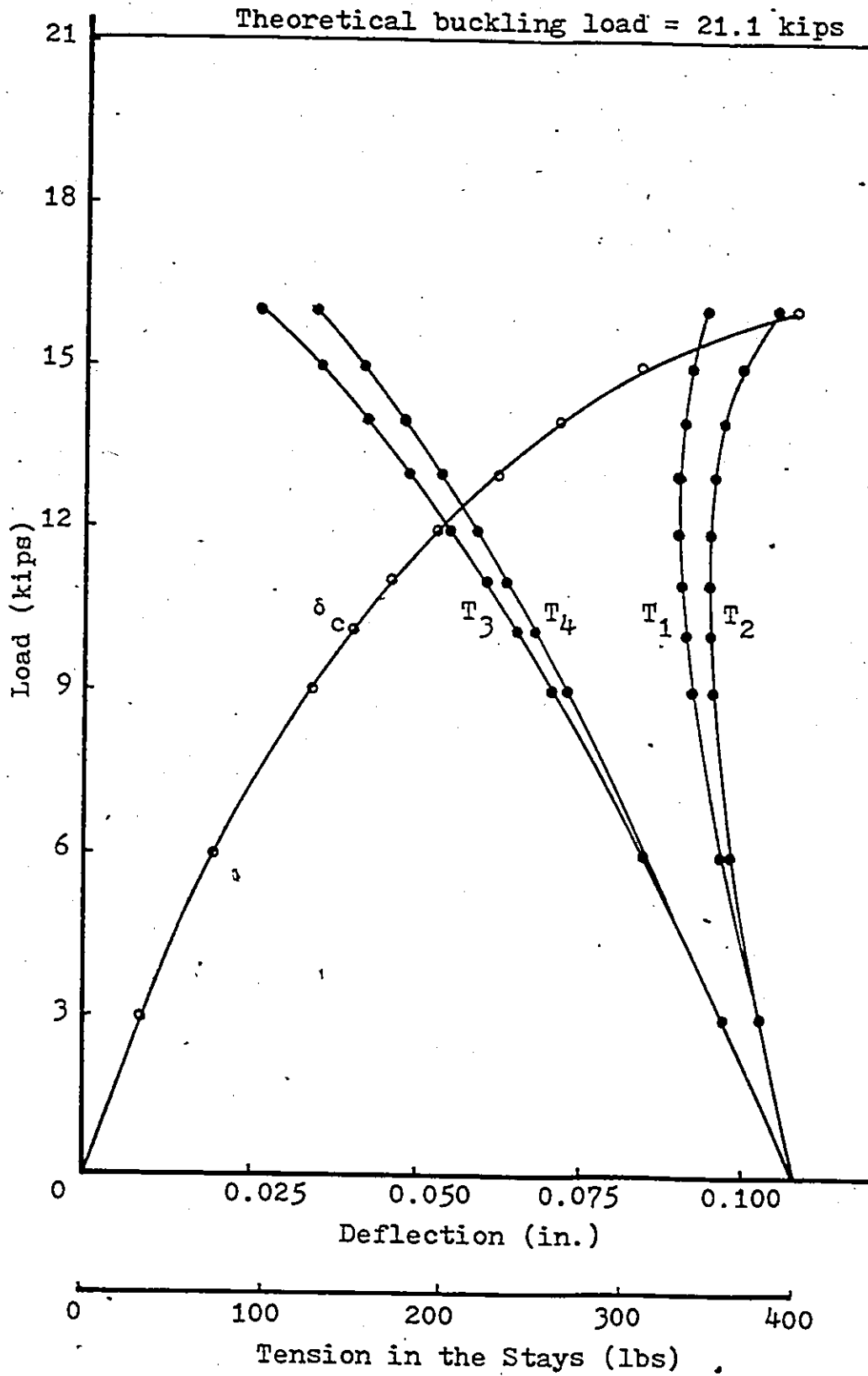


Fig. 6.19 Load versus Deflection and Tension in the Stays for an Initial Pretension of 400 lbs.

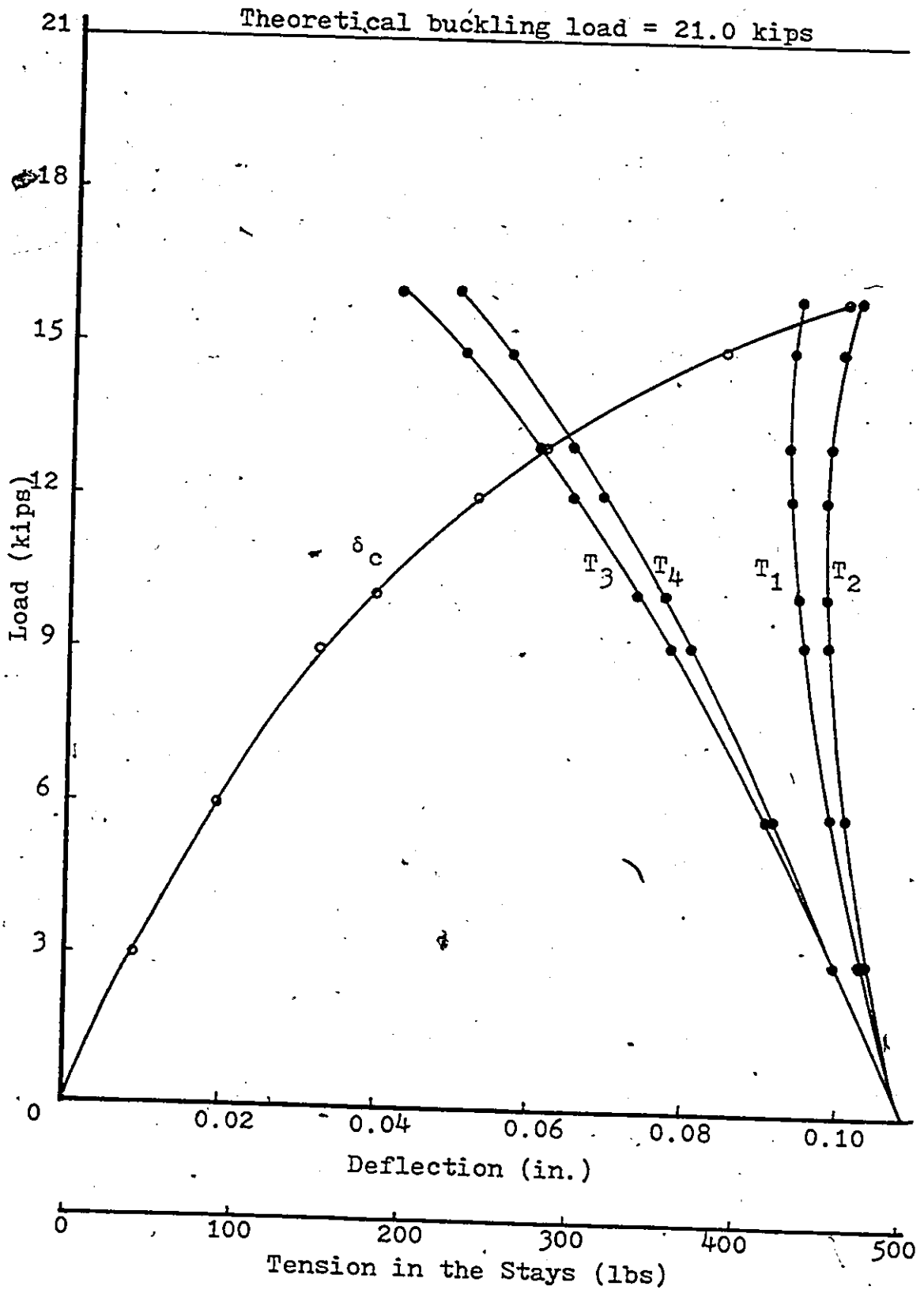


Fig. 6.20 Load versus Deflection and Tension in the Stays for an Initial Pretension of 500 lbs.

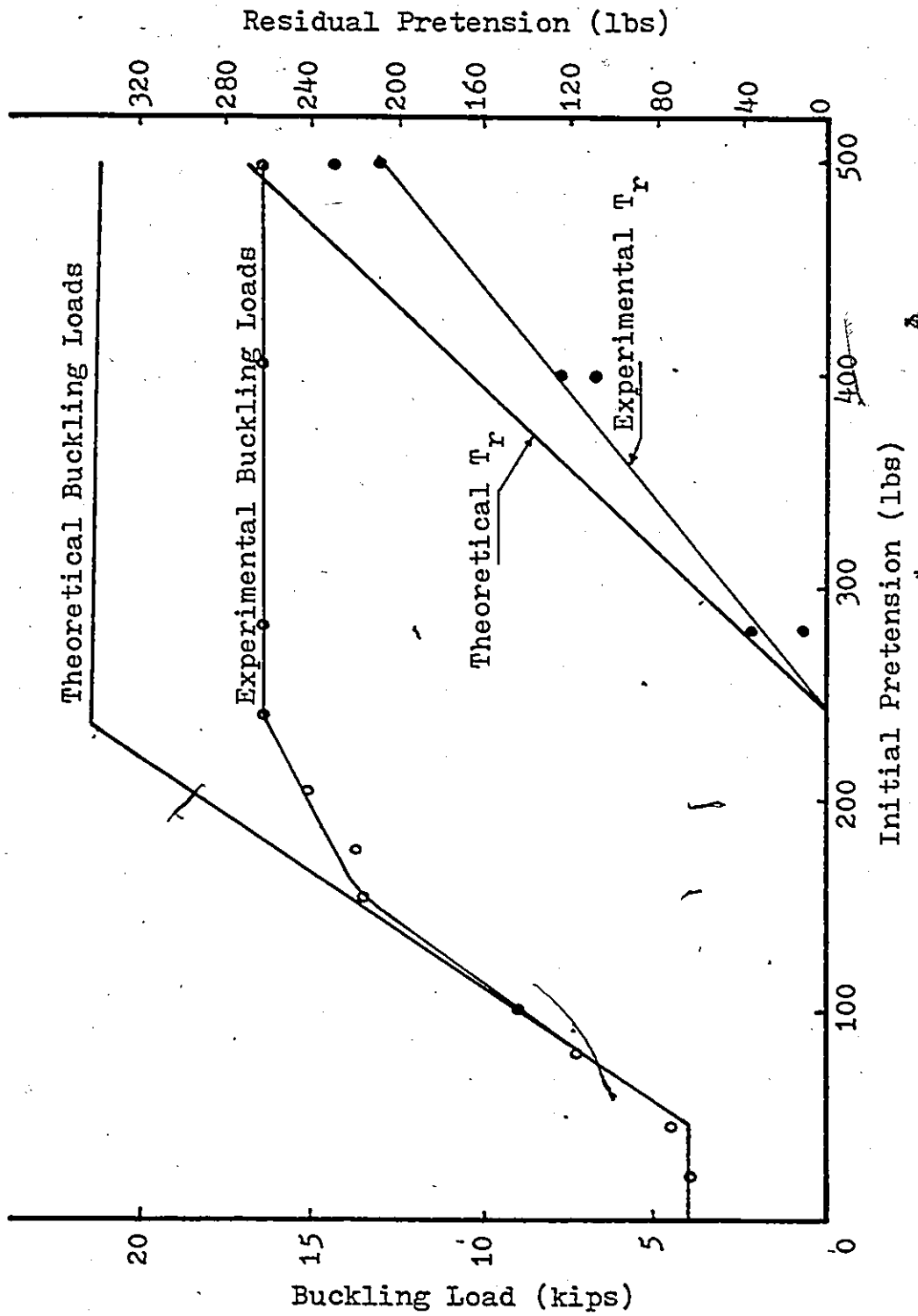


Fig. 6.21 Comparison between Theoretical and Experimental Buckling Loads and Residual Pretension.

APPENDIX I
LISTING OF COMPUTER PROGRAM

FORTRAN IV G LEVEL 21

MAIN

DATE = 77093

06/24/30

```

*****
*** THE EFFECT OF INITIAL PRETENSION ON A SINGLE CROSS-ARM STAYED COLUMN ***
*****
0001      DIMENSION EMK(10,10) ,GMK(10,10),XL(10),X(100),EMK1(100),GMK1(100)
0002      *** INPUT DATA ***
0003      READ THE NATURE OF THE PROBLEM : IF THE COLUMN HAS 4 CROSSLARMS SET IN A
          CRUCIFIELD FORM PUT IF20=0 . IF THE COLUMN HAS ONLY TWO CROSSLARMS SET IN
          THE PLANE OF BUCKLING ( THE COLUMN IS PREVENTED FROM BUCKLING IN THE
          PERPENDICULAR PLANE AS IN THE CASE OF AN EXPERIMENT ) PUT IF20= ANY NUMBER
          READ 45 , IF20
0004      45 FORMAT(I3)
          PROPERTIES OF COLUMN . THEN CROSS-ARMS THEN STAYS
          (LENGTH, OUTER DIAM., INNER DIAM., MODULUS OF ELASTICITY FOR COL. AND
          CROSS-ARMS & DIAM., MODULUS OF ELASTICITY FOR STAYS ( AND INNER
          DIAMETER IF STAYS ARE HOLLOW ) )
0005      READ 1, CL, DO, DI, EC
0006      READ 1, CAL, DAO, DAI, EA
0007      READ 1, DS, ES, OIS
          1 FORMAT(4F10.0)
          C *** CALCULATE PROPERTIES OF THE STAYED COLUMN ***
0008      PI=4.0*ATAN(1.0)
0009      AC=PI*(EC**2-DI**2)/4.0
0010      ACA=PI*(CAO**2-DAI**2)/4.0
0011      AS=PI*DS**2/4.0
0012      SL=SQRT((CL/2.0)**2+CAL**2)
0013      CI=PI*(EC**4-DI**4)/64.0
0014      CIA=PI*(CAO**4-DAI**4)/64.0
0015      SI=PI*(DS**4-DIS**4)/64.0
0016      SE=PI**2*EC*CI/CL**2
          C *** CALCULATE MAXIMUM BUCKLING LOAD FOR THE GIVEN COLUMN ***
0017      CALL SCCMEK(CL,AC,EC,CI,CAL,ACA,EA,CIA,SL,AS,ES,ENK)
0018      CALL SCCMGK (CL,GMK)
0019      CALL ARRAY (2,10,10,10,10,EMK1,ENK)
0020      CALL ARRAY (2,10,10,10,10,GMK1,GMK)
0021      CALL NRCOT(10,GMK1,EMK1,XL,X)
0022      PMAX=1./XL(1)
          C *** CALCULATE MINIMUM , OPTIMUM & MAXIMUM PRETENSION ***
0023      RA=CL/SL
0024      RB=(AC*EC*SL**2)/(AS*ES*CL**2)
0025      RC=(AC*EC*CAL**3)/(ACA*CA**SL*CL**2)
0026      IF (IF20.NE.0) GO TO 27
0027      CF=2.0*RA+4.0*RB+8.0*RC
0028      TOPT=FMAX/CF
0029      TMIN=PE/CF
0030      TMAX=FMAX*SL/(2.*CL)
0031      GO TO 28
0032      27 CE= RA+4.0*RB+8.0*RC
0033      TOPT=PMAX/CE
0034      TMIN= PE/CE
0035      TMAX=PMAX*SL/CL
          C *** WRITE PROPERTIES OF THE GIVEN SINGLE CROSS-ARM STAYED COLUMN ***
0036      28 PRINT 16
0037      16 FORMAT(//,10X,'UNITS ARE INCHES AND KIPS',//)
0038      IF (IF20.NE.0) GO TO 30
0039      PRINT 32
0040      32 FORMAT(10X,'*** THE COLUMN HAS 4 CROSS-ARMS SET IN 2 PERPENDICULAR
          PLANES. BUCKLING OCCURS IN ONE OF THE PLANES OF CROSS-ARMS',//)
          GO TO 31
0041      30 PRINT 29
0042      29 FORMAT(10X,'*** THE COLUMN HAS 2 CROSS-ARMS ONLY SET IN ONE PLANE
          WHICH IS THE PLANE OF BUCKLING.',//)
          PRINT 40.
0043      40 FORMAT(14X,'( THE COLUMN IS RESTRICTED FROM BUCKLING IN THE PERPEN
          DICULAR DIRECTION )',//)
0044      31 PRINT 5
0045      5 FORMAT(23X,'MEMBER',10X,'LENGTH',7X,'OUTER',7X,'INNER',4X,'AREA',
          12X,'MOMENT',7X,'MODULUS')
          PRINT 7
0046      7 FORMAT(32X,'DIAM.',7X,'DIAM.',18X,'OF INERTIA',2X,'OF ELASTICITY',
          1//)
          PRINT 6,CL,DO,DI,AC,CI,EC
0047      6 FORMAT(23X,'COLUMN',F16.3,F12.3,F12.3,2F13.4,F14.1,/)
          PRINT 8,CAL,CAO,DAI,ACA,CIA,EA
0048      8 FORMAT(23X,'CROSS-ARM',F13.3,2F13.4,F14.1,/)
0049      PRINT 9,SL,OS,OIS,AS,SI,ES
0050
0051
0052
0053
0054

```



```

FORTRAN IV G LEVEL 21                MAIN                DATE = 77098                06/24/30

0053      9 FORMAT(2JX,'STAY',F10.3,F12.3,F12.4,F14.1,/)
0056      PRINT 10 , TMIN , TPI
0057      10 FORMAT(4X,'MINIMUM EFFECTIVE PRETENSION =',F9.5,' KIPS',6X,'CORR
DETERMINING MINIMUM BUCKLING LOAD =',F10.3,' KIPS',/)
0058      PRINT 11 , TOPT , PMAX
0059      11 FORMAT(10X,'OPTIMUM PREDICTED PRETENSION =',F9.5,' KIPS',6X,'CORR
DETERMINING MAXIMUM BUCKLING LOAD =',F10.3,' KIPS',/)
0060      PRINT 12 , TMAX
0061      15 FORMAT(10X,'MAXIMUM POSSIBLE PRETENSION =',F9.5,' KIPS',6X,' NO
2 APPLIED LOAD IS REQUIRED FOR BUCKLING',/)
C *** WRITE SHAPE OF BUCKLING ( EIGENVECTORS ) ***
0062      PRINT 3
0063      7 FORMAT(9X,'BUCKLING SHAPE
RELATIVE VALUES ARE GIVEN ',/)
0064      PRINT 17 , X(2)
0065      17 FORMAT(2JX,'HORIZONTAL DEFLECTION AT THE MIDDLE OF THE UPPER HALF
OF THE COLUMN =',E12.4)
0066      PRINT 18 , X(4)
0067      18 FORMAT(7.8X,'THE CROSS-ARM LEVEL',2HX,' =',E12.4,/)
0068      PRINT 19 , X(6)
0069      19 FORMAT(48X,'THE MIDDLE OF THE LOWER HALF OF THE COLUMN =',E12
1.4)
0070      PRINT 20 , X(1)
0071      20 FORMAT(7.2JX,'THE SLOPE AT THE UPPER END OF THE COLUMN',2X,' =',E
E12.4)
0072      PRINT 21 , X(3)
0073      21 FORMAT(7.36X,'THE MIDDLE OF THE UPPER HALF OF THE COLUMN',17X,' =',
C,E12.4,/)
0074      PRINT 22 , X(5)
0075      22 FORMAT(30X,'THE CROSS-ARM LEVEL',40X,' =',E12.4,/)
0076      PRINT 23 , X(7)
0077      23 FORMAT(30X,'THE MIDDLE OF THE LOWER HALF OF THE COLUMN',17X,' =',E
E12.4,/)
0078      PRINT 24 , X(8)
0079      24 FORMAT(30X,'THE LOWER END OF THE COLUMN',32X,' =',E12.4,/)
0080      PRINT 25 , X(9)
0081      25 FORMAT(23X,'THE VERTICAL DEFLECTION AT THE END OF THE CROSS-ARMS',
S,' OPPOSITE DIR.' =',E12.4,/)
0082      PRINT 26 , X(10)
0083      26 FORMAT(23X,'THE SLOPE AT THE END OF THE CROSS-ARMS ( BOTH IN THE S
SAME DIRECTION ) =',E12.4,/)
C *** READ INITIAL PRETENSIONS ( WHICH THE CORRESPONDING BUCKLING LOADS ARE
REQUIRED )
C *** EACH INITIAL PRETENSION IN ONE CARD
C *** ADD A BLANK CARD TO END THE GIVEN INITIAL PRETENSIONS
0084      4 READ 39 , TI
0085      39 FORMAT(F10.0)
0086      IF(TI.EQ.0.0) GO TO 43
C *** CALCULATE CRITICAL APPLIED LOAD & RESIDUAL TENSION IN THE STAYS ***
0087      IF(TI.LE.TMAX) GO TO 41
0088      PRINT 42 , TI
0089      42 FORMAT(9X,'INITIAL PRETENSION EMPLOYED =',F9.5,' KIPS',6X,'COLU
UMN BUCKLES BEFORE REACHING THIS INITIAL PRETENSION',/)
0090      GO TO 4
0091      41 IF(TI.GT.TOPT) GO TO 2
0092      IF (IF2C.NE.0) GO TO 33
0093      PA=TI*CF
0094      GO TO 34
0095      33 PA=TI*CE
C *** WRITE GIVEN PRETENSION , CRITICAL APPLIED LOAD & RESIDUAL PRETENSION ***
0096      34 PRINT 12 , TI , PA
0097      PRINT 14
0098      14 FORMAT (10X,'CORRESPONDING RESIDUAL TENSION IN THE STAYS AT INSTAN
NT OF BUCKLING =',F11.3,' KIPS',/)
0099      GO TO 4
0100      2 CAP=1./(4.*RB+8.*RC)
0101      CA1=PMAX*CAP
0102      CA2=2.*CAP*CL/SL
0103      CA3=CAP*CL/SL
0104      IF (IF2C.NE.0) GO TO 35
0105      TF=TI-CA1+CA2*TI
0106      GO TO 34
0107      35 TF=TI-CA1+CA3*TI
0108      36 RF=RE*SL/CL
0109      RE=RC*SL/CL
0110      IF (IF2C.NE.0) GO TO 37
0111      CP=1.+(2.*RF+4.*RE)
0112      C1=PMAX*CP

```

```

FORTRAN IV G LEVEL 21                MAIN                DATE = 77098                06/24/30

0113      C2=2.*CP*CL/SL
0114      PA=C1-C2*TI
0115      GO TO 38
0116      37 CP=1.0+1.0/(4.0*RF+8.0*RE)
0117      C1=PMAX*CP
0118      C2=CP*CL/SL
0119      PA=C1-C2*TI
C *** WRITE GIVEN PRETENSION , CRITICAL APPLIED LOAD & RESIDUAL PRETENSION ***
0120      38 PRINT 12 , TI , PA
0121      12 FORMAT(9X,'INITIAL PRETENSION EMPLOYED =',F9.5,' KIPS',6X,'CORR
RESPONDING EXPECTED BUCKLING LOAD =',F10.3,' KIPS',/)
0122      PRINT 13 , TF
0123      13 FORMAT(10X,'CORRESPONDING RESIDUAL TENSION IN THE STAYS AT INSTANT
1 OF BUCKLING =',F11.3,' KIPS',/)
0124      GO TO 4
0125      43 STOP
0126      END

```

FORTRAN IV G LEVEL 21

SCCMEK

DATE = 77098

06/24/30

```

0001      SUBROUTINE SCCMEK(CL,AC,FC,CI,CAL,ACA,EA,CIA,SL,AS,ES,LWK)
0002      DIMENSION EK(10,10),CK(6,6),IVC(21)
0003      DATA IVC/0,0,1,2,0,3,4,0,5,6,C,7,0,0,8,4,9,10,4,-9,10/
0004      DO 1 I=1,10
0005      DO 1 J=1,10
0006      1 EK(I,J)=0.0
0007      K=1
0008      C *** ELASTIC STIFFNESS MATRICES FOR THE ELEMENTS OF THE COLUMN ***
0009      EK(1,1)=12.*EC*CI/CL**3*64.0
0010      EK(2,1)=0.0
0011      EK(2,2)=AC*EC/CL*4.
0012      EK(3,1)=6.*EC*CI/CL**2*16.0
0013      EK(3,2)=0.0
0014      EK(3,3)=EC*CI/CL*16.
0015      GO TO 30
0016      C *** ELASTIC STIFFNESS MATRICES FOR THE CROSS-ARMS ***
0017      40 EK(1,1)=ACA*EA/CAL
0018      EK(2,1)=0.0
0019      EK(2,2)=12.*EA*CIA/CAL**3
0020      EK(3,1)=0.0
0021      EK(3,2)=6.*EA*CIA/CAL**2
0022      EK(3,3)=4.*EA*CIA/CAL
0023      GO TO 30
0024      C *** ELASTIC STIFFNESS MATRICES FOR THE POSITIVE INCLINED STAYS ***
0025      50 EK(1,1)=CAL**2/SL**2*AS*ES/SL
0026      EK(2,1)= (CAL*CL/2./SL**2)*(AS*ES/SL)
0027      EK(2,2)=CL**2*AS*ES/4./SL**3
0028      EK(3,1)=0.0
0029      EK(3,2)=0.0
0030      EK(3,3)=0.0
0031      GO TO 30
0032      C *** ELASTIC STIFFNESS MATRICES FOR THE NEGATIVE INCLINED STAYS ***
0033      60 EK(2,1)=-EK(2,1)
0034      EK(3,2)=-EK(3,2)
0035      30 EK(4,1)=-EK(1,1)
0036      EK(4,2)=-EK(2,1)
0037      EK(4,3)=-EK(3,1)
0038      EK(4,4)=EK(1,1)
0039      EK(5,1)=-EK(2,1)
0040      EK(5,2)=-EK(2,2)
0041      EK(5,3)=-EK(3,2)
0042      EK(5,4)=EK(2,1)
0043      EK(5,5)=EK(2,2)
0044      EK(6,1)=EK(3,1)
0045      EK(6,2)=EK(3,2)
0046      EK(6,3)=EK(3,3)/2.
0047      EK(6,4)=-EK(3,1)
0048      EK(6,5)=-EK(3,2)
0049      EK(6,6)=EK(3,3)
0050      DO 20 I=1,5
0051      JJ=I+1
0052      DO 20 J=JJ,6
0053      20 EK(I,J)=EK(J,I)
0054      C *** CORRESPONDING V C TABLE ***
0055      IF (K.EC.1) GO TO 10
0056      IF (K.EC.4) GO TO 15
0057      IF (K.EC.6) GO TO 18
0058      IF (K.EC.8) GO TO 21
0059      11 K=2
0060      DO 2 I=1,6
0061      2 IVC(I)=IVC(I+3)
0062      GO TO 10
0063      12 K=3
0064      DO 3 I=1,6
0065      3 IVC(I)=IVC(I+6)
0066      GO TO 10
0067      13 K=4
0068      DO 4 I=1,6
0069      4 IVC(I)=IVC(I+9)
0070      GO TO 10
0071      15 K=7
0072      DO 7 I=1,3
0073      7 IVC(I)=IVC(I+15)
0074      DO 8 I=4,6
0075      8 IVC(I)=IVC(I+3)
0076      GO TO 10
0077      16 K=6
0078      DO 9 I=1,3

```

FORTRAN IV G LEVEL 21

SCCMEK

DATE = 77098

06/24/30

```

0074          9 IVC(I)=IVC(I+6)
0075          DO 14 I=4,6
0076          14 IVC(I)=IVC(I+15)
0077             GO TO 10
0078          18 K=7
0079             IVC(2)=9
0080             IVC(3)=10
0081             IVC(4)=0
0082             IVC(5)=0
0083             IVC(6)=1
0084             GO TO 10
0085          19 K=8
0086             DO 17 I=1,6
0087          17 IVC(I)=IVC(I+12)
0088             IVC(5)=-9
0089             GO TO 10
0090          21 K=9
0091             DO 24 I=1,3
0092          24 IVC(I)=IVC(I+18)
0093             IVC(4)=0
0094             IVC(5)=0
0095             IVC(6)=1
0096             GO TO 10
0097          22 K=10
0098             DO 23 I=1,6
0099          23 IVC(I)=IVC(I+12)
0100          10 DO 5 I=1,6
0101             IL=IVC(I)
0102             IF(IL.EC.0) GO TO 5
0103             DO 6 J=1,6
0104             IN=IVC(J)
0105             IF(IN.EC.0) GO TO 6
0106             IL1=IABS(IL)
0107             IN1=IABS(IN)
0108             JJ=IL1/IL
0109             KK=IN1/IN
0110             EMK(IL1,IN1)=EMK(IL1,IN1)+JJ*KK*EK(I,J)
0111          6 CONTINUE
0112          5 CCNTIAUE
0113             IF (K.EC.1) GO TO 11
0114             IF (K.EC.2) GO TO 12
0115             IF (K.EC.3) GO TO 13
0116             IF (K.EC.4) GO TO 40
0117             IF (K.EC.5) GO TO 16
0118             IF (K.EC.6) GO TO 50
0119             IF (K.EC.7) GO TO 19
0120             IF (K.EC.8) GO TO 60
0121             IF (K.EC.9) GO TO 22
0122             RETURN
0123             ENC

```

FORTRAN IV G LEVEL 21

SCCMGK

DATE = 77098

06/24/30

```

0001 SUPRCLINE SCCMGK (CL,GMK)
0002 DIMENSION GK(6,6),GHK(10,10),IVC(15)
0003 DATA IVC/0.0,1.2,0.3,4.0,5.0,C.7.0,0.8/
0004 DO 1 I=1,13
0005 DO 1 J=1,10
0006 1 GK(I,J)=0.0
0007 GK(1,1)=24./(5.*CL)
0008 GK(2,1)=0.0
0009 GK(2,2)=0.0
0010 GK(3,1)=1./10.
0011 GK(3,2)=0.0
0012 GK(3,3)=CL/30.
0013 GK(4,1)=-GK(1,1)
0014 GK(4,2)=GK(2,1)*(-1)
0015 GK(4,3)=-GK(3,1)
0016 GK(4,4)=GK(1,1)
0017 GK(5,1)=-GK(2,1)
0018 GK(5,2)=GK(2,2)*(-1)
0019 GK(5,3)=-GK(3,2)
0020 GK(5,4)=GK(2,1)
0021 GK(6,1)=GK(2,2)
0022 GK(6,2)=GK(3,1)
0023 GK(6,3)=-GK(3,2)/4.
0024 GK(6,4)=-GK(3,1)
0025 GK(6,5)=GK(3,2)*(-1)
0026 GK(6,6)=GK(3,3)
0027 DO 2 I=1,5
0028 JJ=I+1
0029 CC 2 J=JJ,6
0030 2 GK(I,J)=GK(J,I)
0031 K=1
0032 3 DO 4 I=1,6
0033 DO 4 J=1,6
0034 IL=IVC(I)
0035 IN=IVC(J)
0036 IF(IL*IN.EQ.0) GO TO 4
0037 IL1=IABS(IL)
0038 IN1=IABS(IN)
0039 JJ=IL1/IL
0040 KK=IN1/IN
0041 GK(IL1-IN1)=GHK(IL1,IN1) + JJ*KK*GK(I,J)
0042 4 CONTINUE
0043 IF (K.EQ.2) GO TO 6
0044 IF(K.EQ.3) GO TO 7
0045 IF(K.EQ.4) GO TO 10
0046 K=2
0047 DO 5 I=1,6
0048 5 IVC(I)=IVC(I+2)
0049 GO TO 3
0050 6 DO 8 I=1,6
0051 8 IVC(I)=IVC(I+6)
0052 K=3
0053 GO TO 3
0054 7 DO 9 I=1,6
0055 9 IVC(I)=IVC(I+9)
0056 K=4
0057 GO TO 3
0058 10 RETURN
0059 END
0060

```

APPENDIX II

DEFLECTION OF A RING BEAM UNDER TENSION

The deflection of a ring beam* subjected to a tension force along one of its diameters can be calculated using Castigliano's theorem. The theorem states that if external forces act on an elastic member, the displacement, in the direction of any one of the forces, of the point of application of the force is equal to the partial derivative of the total elastic strain energy in the member with respect to the force. This can be written as:

$$\delta_b = \frac{\partial U}{\partial T} \quad (A.1)$$

in which δ_b = the deflection of the ring beam in the direction of the applied tension force T, and U = the total strain energy in the ring beam.

The total strain energy of the ring beam shown in Fig. A.1 can be obtained by summing the work done by the internal moments and forces acting on each differential element of the beam. This can be expressed as:

$$U = \frac{1}{2} \int \frac{N^2 ds}{E_b A_b} + \frac{1}{2} \int \frac{V^2 ds}{G_b A_b} + \frac{1}{2} \int \frac{M^2 ds}{E_b I_b} \quad (A.2)$$

* For more details, see reference (9).

in which U = the total strain energy in the beam, N = the normal force acting on a differential element of length ds , V = the shearing force acting on the element, M = the bending moment acting on the differential element, A_b = the cross-sectional area of the beam, E_b = its modulus of elasticity, G_b = its modulus of rigidity, and I_b = its moment of inertia.

Substituting for U from Eq. A.2 into Eq. A.1 yields:

$$\delta_b = \int \frac{N}{E_b A_b} \frac{\partial N}{\partial T} ds + \int \frac{V}{G_b A_b} \frac{\partial V}{\partial T} ds + \int \frac{M}{E_b I_b} \frac{\partial M}{\partial T} ds \quad (\text{A.3})$$

For convenience, one quadrant of the ring beam is studied. In Fig. A.2, if section B-B is assumed to remain fixed, the vertical deflection of the plane A-A due to the forces acting on the quadrant will give one half of the total deflection of the ring beam. On any section C-C making an angle θ with section A-A, the direct normal force, N , the shearing force, V , and the bending moment, M , are given by the following equations:

$$N = \frac{T}{2} \cos \theta \quad (\text{A.4})$$

$$V = \frac{T}{2} \sin \theta \quad (\text{A.5})$$

$$M = M_A + \frac{TR}{2}(1 - \cos \theta) \quad (\text{A.6})$$

in which M_A = the internal moment at section A-A, and

R = the mean radius of the ring beam.

M_A could be found using the fact that sections A-A and B-B remain planes at right angles to each other because of symmetry. This is satisfied by:

$$\int_0^{\frac{1}{2}\pi} \Delta d\theta = 0 \quad (A.7)$$

in which $\Delta d\theta$ = the change in the angle $d\theta$ between two normal sections, a differential distance apart, after deformation as shown in Fig. A.2.

For an initially straight beam, the rate of change of slope of the elastic curve is given by:

$$\frac{d^2y}{dx^2} = \frac{M}{EI} \quad (A.8)$$

For the ring beam, which is initially curved, the rate of change of slope of the elastic curve is given by:

$$R_{cs} = \frac{\Delta d\theta}{R d\theta} \quad (A.9)$$

Since the depth of the section is small relative to the radius of curvature R , the influence of the initial curvature of the ring beam can be neglected. In this case, Eq. A.8 can be equated to Eq. A.9, and solving for the change in the angle $d\theta$ in terms of the internal moment M yields:

$$\Delta d\theta = \frac{MR d\theta}{E_b I_b} \quad (A.10)$$

By substituting the value of $\Delta d\theta$ from Eq. A.10, Eq. A.7 becomes:

$$\int_0^{\frac{1}{2}\pi} \frac{MRd\theta}{E_b I_b} = 0 \quad (\text{A.11})$$

Substituting the value of M from Eq. A.6 into Eq. A.11, and considering R , E_b and I_b as constants, the following equation may be obtained:

$$\int_0^{\frac{1}{2}\pi} M_A d\theta + \frac{1}{2} \int_0^{\frac{1}{2}\pi} TR d\theta - \frac{1}{2} \int_0^{\frac{1}{2}\pi} TR \cos \theta d\theta = 0 \quad (\text{A.12})$$

Solving Eq. A.12, the internal moment at section A-A can be expressed as:

$$M_A = \frac{TR}{2} \left(\frac{2}{\pi} - 1 \right) \quad (\text{A.13})$$

Since $2/\pi$ is less than 1, M_A is negative. Hence, it increases the radius of curvature of the quadrant. The bending moment on section C-C can be obtained by substituting the value of M_A from Eq. A.13 into Eq. A.6 which yields:

$$M = \frac{TR}{2} \left(\frac{2}{\pi} - \cos \theta \right) \quad (\text{A.14})$$

For the calculation of the vertical deflection of the quadrant, the partial derivatives of the internal forces and moment with respect to the vertical load in the quadrant, $T/2$, should be obtained from Eq. A.4, A.5 and A.14 as

follows:

$$\frac{\partial N}{\partial \left(\frac{T}{2}\right)} = \cos \theta \quad (\text{A.15})$$

$$\frac{\partial V}{\partial \left(\frac{T}{2}\right)} = \sin \theta \quad (\text{A.16})$$

$$\frac{\partial M}{\partial \left(\frac{T}{2}\right)} = R \left(\frac{2}{\pi} - \cos \theta \right) \quad (\text{A.17})$$

Substituting the values of the partial derivatives from Eqs. A.15, A.16 and A.17 into Eq. A.3, the following expression for half of the total deflection of the ring beam can be obtained:

$$\frac{1}{2} \delta_b = \int_0^{\frac{1}{2}\pi} \frac{T \cos^2 \theta}{2 E_b A_b} R d\theta + \int_0^{\frac{1}{2}\pi} \frac{T \sin^2 \theta}{2 G_b A_b} R d\theta + \int_0^{\frac{1}{2}\pi} \frac{TR^3}{2 E_b I_b} \left(\frac{2}{\pi} - \cos \theta \right)^2 d\theta \quad (\text{A.18})$$

Solving Eq. A.18, the required deflection of the ring beam due to a tension force, T , along one of its diameters is given by:

$$\delta_b = \frac{\pi TR}{4 E_b A_b} + \frac{\pi TR}{4 G_b A_b} + \frac{TR^3}{4 E_b I_b} \left(\pi - \frac{8}{\pi} \right) \quad (\text{A.19})$$

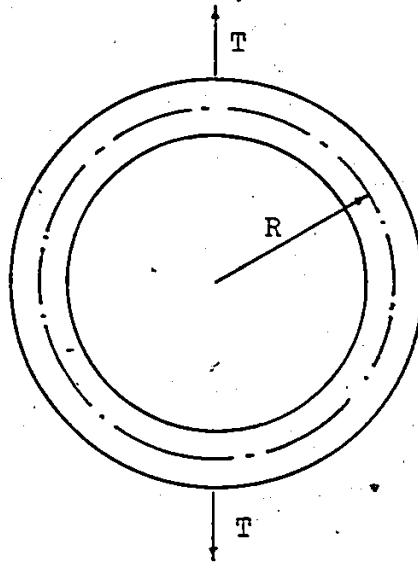


Fig. A.1 Ring Beam Subjected to Tension Force Along One of its Diameters.

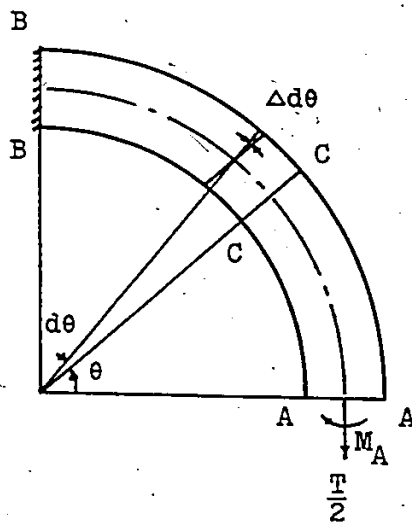


Fig. A.2 Quadrant of the Ring Beam and Differential Element to Be Studied.

BIBLIOGRAPHY

1. Chu, K. H., and Berge, S. S., "Analysis and Design of Struts with Tension Ties", Journal of the Structural Division, ASCE, Vol. 89, No. ST1, Proc. Paper 3414, Feb., 1963, pp. 127-163.
2. Mauch, H. R., and Felton, L. P., "Optimum Design of Columns Supported by Tension Ties", Journal of the Structural Division, ASCE, Vol. 93, No. ST3, Proc. Paper 5281, June, 1967, pp. 210-220.
3. Ellis, J. S., "The R. M. C. Design-Build-Test Projects", Engineering Education, ASEE, Vol. 62, No. 3, Dec., 1971, pp. 294-296.
4. Pearson, K. M., "The Behaviour of a Stayed Column with Varying Stay Tension and Cross Member Length", Thesis presented to the Royal Military College of Canada, Kingston, Ontario, Canada, in partial fulfillment of the requirements for the degree of Bachelor of Engineering, 1971.
5. Clarke, J. C., "The Behaviour of a Single Stayed Column", Thesis presented to Queen's University, Belfast, Ireland, in partial fulfillment of the requirements for the honours degree in Civil Engineering, 1972.
6. Smith, R. J., McCaffrey, G. T., and Ellis, J. S., "Buckling of a Single-Crossarm Stayed Column", Journal of the Structural Division, ASCE, Vol. 101, No. ST1, Proc. Paper 11071, Jan., 1975, pp. 249-268.
7. Khosla, C. M., "Buckling Loads of Stayed Columns Using the Finite Element Method", Thesis presented to the University of Windsor, Windsor, Ontario, Canada, in partial fulfillment of the requirements for the degree of Master of Applied Science, 1975.
8. Temple, M. C., "Buckling of Stayed Columns", Journal of the Structural Division, ASCE, Vol. 103, No. ST4, Proc. Paper 12894, April, 1977, pp. 839-851.
9. Seely, F. B., and Smith, J. O., "Advanced Mechanics of Materials", John Wiley and sons, Inc., 2nd ed., 1957.
10. "System/360 Scientific Subroutine Package, H20-205-3, Version III Programmer's Manual", IBM, Armonk, N. Y. ✓

VITA AUCTORIS

HISHAM HUSSEIN HAFEZ

The author was born on February 10, 1951, in Cairo, Egypt. In 1968, he completed his secondary school education at "Collège des Frères, De La Salle", Cairo, Egypt. Then, he joined the Faculty of Engineering, Cairo University where he was granted a financial scholarship for five consecutive years. In 1973, he graduated from Cairo University with a degree of Bachelor of Civil Engineering with a rate of appreciation of Distinction with honours. After graduation, the author spent two years working as a teaching and research assistant in the Civil Engineering Department at Cairo University.

In 1975, he joined the Civil Engineering Department at the University of Windsor, Windsor, Ontario, Canada, as a teaching and research assistant. The author prepared this thesis in partial fulfillment for the requirements for the degree of Master of Applied Science at the University of Windsor.